2011

# The role of Ad-36 and its E4orf-1 protein in modulating glycemic control

Emily Jane Dhurandhar
*Louisiana State University and Agricultural and Mechanical College*

# THE ROLE OF AD-36 AND ITS E4ORF-1 PROTEIN IN MODULATING GLYCEMIC CONTROL

A Dissertation
Submitted to the Graduate Faculty of the
Louisiana State University and
Agricultural and Mechanical College
in partial fulfillment of the
requirements for the degree of
Doctor of Philosophy

In

The School of Human Ecology

Emily Dhurandhar
B.S., Michigan State University, 2006
August 2011

## Acknowledgements

I owe my deepest gratitude to Dr. Nikhil Dhurandhar, who has expertly guided me in the completion of this dissertation, and has held me to the highest standards throughout my doctoral degree. With patient attention, he has cultivated my scientific thinking ability. Dr. Dhurandhar's accessibility, fantastic teaching ability, and kindness make him an exceptional mentor, and I am very thankful for his mentorship.

I thank Dr. Roy Martin, Dr. Frank Greenway, Dr. Jianping Ye, Dr. Michael Keenan, and Dr. Christina Sabliov for their counsel on my research projects. I am grateful to have received the benefit of their experience and expertise. Also, I would like to thank my lab-mates: Dr. Rashmi Krishnapuram, Dr. Olga Dubussion, Heather Kirk-Ballard, Nazar Mashtilar, Ying Yu, and Dr. Vijay Hegde for their help. Their teachings and support in the lab have been indispensible. Lastly, I cannot convey adequate thanks to my husband Rohan Dhurandhar, parents Deborah and Robert McAllister, and mother-in-law Amrita Dhurandhar for their constant support throughout my doctoral degree.

## Table of Contents

## List of Tables

## List of Figures

## List of Abbreviations

Body Mass Index (BMI)
Type 2 Diabetes Mellitus (T2DM)
De novo lipogenesis (DNL)
Food and Drug Administration (FDA)
National Heart, Lung, and Blood Institute (NHLBI)
American Heart Association (AHA)
Nonalcoholic Fatty Liver Disease (NAFLD)
Insulin Receptor (IR)
Insulin Receptor Substrate 1 (IRS-1)
Insulin Receptor Substrate 2 (IRS-2)
Phosphatidyl Inositol 3-Kinase (PI3K)
Metabolically Healthy Obese (MHO)
Interleukin-6 (IL-6)
C-Reactive Protein (CRP)
Tumor Necrosis Factor alpha (TNF-α)
Interleukin 1-beta (IL-1β)
Interleukin-18 (IL-18)
Monocyte Chemotactic Protein-1 (MCP-1)
Jun-Terminal Kinase (JNK)
Nuclear Factor Kappa-Light-Chain-Enhancer of Activated B Cells (NF-κB)
Crown-Like Structures (CLS)
Platelet Derived Growth Factor (PDGF)
Hypoxia-Inducible Factor alpha (HIF-1α)
Thiazolidinedione (TZD)
Extracellular Matrix (ECM)
AMP-activated Protein Kinase (AMPK)
Non Alcoholic Steatohepatitis (NASH)
Adenovirus type 36 (Ad36)
Western Blot (WB)
Macrophage Colony Stimulating Factor (MCSF)
Interferon-gamma (INF-γ)
Interleukin-10 (IL-10)
Toll-like Receptor 4 (TLR-4)
Mouse Embryonic Fibroblasts (MEF)
Phosphate Buffered Saline (PBS)
Peroxisome Proliferator Activator Receptor gamma (PPARγ)
CCAAT Enhancer Binding Protein beta (C/EBPβ)
Glycerol 3-Phosphate Dehydrogenase (G3PDH)
Norepinephrine (NE)
Human Adipose Tissue Derived Stem Cells (hASC)
Methylisobutylxanthine, Dexamethasone, and Insulin (MDI)
PDZ-domain Binding Motif (PBM)
Mitogen Activated Protein Kinase (MAPK)
High Fat Diet (HFD)

Knock Out (KO)
Sterol Regulatory Element Binding Protein-1c (SREBP-1c)
2-Deoxy-D-glucose (2DG)
Phosphate Buffered Saline (PBS)
Bovine Serum Albumin (BSA)
Hepatitis C Virus (HCV)
Radioactive Counts Per Minute (CPM)

## Abstract

Current treatment strategies for Type 2 Diabetes Mellitus (T2DM) include a range of anti-diabetic drugs, supplemented by lifestyle modifications to reduce dietary fat intake and body fat. However, for their anti-diabetic action, most drugs recruit insulin signaling pathways, which are already impaired in T2DM. Also, compliance and success in achieving sustained improvements in diet or obesity over the long term is marginal. Therefore, an agent that improves diabetes independent of insulin signaling or lifestyle changes may be highly useful. Human adenovirus Ad36 offers such a model. Ad36 improves glycemic control in chow-fed mice or rats and attenuates diabetes and hepatic steatosis in high fat(HF)-fed mice, despite the HF intake and without reducing adiposity. In human adults, natural Ad36 infection predicts better glycemic control and lower hepatic lipid stores. Ex-vivo cell signaling studies suggest that in mice, Ad36 activates Ras-mediated phosphatidyl- inositol 3-kinase (PI3K) pathway (Ras/PI3K) to up-regulate glucose uptake in skeletal muscle and adipose, and suppresses glucose output from the liver. This study determined if the anti-diabetic properties of Ad36 could be creatively harnessed. Objective 1 determined that Ad36 seropositivity was associated with improved glycemic control and lower hepatic lipids in Caucasian, Hispanic, and African American children and adolescents. Objective 2 determined which of the conventional contributors of insulin sensitivity are modulated by Ad36. *In vitro*, Ad36 increased preadipocyte differentiation, de-novo lipogenesis, and fat oxidation. Ad36 increased the proportion of small adipocytes in mice on a chow diet, whereas in HF-fed mice, Ad36 increased the proportion of large adipocytes. Adipose tissue macrophage infiltration and angiogenesis were not affected by Ad36. Objective 3 determined the E4orf1 protein of

Ad36 mediates its anti-hyperglycemic property. E4orf1 is sufficient and necessary to improve glucose uptake. Mirroring the actions of Ad36, *in vitro*, E4orf1 also up-regulates the Ras/PI3K pathway, and adiponectin –an insulin sensitizing adipokine, and down-regulates inflammatory cytokine expression. E4orf1 increases glucose uptake in, preadipocytes and adipocytes. In hepatocytes, E4orf1 reduces glucose output and the metabolic studies indicate it favors less hepatic lipid storage. Overall, this study offers a broad foundation to further determine the potential of E4orf1 as an anti-diabetic agent.

# Chapter 1. Introduction

## 1.1 Obesity Prevalence, Treatment, Causes

Obesity prevalence has risen to epidemic proportions across the globe and has spread to almost every demographic(1), while the driving causes remain unclear(2). Obesity is characterized by excess body fat, and is clinically defined by Body Mass Index (BMI). BMI is body mass in kilograms divided by the square of height in meters, and represents weight adjusted for height. BMI between 25.0-29.9 is overweight, and over 30.0 is obese. Several classes of obesity were more recently defined by the World Health Organization, with 30.0-34.9 defined as class I, 35.0-39.9 as class II, and above 40 as class III obesity.

Obesity was first recognized as a health threat by health insurance companies in the 1950's (3). Tracking of obesity prevalence in the United States began in the 1960's, and prevalence was fairly stable between 1960-1980 (4; 5). Following 1980, however, prevalence climbed 8% in one decade, from 14.5% to 22.5% (4). Prevalence continued to increase through the 1990's, to 30.5% by 2000(6), but prevalence remained somewhat stable through the last decade, with rates only increasing slightly to 33.8% (7). Increasing obesity prevalence trends were only statistically significant for men, not women over the last decade (7). Currently, 68% of adults are overweight or obese in the United States. Childhood and adolescent obesity prevalence is also on the rise. Prevalence of BMI above the $95^{th}$percentile has increased three-fold since 1980 in children and adolescents, and prevalence has remained stable but high at approximately 17% (8; 9).

Obesity is associated with increased risk for Type 2 Diabetes Mellitus (T2DM), certain cancers, coronary heart disease, hypertension, sleep apnea, osteoarthritis, liver and gallbladder disease, and stroke (10), and its effective prevention and treatment is crucial. The most common

treatment for overweight or moderately obese individuals consists of behavioral, diet, and exercise modifications for weight loss. Obesity is considered a result of positive energy balance, therefore reducing caloric intake and increasing energy expenditure to induce negative energy balance is the objective of these modifications. Commercially available programs for the general public, such as Weight Watchers, produce only modest weight loss and have high drop-out rates and high weight regain post intervention (11). In addition, most individuals do not achieve their weight loss goals, and 50% are not able to achieve even what they themselves would consider a "disappointing" amount of weight loss (12). Both weight loss interventions and public awareness regarding weight loss as treatment for obesity and its co-morbidities have failed to slow the obesity epidemic or improve obesity rates at a community level (1; 13-16). Furthermore, scientific weight loss interventions with trained dieticians and consistent counseling are only marginally effective at an individual level. Studies that carefully control caloric intake and physical activity are initially successful, but most participants regain the weight lost one year post intervention (17; 18). Even follow up interventions with the purpose of helping participants maintain weight loss are often unsuccessful (19) except for few effective techniques such as consistent self-weighing (20) and very high continued physical activity levels (21), which have a very limited acceptance and applicability. As a result, behavioral weight loss treatment has had little impact on the obesity epidemic.

Pharmacological agents provide support for weight loss, but serious side effects, marginal efficiency of the available drugs, or low enthusiasm in approval of new drugs by the Food and Drug Administration (FDA) have limited their use (22; 23). Currently, only one drug (Orlistat) is approved for long term use in obesity treatment. Bariatric surgery is very effective in inducing large weight losses in severely obese subjects and improves their health risks and reduces mortality (24). However, there are many limitations about bariatric surgery. At present, it is

offered mainly to severely obese subjects, in whom the risk due to comorbidities of obesity outweighs that of a surgical procedure. Bariatric surgery patients may even regain a large portion of the weight initially lost 5-10 years post operative (25). Importantly, considering the resource-intense nature of this approach, surgery is unlikely to be a treatment for 67% of the adults suffering from overweight or obesity in the US or millions other globally. Thus, although conventional weight loss approaches may succeed in improving health risks at individual levels, achieving and maintaining weight loss is highly challenging at a community level. Alternative therapies are urgently needed to alleviate obesity related comorbidities, either by effectively reducing obesity, or by improving metabolic health independent of weight loss.

Obesity is a complex, multifactorial disorder, which may explain the difficulty of reducing weight simply by increasing energy expenditure and decreasing energy intake. Per capita energy availability, food intake (26-28), and eating patterns such as eating away from home and snacking have increased since the 1980's (29). The built environment has changed as well, which may be associated with obesity and less physical activity (28; 30). The environment in developed countries has changed drastically and has been recently termed "obesogenic", however, the response of a given individual to this environment varies greatly. Evidence suggests a biological predisposition determines our response to an obesogenic environment (31).

A complex system controlling energy balance exists between the hypothalamus, adipose tissue and the gastro-intestinal system, all of which integrate nutrient and environmental cues (32; 33). When this system is functional, body adiposity remains fairly stable. Healthy individuals recover from long-term overfeeding lasting 100 days, and return to normal weight 4 months after resuming a normal diet(34). Perturbations in body weight can be effectively countered by the body's physiological responses in an attempt to return to its stable state (35). The ability of individuals to adapt to positive energy balance is, however, variable. Humans

have high variation in energy expenditure, with approximately 10% variation in total energy expenditure in healthy men (36; 37). Weight gained over time is associated with 24 hr energy expenditure at baseline, and this association is familial (38). When exposed to long term overfeeding, a large range of weight gain occurs, and variation in weight gain is three times more between identical twin pairs than within pairs (39). A similar phenomenon was reported for weight loss, induced in identical twin pairs exposed to long term high levels of exercise (40). Evidence thus suggests a strong genetic component may predict an individual's response to an obesogenic environment.

Many genes have been associated with obesity; as of 2005, 176 cases of monogenic obesity from mutations in 11 different genes, 50 loci involved in Mendelian disorders related to obesity, and 127 more candidate genes with 22 having 5 or more supportive studies have been identified(41). A leptin receptor mutation, for example, causes leptin resistance due to absence of weight-controlling feedback of leptin from adipose tissue (42). Variations in FTO gene, as another example, are strongly related to energy intake and obesity (43).

In addition, several alternative contributors to the obesity epidemic unrelated to physical activity and caloric consumption have been recently identified, such as infections, epigenetics, intrauterine environment, maternal age at birth, assortative mating, endocrine disruptors, pharmaceutical iatrogenesis, reduction in variability of ambient temperatures, greater fecundity in more obese individuals, and sleep debt (44). These factors may alter weight-regulating mechanisms, or interact with a genetic predisposition to obesity- and combined with an obesogenic environment, lead to obesity.

**1.2 Obesity and Metabolic Syndrome**

Obesity is highly associated with the development of Metabolic Syndrome. As defined by the National Heart, Lung, and Blood Institute (NHLBI) and American Heart Association

(AHA), Metabolic Syndrome is characterized by three or more of the following: large waist circumference (≥ 40 in for men, 35 in for women), high blood pressure (≥ 130/85 mmHg), high fasting blood sugar (≥ 100 mg/dL), low HDL cholesterol (men ≤ 40 mg/dL, women ≤ 50 mg/dL), and high triglycerides (≥ 150 mg/dL). Metabolic Syndrome increases the risk of cardiovascular disease and T2DM, kidney disease, nonalcoholic fatty liver disease (NAFLD), peripheral artery disease, and stroke. It is considered one of the top causes of mortality in developed countries (45-47). In the United States, the overall prevalence of Metabolic Syndrome is approximately 22%. The prevalence of metabolic syndrome is 4.6%, 22.5%, and 59.6% for normal weight, overweight, and obese men, with similar trends in women (48). In children, the prevalence also increases with the severity of obesity, and 50% of severely obese (BMI z score above 2.5) children have metabolic syndrome (49). Therefore, excess body fat is highly associated with development of metabolic syndrome.

### 1.3 Metabolism in Type 2 Diabetes Mellitus

The United States alone has 26 million diabetics and 79 million prediabetic persons (http://www.cdc.gov/diabetes/pubs/pdf/ndfs_2011.pdf). T2DM is defined as having fasting blood glucose ≥ 126 g/dL. T2DM is characterized by a chronic state of insulin resistance, and is often accompanied by symptoms of Metabolic Syndrome. Insulin action is impaired at the signaling level in these individuals. Normally, after Insulin binds to the Insulin Receptor (IR), Insulin Receptor Substrate 1 and 2 (IRS1/IRS2) are activated via tyrosine phosphorylation, which in turn activates Phosphatidyl inositol 3-kinase (PI3K) (50) – this is considered proximal insulin signaling. PI3K phosphorylates and activates AKT (PKB), which leads to translocation of glucose transporter Glut4 to the cell membrane, resulting in cellular glucose uptake (50) – this signaling is conventionally considered as distal insulin signaling. In addition, in the liver, PI3K

activation also suppresses gluconeogenesis, and increases glycogen and protein synthesis. Activation of SREPB-1c via hepatic insulin signaling increases lipid synthesis (50). In T2DM , however, proximal insulin signaling is impaired at the level of IR, IRS1/2, and PI3K (50-53). Because insulin signaling is defective, blood glucose remains elevated, and as a result, the pancreas receives constant stimulation to secrete more insulin to improve glucose disposal. Pancreatic beta cells therefore become necrotic, and over time are unable to secrete insulin in quantities sufficient for maintenance of normoglycemia (54; 55). Other pathologies of pancreatic beta cells have also been suggested, which could contribute to impaired insulin signaling (56).

Impaired insulin signaling has several metabolic outcomes. Glucose is not cleared by adipose tissue and muscle, two of the main tissues involved in glucose clearance. Due to hepatic insulin resistance, gluconeogenesis is not suppressed in postprandial state, so hepatic glucose output is uncontrolled. Also, due to insulin resistance, hepatic de novo lipogenesis (DNL) is not stimulated, which impairs clearance of cellular glucose. These are some of the key contributions of the liver to hyperglycemia in insulin resistant state. In adipose tissue, lipid uptake is not stimulated by insulin, and lipolysis in adipocytes is not suppressed by insulin in an insulin resistant state. Therefore, systemic levels of free fatty acids increase, which could promote the deposition of these lipids ectopically in tissues such as the liver, skeletal muscle or heart, which further impairs glucose disposal by these tissues.

### 1.4 Metabolically Healthy Obesity- Adipose Tissue and Liver in the Regulation of Glycemic Control

Many factors influence the metabolic profile of an obese individual; those who smoke less, exercise more, have smaller waist circumferences, and who are non-Hispanic or non-African American are metabolically healthier (57; 58). Although approximately 60% of obese

persons have metabolic syndrome, 40% of obese adults do not have metabolic syndrome, and are apparently "metabolically healthy" for many disease markers. This population, referred to as metabolically healthy obese (MHO), has better insulin sensitivity, high density lipoprotein levels, triglyceride levels, (59) and inflammatory profiles (60) than the obese metabolically abnormal population. It has even been suggested that obesity in these individuals may be protective against co-morbidities (61). Furthermore, normal weight persons can also demonstrate the unhealthy metabolic profile typical of an obese person (62; 63). Nearly one quarter of the normal weight American population is metabolically abnormal, and those with higher waist circumference, greater age, and lower physical activity fall into this category (58). Another example is the normal weight Asian Indian population which has particularly high percent body fat in addition to hyperlipidemia, insulin resistance, high ectopic lipid deposition in skeletal muscle, and a high level of inflammatory markers (64-66). Thus, many factors besides adiposity seem to determine the metabolic health of an individual.

The exact mechanisms for obesity leading to Metabolic Syndrome and its related co-morbidities are not well understood, and comparing metabolically healthy obese to metabolically abnormal obese is one approach to better understand this complex relationship. Recent research suggests many adipose tissue and liver characteristics distinguish obesity with metabolic abnormalities and insulin resistance from metabolically healthy obesity.

### 1.4.1 Adipose Tissue and Glycemic Control

While adipose tissue was once considered simply a storage organ, it is now considered an endocrine organ that influences metabolic health and insulin sensitivity (67). Several factors, termed adipokines, are secreted from adipose tissue and regulate insulin action, lipid metabolism, and energy expenditure. For example, adiponectin is secreted from adipocytes and is an insulin

sensitizing, anti-inflammatory adipokine (68). Resistin on the other hand, another adpokine secreted from adipose tissue, is pro-inflammatory and associated with insulin resistance in rodents (69). In addition, adipose tissue is vital for efficient storage of fatty acids, which are otherwise metabolically toxic as in the case of lipodystrophy. A relative lack of adipose tissue in lipodystrophy causes marked insulin resistance, which can be reversed by restoration of adipose tissue (70; 71). Appropriately functioning adipose tissue is therefore imperative for metabolic health. Several other characteristics of adipose tissue such as adipose tissue distribution, inflammation, macrophage infiltration, hypoxia, adipose tissue expandability and remodeling, adipocyte size, and adipokine seceratory profile have been associated with insulin resistance.

**1.4.1a Adipose Tissue Distribution**

Distribution pattern of adipose tissue throughout the body is associated with insulin resistance. Although BMI is related to development of metabolic abnormalities, visceral fat, estimated by waist circumference or wait-to-hip ratio, is often a better predictor of health risk (72-74). Gluteal and femoral adipose depots, on the other hand, may be more protective against the development of metabolic abnormalities (75). In response to a high fat diet, visceral fat up-regulates lipoprotein lipase and hormone sensitive lipase more so than subcutaneous fat, which may release more free fatty acids and contribute to increased systemic free fatty acids, and ectopic lipid deposition in liver and skeletal muscle (76). Visceral fat secretes more inflammatory cytokines that may contribute to insulin resistance. Particularly, Interleukin-6 (IL-6) expression is up-regulated in visceral adipose tissue, which in turn may increase C-reactive protein secretion from the liver (77; 78). Alternatively, reduction of visceral obesity reverses hepatic insulin resistance (79).

Inflammation may also be a factor in the relationship between visceral fat and insulin resistance, as macrophage infiltration is greater in visceral adipose tissue of insulin resistant

subjects (80; 81). These macrophages may be a source of adipokines visfatin and resistin (80), both of which may be associated with insulin resistance. In addition, insulin-sensitizing adipokine adiponectin is negatively associated with visceral fat (82). Therefore, increased visceral fat lipolysis, inflammation, and changes in adipokine secretion may contribute to the association between visceral obesity and insulin resistance.

**1.4.1b Adipose Tissue Inflammation**

Inflammation is a potential contributor to Metabolic Syndrome and insulin resistance in obesity(83). C-reactive protein (CRP), a marker of inflammation, is markedly up-regulated in obese individuals with Metabolic Syndrome (84). Expression of pro-inflammatory cytokines and chemokines such as Tumor Necrosis Factor alpha (TNF-α)(85; 86), Interleukin 6 (IL-6)(87), Interleukin 1-beta (IL-1β) (88), Interleukin-18 (IL-18)(89), and Monocyte chemotactic protein-1 (MCP-1)(90) in adipose tissue inhibits insulin signaling and/or is associated with insulin resistance. Cytokine expression is elevated in adipose tissue of obese persons, especially in insulin resistant obese more so than insulin sensitive obese (91). Activity of inflammatory pathway transcription factors, such as Jun-terminal kinase (JNK) and nuclear factor kappa-light-chain-enhancer of activated B cells (NF-κB), is also up-regulated in adipose tissue of obese, insulin resistant persons, which down-regulates insulin signaling, leading to insulin resistance (91-93). Interestingly, inflammatory cytokine expression decreases with weight loss and resembles that of a lean individual in response to very low calorie diet (94).

Macrophage populations in adipose tissue may play a major role in mediating inflammation and insulin resistance, although the role of macrophages is not completely understood. Macrophage infiltration into adipose tissue is associated with obesity and adipocyte hypertrophy (95-97), likely through increased MCP-1 secretion from adipocytes (90; 98), Macrophages in obese adipose tissue tend to aggregate in crown-like structures (CLS) (97),

which aggregate around necrotic adipocytes(97; 99), and weight loss reduces macrophage infiltration (97). On the other hand, macrophages also aid with development of new blood vessels in response to inflammation (100) and ischemia (101), possibly through platelet derived growth factor (PDGF) (102), and therefore may be involved in adipose tissue growth and remodeling (102; 103).

In addition, inflammation may contribute to insulin resistance through increasing systemic free fatty acids. Inflammatory cytokines such as TNF-α, which increase lipolysis in adipocytes, are increased with insulin resistance (104). Uncontrolled lipolysis contributes to increased systemic levels of free fatty acids, which may contribute to insulin resistance through several mechanisms. First, free fatty acids enhance pancreatic response to glucose and may lead to hyperinsulinemia (105; 106), and hyperinsulinemia is enough to induce insulin resistance due to an innate feedback loop downstream of insulin signaling that inhibits IRS-1 (107). In skeletal muscle, impaired fatty acid oxidation may lead to buildup of diacylglycoerol (108), which mediates insulin resistance (107).

**1.4.1c Adipose Tissue Hypoxia**

Adipose tissue hypoxia is another factor associated with insulin resistance and inflammation (109; 110). As adipocytes undergo hypertrophy and adipose tissue expands in response to positive energy balance, increased vascularization must occur to allow expansion, and prevent hypoxia and inflammation (111). Obesity and insulin resistance are associated with adipose tissue hypoxia. Hypoxia-inducible factor alpha (HIF-1α), the key hypoxia induced transcription factor, is elevated in diet induced and *ob/ob* obese models (112). Exposing human and rodent adipocytes or macrophages to hypoxia induces expression of inflammatory cytokines, and exposing preadipocytes to hypoxia inhibits differentiation (112). In mice, adipose tissue of obese animals (*ob/ob* mice) demonstrates a marked 70% reduction in $O_2$ partial pressure and a

marked reduction in adiponectin compared to control lean mice (113). In humans, obesity is also linked to increased adipose tissue HIF-1α expression, which is improved after bariatric surgery induced weight loss (97; 114). Thus, obesity is associated with hypoxia in adipose tissue.

Hypoxia in adipose tissue may also contribute to insulin resistance through several mechanisms (109). Hypoxia and related inflammation increases adipocyte death (99; 110; 115), which may in turn contribute to increased systemic free fatty acids. In addition, hypoxia suppresses insulin induced glucose uptake in 3T3-L1 adipocytes, and therefore may cause insulin resistance locally in adipose tissue (110). Adipokine secretion is also altered by hypoxia; it may induce leptin expression (116) and suppresses anti-inflammatory adiponectin expression (117; 118).

**1.4.1d Adipose Tissue Expandability**

Adipose tissue expandability also influences insulin sensitivity (119). If the expansion threshold is limited during positive energy balance, new adipocytes may not get recruited. Instead, the existing adipocytes may undergo hypertrophy, but eventually become insulin resistant and necrotic. Adipocyte death may in turn cause systemic free fatty acid "spill over" and ectopic lipid deposition (119). If adipose tissue is able to recruit new adipocytes and respond with hyperplastic expansion, however, and effectively "remodel" in response to positive energy balance, it retains its function in maintaining insulin sensitivity. T2DM drug class Thiazolidinedione (TZD) is a well known example of an agent which remodels adipose tissue. TZDs are agonists of PPARγ, the predominant regulator of adipogenesis (120), and increase insulin sensitivity (121). TZDs reverse glucose intolerance in obese Zucker rats not by changing adipose tissue mass, but rather by decreasing mean adipocyte size (122). Treatment with TZDs specifically expands subcutaneous adipose tissue (123; 124), increasing the ratio of subcutaneous / visceral adipose tissue mass (125). A shift from hypertrophic to hyperplastic subcutaneous

adipose tissue occurs, as indicated by greater number of smaller adipocytes (125-127). This shift to hyperplastic expansion of adipose tissue is thought to be the mechanism by which TZDs increase insulin sensitivity (128). This hypothesis is also supported by the association of impaired adipogenesis with insulin resistance (129). Thus, expansion of adipose tissue appears to accommodate incoming lipid in adipose tissue, thereby, preventing its ectopic storage and the consequential deterioration in glycemic control.

Several animal models of excessive adipose tissue expansion have demonstrated improved insulin sensitivity (68; 130). Collagen VI is one of the predominant components in the extracellular matrix (ECM) that surrounds adipose tissue, which must be rearranged upon adipose tissue expansion (130). On a high fat diet or ob/ob genetic background, Collagen VI knock-out mice have uninhibited adipose tissue expansion, yet improved insulin sensitivity (130). Collagen VI KO *ob/ob* mice are characterized by larger adipocytes, improved lipid clearance, lower inflammation and improved insulin sensitivity in adipose tissue, less pancreatic hyperplasia, and less adipocyte death compared to *ob/ob* controls (130). Alternatively, excessive Collagen VI gene expression is also related to impaired insulin sensitivity, as *db/db* mice have greater collagen expression compared to wild type mice, and collagen expression decreases following TZD treatment of wild type mice (130).

The involvement of fibrosis in adipose tissue dysfunction in humans is evident in Asian Indians, who are insulin resistant at a lower BMI compared to Caucasians (45-47) and have greater expression of Collagen VI (130). In human obesity, expression of extra-cellular matrix components is up-regulated and may be mediated by the response of preadipocytes to high levels of inflammation (131; 132). Therefore, expandability of adipose tissue may be directly affected by the extra-cellular matrix, and may influence insulin sensitivity.

Collectively, it is postulated that increased lipid storage demands result in expansion of adipose tissue mass. Expanding adipose tissue increases oxygen demands, resulting in hypoxia. This hypoxia stimulates angiogenesis for supplying oxygen through increased blood supply, allowing the formation of new adipose tissue. Thus, hypoxia, angiogenesis and adipose tissue expansion together offer increased capacity to store lipid, thereby preventing systemic free fatty acid increase and ectopic fat deposition.

**1.4.1e Adipose Tissue Adiponectin**

Adiponectin may be one of the most important insulin sensitizing adipokines. Adipose tissue specific overexpression of adiponectin in *ob/ob* mice improves insulin sensitivity despite marked obesity (68). These mice have lower ectopic lipid deposition in liver and skeletal muscle, greater adipogenesis, smaller adipocyte size, lower triglycerides, less macrophage adipose tissue infiltration, less systemic inflammation, less pancreatic hyperplasia, and lower fasting glucose and insulin levels compared to *ob/ob* control mice (68). On the other hand, hypoadiponectinemia is associated with insulin resistance in rodents, non-human primates, adults and children (82; 133-137), and adiponectin receptor ApidoR1 and AdipoR2 expression is reduced in insulin resistance (138; 139).

Adiponectin may influence insulin resistance in several ways. First, adiponectin has systemic effects on glucose and lipid metabolism. Through its receptors, adiponectin robustly up-regulates AMP-activated protein kinase (AMPK) activation in the liver, thereby increasing fatty acid oxidation and decreasing hepatic glucose production and output (140-142). Certain isoforms of adiponectin may have a similar effect on AMPK in skeletal muscle, increasing glucose uptake and fatty acid oxidation (143). The systemic action of adiponectin is dependent on expression levels of adiponectin receptors AdipoR1 and AdipoR2 (144). AdipoR1 is abundantly expressed in skeletal muscle, whereas AdipoR2 is expressed in liver (144). During

fasting, adiponectin receptors are up-regulated, likely for stimulation of fat oxidation and hepatic glucose output, and they are down-regulated postprandially (138). This mechanism is regulated by insulin mediated activation of PI3K, which phosphorylates and inactivates transcriptional forkhead transactivator FOXO1 (138). Adiponectin therefore improves systemic glucose clearance by suppressing glucose output from the liver, decreasing steatosis of the liver by up-regulating fatty acid oxidation, and increasing glucose uptake in skeletal muscle.

The autocrine-paracrine action of adiponectin in adipose tissue may improve inflammation, increase glucose uptake and improve insulin resistance. Chronic inflammation and hypoxia normally present in obesity suppresses adiponectin secretion (113). Adiponectin suppresses TNF-α expression, suggesting it has anti-inflammatory properties (145). Adiponectin receptors are expressed in adipose tissue macrophages, and adiponectin has anti-inflammatory action on these cell types (146). In fact, adiponectin desensitizes macrophages to pro-inflammatory stimuli (146), and switches macrophages to anti-inflammatory phenotype (147). Adiponectin also activates AMPK in adipocytes and increases glucose uptake, and reverses TNF-α induced insulin resistance in adipocytes (148) . Lastly, adiponectin up-regulates angiogenesis, and therefore may prevent hypoxia in adipose tissue (149; 150).

**1.4.1f Adipocyte Size**

Adipocyte size is also a marker of insulin sensitivity and adipose tissue metabolic health. Several reports have found an association between insulin resistance and large subcutaneous adipocyte size (151-153). This is apparent in Pima Indians, a population with marked obesity and insulin resistance, with a 20% increase in fat cell size in T2DM subjects compared to those with normal glucose tolerance (153). Mean adipocyte size is negatively correlated with insulin sensitivity after adjusting for body fatness (153).

Several mechanisms may link large adipocyte size and insulin resistance. Large adipocyte size may be a result of decreased capacity for adipogenesis (129), whereby mature adipocytes become hypertrophic because new cells are not being recruited in response to positive energy balance. Also, adipocyte size is positively correlated to expression of pro-inflammatory cytokines and chemokines (154), suggesting dysfunctional hypertrophic adipocytes may be pro-inflammatory. In addition, large adipocytes have higher rates of basal lipolysis than small adipocytes and may therefore increase systemic free fatty acids (155). Lastly, large adipocytes in both omental and subcutaneous adipose tissue are associated with hepatic lipid accumulation and fibrosis (156).

Conversely, small adipocyte size is associated with improved insulin sensitivity, as demonstrated with TZD treatment (126-128) and adipose tissue specific adiponectin over expressing mice (68). Metabolically healthy obesity is associated with smaller omental adipocyte size, but not smaller subcutaneous adipocyte size, compared to metabolically abnormal obesity (156; 157). Small adipocytes secrete more adiponectin (122; 158), which may contribute to improved insulin sensitivity. It should be noted, however, that Collagen VI knock-out mice demonstrate larger adipocyte size and better insulin sensitivity compared to controls. This contradictory finding suggests adipocyte size is a function of adipose tissue remodeling capacity. In the absence of the extra cellular matrix, with uninhibited adipose tissue expansion, perhaps large adipocytes have “room to grow” and are therefore less problematic. Also, large fat cell size was negatively correlated with insulin resistance in non-diabetic subjects, suggesting other factors may play a more important role after progression to T2DM(151).

### 1.4.2 Hepatic Regulation of Insulin Sensitivity

Hepatic functioning is also vital for maintenance of normoglycemica. Prevalence of fatty liver due to excessive lipid accumulation is 15% in normal weight individuals, but rises to 65% and 80% in obese and morbidly obese subjects, respectively (159-163). Many changes can lead to hepatic triglyceride accumulation; however, excess de novo lipogenesis (164; 165) and lower lipid export from liver (166; 167) are major contributors of NAFLD. NAFLD prevalence is extremely high in T2DM (69.5%) (168). NAFLD can be present without T2DM, however, those patients are generally younger with a less advanced stage of the problem, whereas those with T2DM have a more severe form including cirrhosis (169) or Non Alcoholic Steatohepatitis (NASH) (170). NASH is a more advanced stage of NAFLD, which includes inflammation and fibrosis in addition to lipid accumulation. Fatty liver is associated with insulin resistance independent of BMI, percent body fat, and visceral fat (159; 171-175). In addition, hepatic triglyceride content is the best predictor of impaired insulin action in liver, skeletal muscle, and adipose tissue, independent of body fat and BMI (172). NAFLD improves after bariatric surgery, and gene expression of inflammation and fibrosis are lower 1 year post surgery (176).

Several associations have been reported between hepatic steatosis and other contributors to insulin resistance(159). Many adipose tissue factors are highly correlated with steatosis. Adipose tissue macrophage infiltration and inflammation are closely linked to severity of NAFLD and fibrosis independent of body fatness (81; 177). Specifically, omental macrophage content and adiponectin levels are the best predictors of hepatic fibroinflammatory lesions (81). IL-1β secretion from adipocytes in response to activated macrophages and TNF-α may mediate the effect of adipose tissue inflammation on hepatic insulin resistance (178). Adiponectin secretion from adipocytes is also likely to play a large role in steatosis, as adiponectin induces fatty acid oxidation (141), is inversely associated with hepatic steatosis (179; 180), and

adiponectin therapy corrects steatosis in mice (159; 180). Local hepatic inflammation may also play a role in insulin resistance. Liver-specific activation of NF-κB is sufficient to induce hepatic insulin resistance and moderate systemic insulin resistance and has similar effects to high fat diet (181). Lastly, hepatic lipid accumulation may result in build-up of fatty acid compounds such as diacylglycerol that have negative feedback on insulin signaling (182). Thus, hepatic lipid is a strong contributor to insulin resistance.

Many characteristics of adipose tissue and liver therefore contribute to insulin resistance and distinguish metabolically healthy from metabolically unhealthy obesity. Reducing obesity leads to improvements in obesity-associated metabolic comorbidities (183-185), however, compliance with lifestyle modifications for weight loss is highly challenging for the general population. As a result, drug therapies are a promising alternative for improvement of hyperglycemia. Specifically, drug therapies that improve hyperglycemia without weight loss and despite continued consumption of a high fat diet would be of practical benefit.

Current drug therapies improve insulin secretion, insulin action at the receptor level, or enhance the insulin signaling pathway. Insulin signaling is impaired in the T2DM condition (50-53; 186; 187), however, diminishing the effectiveness of treatments that target these weakened pathways. For these reasons, an agent that improves glycemic control despite continued consumption of a high fat diet, without weight loss, which bypasses insulin and insulin signaling through an alternative pathway, may be more effective than treatments available currently. Interestingly, human Adenovirus type 36 (Ad36) infection increases glucose disposal despite impaired proximal insulin signaling (188; 189), improves glycemic control in mice on a high fat diet without weight loss (190), and offers an excellent template for the study of such alternative pathways.

### 1.5 Ad-36 and its E4orf1 Protein for Improvement of T2DM

Human adenovirus Ad36 infection is a model to study metabolically healthier obesity for the prevention of metabolic complications in obesity. Ad36 is a serologically unique human adenovirus, compared to 50 other serotypes of human adenoviruses, and belongs to subgroup D (191). It was first isolated in 1978 in Germany, from a fecal sample obtained from a girl who was suffering from diarrhea (191). Human adenoviruses cause a range of symptoms depending on the serotype, including conjunctivitis, gastroenteritis, and upper respiratory distress. Ad36 causes obesity in animal models (192-194) and is associated with human obesity (195; 196), yet its infection is associated with better lipid, cholesterol (195), and insulin sensitivity profiles (188; 197). Ad36 infection increases glucose uptake in diabetic and non-diabetic skeletal muscle and adipose tissue explants (188; 189) and attenuates high fat diet-induced hyperglycemia in mice (190). Studying the favorable effect of Ad36 on metabolic consequences of obesity may provide insight to novel treatments that improve glycemic control despite adiposity. Using infection as treatment for metabolic syndrome is not practical; however, identifying the viral protein that is responsible for influencing glucose disposal may help in developing a novel anti-diabetic therapeutic agent. A background for this approach is provided below.

#### 1.5.1 Animal Models of Ad36-Induced Obesity

Several animal experiments clearly demonstrate the effect of Ad36 on increasing adiposity. Chickens, mice, rats and marmosets (non-human primates) all have greater adiposity in response to Ad36 infection at various ages and infection routes (192-194; 197).
Ad36 infection and subsequent adiposity are both transmittable. Ad36 infection could be transmitted within 12 hours from experimentally infected animal to uninfected cage mates(192). When blood obtained 36 h after infecting chickens with Ad36 was injected intravenously into a

new set of animals, the recipient animals became infected with Ad36 and developed obesity (192). In addition to fulfilling Koch's postulate, this experiment demonstrates blood-borne mode of transmission of Ad36.

A species specific effect of Ad36 on adiposity has been observed as described below (192-194; 197). In chickens, Ad36 did not increase weight significantly, however, acutely and significantly increased body fatness. Rodent and marmoset models show a more gradual onset of significant weight gain. Six months after Ad36 infection, marmosets show a 3 fold increase in body weight gain and 56% greater body fat compared to uninfected controls. Prevalence of obesity ranged from 60 to 100% in various animal experiments compared to 12 to 23% prevalence in the uninfected controls.

Ad36 spreads to several organs, including the kidneys, liver, lungs, heart, spleen, skeletal muscle and adipose tissue only 2 days following infection, as determined by Ad36-specific DNA (198). The presence of Ad36 in adipose tissue is particularly intriguing considering the role of Ad36 on adiposity. The amount of Ad36 DNA in adipose tissue significantly correlated with the amount of adipose tissue (193). Viral mRNA is also detectable in adipose tissue, suggesting active viral replication. Collectively, these studies indicated that Ad36 may directly influence adipose tissue and induce its expansion.

As expected, the increase in adiposity by Ad36 is also accompanied by the up-regulation of the adipogenic gene cascade. Ad36 robustly up-regulates PPARγ (peroxisome proliferator activator receptor gamma), C/EBPβ (CCAAT enhancer binding protein β), and G3PDH (glycerol 3-phosphate dehydrogenase) compared to uninfected controls (197). However, Ad36 increases adiposity as well, which may confound the comparison of adipogenic gene expression in adipose tissue of lean vs. obese (Ad36 infected) animals. Therefore, the adipose tissue gene expression was compared between selected animals from the Ad36 infected and uninfected groups matched

for body weight and adiposity. This comparison showed that although their adipose tissue mass was matched, Ad36 increased the adipose tissue expression of PPARγ up to 30 fold as well as the expression of C/EBPβ and G3PDH by several fold (197) .

A criticism of animal studies with Ad36 induced adiposity is that high, experimental doses of virus may not reflect natural infection. Significant adiposity does occur, however, in naturally infected rhesus monkeys (194). Over a 90 month period rhesus monkeys at the Wisconsin Regional Primate Research Center were tested for Ad36 seropositivity due to spontaneous natural infection. Their data were compared 18 months before and 18 months after seroconversion. After the seroconversion, monkeys gained 15% body weight reduced serum cholesterol by 23% (194). Body weights of these monkeys were stable previous to the time of infection. All 15 monkeys in the study eventually became infected throughout the 90 month study, indicating a high transmissibility and relative epidemic in this population of monkeys. The drop in cholesterol and increase in body weight was independent of age upon natural infection, thus these effects were not due to age but were specific to the virus. This is the only prospective study to date on natural infection of Ad36 and the induction of adiposity, and it is indicative of the ability of Ad36 to induce weight gain in an otherwise healthy population.

In addition to increased adiposity, Ad36 also induces better insulin sensitivity in male Wistar rats (197). While fasting glucose levels do not differ, fasting insulin levels are significantly lower and HOMA index is improved in Ad36 infected animals. Despite increased body fatness, rats maintained euglycemia with nearly half the insulin level of control mice. Thus, Ad36 increases adiposity, yet prevent the development of adiposity induced insulin resistance. This action is reminiscent of anti-diabetic TZDs. Ad36 also induces higher circulating levels of leptin, which suppresses norepinephrine (NE) signaling in the paraventricular nucleus of the hypothalamus that would normally induce corticosterone secretion

and inflammation to fight infection (199). Rats did indeed show lower NE and corticosterone levels (197). Corticosterone prevents fat deposition and glucose uptake in adipocytes and liberates fatty acids for energy and glycerol for gluconeogenesis, therefore at lower levels of corticosterone, fatty acid deposition can take place and lipolysis is inhibited. Perhaps this endocrine cycle also contributes to insulin sensitivity and increased adiposity in Ad36 infected animals.

### 1.5.2 *In Vitro* Studies

Numerous *in vitro* studies have demonstrated the ability of Ad36 to induce adipogenesis. Since adipose tissue is infected by Ad36 (198), it is logical to investigate the direct effect of Ad36 on adipocytes in cell culture as a mechanism for Ad36 induced adiposity. Ad36 infected 3T3-L1 preadipocytes or human adipose tissue derived stem cells (hASC) differentiate and accumulate lipid to a greater extent than Mock infected or Ad-2 infected negative control cells (200; 201). Ad36 infection is abortive in the 3T3-L1 cell line. Ad36 initiates mRNA expression in 3T3-L1, but virus particles are not formed. Ad36 mRNA expression is enough to induce an adipogenic effect. Cidofovir, an anti-adenoviral agent, abrogates the adipogenic effect of Ad36 on 3T3-L1 cells (200). Importantly, Ad36 can induce adipogenic differentiation even in the absence of the adipogenic induction with an adipogenic cocktail of methylisobutylxanthine, dexamethasone, and insulin (MDI), or even in hASC exposed to osteogenic media (202). Detailed investigation of the effect of Ad36 preadipocyte biology has further characterized how Ad36 may lead to increased adiposity *in vivo*. The adipogenic gene cascade has revealed the entire process from increased cAMP and Wnt-10b down-regulation, to increased phosphatidyl-inositol kinase activity and aP2 is induced with or without MDI in both 3T3-L1 (200; 201) and hASC's (203).

One of six genes expressed from adenoviral early gene E4 (204), E4orf1 is a candidate for the differentiation and proliferation of preadipocytes because of its role in cell cycle regulation. It contains a PDZ-domain binding motif (PBM) which is critical for its ability to induce adipogenesis(203). The E4orf-1 gene of Ad9, which is highly homologous to that of Ad36, is known to activate PI3K (41, 42). Since Ad9 is also known to cause lipid accumulation in 3T3-L1 cells (43), E4orf-1 of Ad36 was investigated as the inducer of adipogenesis as well and was found to be sufficient and necessary to induce adipogenesis, and relies on the PI3K pathway for this induction (188). The PBM of Ad36 E4orf1 is necessary for the adipogenic effect of E4orf1 (203).

**1.5.3 Human Studies**

Ethical considerations preclude experimental infection of humans to demonstrate a cause and effect relationship of Ad36 and obesity in humans. For this reason, only indirect evidence for an association can be obtained. Several reported epidemiological associations between individuals seropositve to Ad36 and BMI, however, are supportive and congruent with evidence from animal and *in vitro* cell culture studies. Seropositivity to Ad36 is associated with obesity in the United States; 30% of obese individuals have been infected, whereas only 11% of lean persons have antibodies to Ad36 (195). Other adenoviruses (Ad-31, Ad-2, and Ad-37) do not have an association with BMI, suggesting the effect is not a characteristic of all adenoviruses in humans. Seropositive individuals had significantly greater BMI compared to their seronegative counterparts within obese as well as non-obese groups. Italian adults also showed a positive association of Ad36 seropositivity and BMI (205), whereas a cohort from the Netherlands and Belgium, and another cohort of United States military personnel did not show this association (206; 207). Antibody positive twins have higher BMI and adiposity than their seronegative twin (195). Increased adiposity in Ad36 infected twins occurs despite identical genetic background.

Ad36 infection is also associated with adiposity in children (208; 209). In Korean children, Ad-36 seropositivity is associated with higher BMI z-score and waist circumference (209; 210). In the United States, prevalence of Ad36 antibodies is 15% overall in adolescents aged 8-18, and of the seropositive children, 78% are obese, while 4% are non-obese (208). This indirect evidence coupled with direct causative effect in animal studies indicates that Ad36 may promote greater adiposity in humans. Ad36 may therefore be another environmental factor, other than diet and exercise that may contribute to increased adiposity.

### 1.5.4 Ad36 and Insulin Sensitivity

Several lines of evidence suggest that Ad36 induces metabolic changes that may favorably alter insulin sensitivity. Ad36 increases glucose uptake by preadipocytes, adipocytes, adipose tissue and skeletal muscle and reduces leptin secretion by adipocytes (188; 189; 211). Local adipocyte hypoleptinemia could contribute to improved adipogenesis and lipid accumulation. Lipid accumulation in Ad36 infected adipocytes may partly be due to de novo lipogenesis increased by the virus (188). Overall, it appears that Ad36 promotes adipogenic commitment and differentiation of adipocyte progenitors, increases glucose uptake by these cells, and increases the conversion of glucose to lipid. This may explain increased adiposity on one hand, and better glycemic control on the other hand that is observed in Ad36 infected animal models. Human ex-vivo studies, as outlined below, have provided further insight into this paradoxical phenomenon of improved insulin sensitivity caused by adipogenic Ad36 and its potential relevance to metabolically healthier human obesity.

Despite increased adiposity in seropositive subjects, Ad36 infection is associated with a decrease in serum cholesterol and triglycerides (195). Ad36 seropositive diabetic and nondiabetic subjects have lower fasting blood glucose and Hb A1C levels than seronegative subjects (188;

190). In addition, Ad36 seropositivity is associated with a lower prevalence of NAFLD (212), which may be related to the mechanism for Ad36 induced improvements in glycemic control.

Ex-vivo human studies demonstrate Ad36 increases glucose disposal in primary skeletal muscle cells and adipose tissue explants from both diabetic and nondiabetic individuals in the basal and insulin stimulated conditions (188; 189). Although Ad36 down-regulates IRS-1 activation, it increases Ras-mediated PI3K activation and Glut4 translocation, leading to increased glucose uptake in both skeletal muscle and adipose tissue (188; 189). Thus, Ad36 infection down-regulates proximal insulin signaling, yet up-regulates the distal insulin signaling. In adipose tissue, increased adiponectin, Glut1, PI3K activation, PPARγ, and decreased inflammatory cytokines such as MCP-1 mRNA expression induced by Ad36 also appear to contribute to improved glucose uptake (188). Collectively, this evidence suggests Ad36 may be able to improve glucose disposal and lipid storage, despite impairing proximal insulin signaling. Possibly, Ad36 recruits adipose tissue, liver and skeletal muscle to effect this change.

The effect of Ad36 on glycemic control was first observed experimentally in rats (197). Infected rats had lower HOMA-IR and maintained normoglycemica with half the fasting insulin levels of control mice, suggesting Ad36 has an insulin-sparing effect (197). This observation was then verified in C57BL/6J mice (190). Ad36 infected mice were fatter, but had had consistently lower fasting glucose and fasting insulin compared to those infected with Mock or Ad2 infected mice (190). In another experiment, Ad36 improved hyperglycemia in mice induced by a high fat diet. Ad36 lowered fasting glucose and insulin up to 20 weeks post infection, and significantly improved glucose clearance following a glucose tolerance test compared to Mock or Ad2 infected mice (190). Probably due to the overwhelming adipogenic effect of high fat diet, there was no difference in adiposity between the three groups of mice. Ad36 appears to increase glucose clearance through a Ras-PI3K mediated Glut4 pathway in

adipose tissue and skeletal muscle (190). Ad36 may also induce fatty acid oxidation in liver and skeletal muscle through increased adiponectin expression in adipose tissue (190). Glucose output may also be suppressed by Ad36, as indicated by lower hepatic Glut2 expression (190). Gene expression indicated that hepatic fatty acid oxidation and export may be up-regulated by the virus(190). Thus despite a high fat diet, Ad36 infection recruited multiple tissues for attenuation of dysglycemia. Ad36 may circumvent impaired proximal insulin signaling through a Ras-mediated pathway for glucose uptake in adipose tissue and skeletal muscle, and suppress hepatic lipid accumulation and glucose output. Collectively, these effects may lead to *in vivo* Ad36-induced improvements in glycemic control.

### 1.5.5 Ras Activation- Glucose Uptake, Angiogenesis, and Cell Transformation

While Ras proteins are a family of GTPases that have been most studied as oncogenes, they have a vital role in signal transduction and regulation of multiple processes that would be vital to viral replication including differentiation, proliferation and cell cycle. Ras has three major isoforms: H-Ras, N-Ras, and K-Ras. Major downstream Ras effectors include the mitogen activated protein kinase (MAPK/ERK) pathway, the p38 MAPK pathway, and the PI3K/mTOR pathway(213). Importantly, Ras regulates many processes that may contribute to glycemic control through these downstream effectors as described below.

Ras plays a role in adipogenesis. Ras is both sufficient(214) and necessary(215) to induce adipogenesis through the PI3K/AKT pathway(216; 217) and the p38 pathway(218). MAPK/ERK activation by Ras may also be involved in the initiation of adipogenesis (219), but this pathway is down-regulated upon progression of adipogenesis (220; 221). Activator complex exchange of CEBPβ, the initiator of adipogenesis, is also stimulated by Ras activation (222). In addition, Ras may function to increase glucose disposal. While Ras does not contribute to

insulin dependent glucose uptake(223), it alone is sufficient to induce glucose uptake(224). Overexpression of H-Ras in adipose tissue is sufficient to increase insulin sensitivity in mice (225), and in general Ras is thought to have insulin mimicking effects on glucose transporter translocation (226; 227). Assuming Ad36 requires Ras to increase glucose uptake, this would explain why insulin has an additive effect *in vitro* on increased glucose uptake in Ad36 infection(188; 189). Finally, Ras downstream effectors can induce angiogenesis via p38 or PI3K activation (228-234), which is crucial for the prevention of hypoxia and insulin resistance in adipose tissue(229). Thus it is possible that Ad36 acts through Ras to improve glycemic control *in vivo*.

Although Ras is known as an oncogene, its activation alone is not sufficient to induce tumor formation. For instance, dysregulated focal adhesion kinase is necessary for Ras activation to result in cell transformation (235). In addition, transgenic over expression of H-Ras in adipose tissue, the specific isoform activated by E4orf1, does not cause tumor formation (225). In several Ad36 infection experiments lasting up to 7 months, animals did not develop tumors (192-194; 197). Therefore, we hypothesize that E4orf1 is not likely to be oncogenic, although this needs to be tested more thoroughly *in vivo*.

### 1.5.6 E4orf1: A Candidate Gene of Ad36 for Improving Glycemic Control

Identifying the viral protein responsible for glucose uptake induced by Ad36 is the next step in isolating the therapeutic potential of the virus, since infection is not a viable treatment option. Many viruses have been exploited for beneficial purposes, and can be used as tools to combat disease. For example, bacteriophages have been explored as antibacterial agents (236), and lytic properties of other viruses have been used to selectively infect and destroy cancer cells(237).

E4orf1 was chosen as a candidate for the glucose clearance effect of Ad36. Adenoviruses have a set of several early genes that encode proteins for evading the host immune system and changing cell function for favorable viral replication, and several late genes that encode structural proteins. Adenoviral gene E4orf1 is transcribed from the first open reading frame of Ad36 early gene 4, and is a 17 kDa, 125 amino acid protein. It is highly homologous to the human ancestral dUTPase gene, and has a PBM region through which it interacts with other proteins containing PDZ regions for scaffolding. E4orf1 of adenovirus Ad9 binds to Dlg1 through its PBM region(238), the complex then translocates to the membrane, where it activates Ras, which in turn activates PI3K (238-240). The E4orf1 protein of Ad36 is 96% homologous to that of Ad9. This entire mechanism is not worked out with Ad36 E4orf1, however, available information suggests a similar mechanism of action for Ad36 E4orf1. For instance, Ad36 requires Ras and PI3K for its adipogenic action, and Ad36 E4orf1 is sufficient and necessary for PI3K activation in hASC's(203). Intact Ad36 E4orf1, but not its PBM mutated form, binds to Dlg1 (unpublished observations). Therefore, we hypothesized that E4orf1 of Ad36 may be sufficient to activate the Ras-PI3K pathway and to increase glucose uptake.

Based on this background, we planned the following objectives for this study:

## 1.6 Objectives

### 1.6.1 Objective 1. To Determine If Ad36 Infection Is Associated with Better Glycemic Control in Children

#### 1A. Association of Ad36 Infection with Glycemic Control in Prepubertal Caucasian and African American Children

#### 1B. Association of Ad36 Infection with Glycemic Control in Hispanic Children

- **Rationale and Expected Outcome**: Association of Ad36 seropositivity and improved glycemic control has been established in adults (188; 190), however,

any relationship between seropositivity and glycemic control in children is unknown. Adenoviruses are a common childhood infection, and Ad36 is associated with obesity in children (208; 210). Childhood is a critical time for adipose tissue deposition, and obesity in childhood is associated with greater likelihood of developing obesity and metabolic complications later in life (241). Therefore, childhood represents a unique opportunity to prevent obesity and its metabolic complications. Identifying factors which may be protective and determining the mechanism may aid in preventing metabolic abnormalities in this vulnerable population. Sera of already characterized prepubertal Caucasian and African American children from the "Mechanisms of the Metabolic Syndrome in Prepubertal Youth (MET)" study (242), and from adolescent Hispanic children from the "LA VIVA FAMILIA" study (243) will be screened for neutralizing antibodies to Ad36. Associations between seropositivity for fasting insulin, glucose, and HOMA IR, and intrahepaic lipid will be tested, and we hypothesize that Ad36 antibody prevalence will be associated with improved glycemic control.

### 1.6.2 Objective 2. Identify the Characteristics of Adipose Tissue and Liver Associated with Ad36 Induced Improvements in Glycemic Control

In animal models, Ad36 infection improves glycemic control in chow fed animals and attenuates high fat diet induced hyperglycemia. In humans, natural Ad36 infection is associated with improved glycemic control. Changes in adipose tissue and liver morphology and metabolism induced by Ad36 will be indicative of the mechanism involved in Ad36 induced improvements in glycemic control and will lay the foundation for future research.

#### 2A. Adipose Tissue

## 2A.1 Adipocyte Metabolism

### 2A.1.1 Spread of Ad36 Infection in Human Adipose Derived Stem Cells

- **Rationale and Expected Outcome**: The effect of Ad36 on 3T3-L1 murine preadipocyte differentiation is well characterized, but its effect on differentiation of human preadipocytes has not been determined. Human multipotent hASC's may be a pertinent model for the study of Ad36 on human preadipocyte differentiation, but successful infection and spread of Ad36 needs to be verified and characterized. We hypothesize that Ad36 will successfully infect and spread in hASC. Mock infected cells will serve as a negative control.

### 2A.1.2 Lipid Accumulation in hASC Following Ad36 Infection with and without MDI

- **Rationale and Expected Outcome:** Many agents that up-regulate adipocyte differentiation improve insulin sensitivity. Ad36 induces differentiation and lipid accumulation in 3T3-L1, even without the induction by differentiation cocktail. If Ad36 increases lipid accumulation in hASC, that may explain improved glycemic control despite increased adiposity associated with Ad36 infection and would indicate relevance to human adipose tissue. Fluorescent BODIPY lipid and DAPI nuclei staining will be used to quantify lipid per cell on a Flexstation fluorescent plate reader, which quantifies intensity of fluorescence. Ad36 infection with and without MDI will be the experimental groups, Mock infected cells with MDI will serve as a positive control, and Mock infected cells

without MDI will be a negative control. We hypothesize that Ad36 will increase lipid accumulation in hASC compared to Mock, with or without MDI.

### 2A.1.3 The Effect of Ad-36 Infection on Lipid Accumulation with Respect to Confluency

- **Rationale and Expected Outcome**: Determining optimal conditions for lipid accumulation following Ad36 infection will both, provide optimal conditions for future experiments, and also provide insight into the mechanism of Ad36 induced lipid accumulation. The response of 3T3-L1 to Ad36 is previously well characterized, but the effect of cellular confluence relative to the time of infection on lipid accumulation is unknown, and will therefore be determined. 3T3-L1 will therefore be infected 1 or 2 days prior to confluence and on the day of confluence, and fixed either 9 days post infection or 9 days post confluence. With this design, cells will either have equal time after virus infection, or equal time post confluence for lipid accumulation. After fixation, cells will be stained with BODIPY for lipid and DAPI nuclei for calculation of lipid per cell, and quantified using Flexstation fluorescent plate reader. We expect that Ad36 may interact synergistically with confluence for induction of lipid accumulation, since the differentiation process begins in response to confluency in 3T3-L1.

### 2A.1.4 De Novo Lipogenesis Time Course Following Ad36 Infection in 3T3-L1

- **Rationale and Expected Outcome**: Ad36 increases cellular lipid accumulation in adipocytes. Increased lipid uptake, or greater de novo lipogenesis from glucose are the two potential sources of this accumulated lipid. Previous data suggested that Ad36 increases lipid uptake in adipocytes. Considering the increased glucose uptake promoted by Ad36, conversion of this glucose to lipids is also a possible mechanism, which will be determined. [14C]-Glucose incorporation into lipids will be determined in a time course following infection with Ad36, Ad2, and Mock. Mock will serve as a negative control, and Ad2 as a control for viral infection. Because Ad36 increases lipid accumulation, we hypothesize that it will up-regulate denovo lipogenesis.

### 2A.1.5 Modulation of Glucose and Palmitate Oxidation in 3T3-L1 by Ad36

- **Rationale and Expected Outcome:** Lipid uptake and storage and glucose uptake is up-regulated by Ad36, however, the fate of these substrates is otherwise unknown. Understanding glucose and lipid disposal mechanisms by Ad36 in different tissues may help explain increased clearance of these substrates by the virus. [14C]- Glucose and [14C]-Palmitate oxidation will therefore be determined in Mock, Ad2, and Ad36 infected 3T3-L1. Mock will serve as a negative control, and Ad2 as a control for viral infection, since it is unknown how viral infection would affect these parameters. We expect that Ad36 may up-regulate glucose

and palmitate oxidation, since it increases uptake and clearance of both substrates, and since viral replication has high energy demands.

## 2A.2 Effect of Ad36 on Adipose Tissue Morphology

### 2A.2.1 Change in Adipocyte Cell Size in C57BL/6J Mice on Chow and High Fat Diet

- **Rationale and Expected Outcome**: Considering that small adipocyte size is correlated with insulin sensitivity, and large adipocyte size is associated with insulin resistance, the effect of Ad36 infection on adipocyte size will be determined. Mock, Ad36 and Ad2 infected adipose tissue from C57BL/6F mice on chow and high fat diet (HFD) will be fixed and processed for staining, and adipocyte diameter will be measured using Image J software after image acquisition. Since Ad36 is an adipogenic agent, we expect that it may increase the population of smaller adipocytes, which may contribute to increased insulin sensitivity in chow and high-fat fed mice infected with Ad36.

### 2A.2.2 Effect of Ad36 on Macrophage Infiltration in C57BL/6J Mice on Chow and HFD

- **Rationale and Expected Outcome**: Macrophage infiltration of adipose tissue is associated with obesity and insulin resistance. Immunohistochemistry staining for macrophages in adipose tissue from Mock, Ad36 and Ad2 infected chow and HFD fed C57BL/6J mice will be quantified using Image J software following image acquisition. Adenoviruses are excellent at evading the host immune system, therefore,

we hypothesize Ad36 may suppress macrophage infiltration in adipose tissue in chow or HFD C57BL/6J mice, which may contribute to improved insulin sensitivity in Ad36 infected animals.

#### 2A.2.3 Effect of Ad36 on Adipose Tissue Vascularization and Angiogenesis

- **Rationale and Expected Outcome**: Adipose tissue angiogenesis is associated with better insulin sensitivity and Ras and PI3K signaling is involved in angiogenesis. Because Ad36 activates Ras and PI3K, we hypothesized that it may increase adipose tissue vascularization, prevent hypoxia, and thus improve insulin sensitivity in mice. Adipose tissue vascularization in Ad36 infected C57BL/6J mice fed chow or HFD will be determined. To test the direct effect of Ad36 on angiogenesis, and to determine the potential relevance of this effect in humans, angiogenesis will be determined in human adipose tissue explants exposed to Ad36. Lastly, the effect of Ad36 on murine endothelial cell tube formation will be determined to elucidate a direct effect of the virus on endothelial cells. For all experiments, Mock, Ad2, and Ad36 infection will be used. We hypothesize that Ad36 may up-regulate angiogenesis, thereby improving hypoxia and insulin resistance through increase in adipose tissue vascularization.

### 2B. Effect of Ad36 on Hepatic Steatosis

#### 2B.1 Effect of Ad36 on Hepatic Steatosis and Glycogen Stores in C57BL/6J Mice on HFD

- **Rationale and Expected Outcome**: Hepatic lipid accumulation can contribute to insulin resistance, and hepatic glycogen stores are often reduced in T2DM. Glycogen content and lipid accumulation will be determined in the livers of high fat fed C57Bl/6J mice infected with Ad36, Ad2, or Mock. A liver specimen from a chow-fed mouse will be used as a positive control for healthy liver. We expect Ad36 may decrease hepatic lipid and increase glycogen content, which may explain attenuated dysglycemia in infected mice on HFD.

### 1.6.3 Objective 3. Determine If the E4orf1 Protein of Ad36 Enhances Glucose Disposal in Adipose Tissue and Liver, and If It Alters Lipid Metabolism in Liver for Lower Lipid Stores

Identifying the viral protein employed by Ad36 to improve glucose disposal and hepatic lipid metabolism could be of therapeutic value. Because E4orf1 is sufficient to induce PI3K activation, we hypothesized that it may regulate glucose and lipid metabolism in these two key tissues for glucose homeostasis. We hypothesize it may increase glucose uptake in adipocytes through the Ras-PI3K pathway used by the virus. We also hypothesize that it may suppress glucose output from the liver, and alter hepatic lipid metabolism for lower hepatic triglyceride accumulation. Although the effect of the whole virus on hepatic metabolism has not been previously characterized, since we are examining the therapeutic potential of E4orf1, we will determine the direct effect of E4orf1 on hepatic metabolism.

#### 3A. Effect of E4orf1 in Adipocytes

##### 3A.1 Is E4orf1 Necessary for Ad36 Induced Glucose Uptake?

- **Rationale and Expected Outcome:** To determine if Ad36 requires E4orf1 for enhancing cellular glucose uptake, E4orf1 will be knocked down by using a

targeted siRNA after Ad36 infection in 3T3-L1. We expect that that knockdown of E4orf1 will abate Ad36 induced glucose uptake.

### 3A.2 Is E4orf1 Sufficient to Increase Glucose Uptake?

- **Rationale and Expected Outcome:** If E4orf1 is responsible for Ad36 induced glucose uptake, its expression alone should be sufficient to increase glucose uptake. This will be tested using multiple systems. First, glucose uptake will be determined following transfection of E4orf1 plasmids in 3T3-L1 preadipocytes and adipocytes, and will be compared to transfection of Null vector control, in presence or absence of insulin. We hypothesize that E4orf1 will increase glucose uptake compared to Null vector in basal and possibly insulin stimulated conditions. Next, an inducible stable E4orf1 expressing 3T3-L1 cell line will be created. This will be used to determine a controlled dose response glucose uptake effect of E4orf1 expression, and we hypothesize that E4of1 expression will induce a dose-response effect. The E4orf1 cell line without induction and an empty vector control cell line will be used as a negative control for comparison.

### 3A.3 The Effect of E4orf1 on De Novo Lipogenesis in 3T3-L1 Preadipocytes

- **Rationale and Expected Outcome:** E4orf1 is adipogenic and increases lipid accumulation, but it is unknown if this is a result of lipid uptake or de novo lipogenesis. If E4orf1 induces glucose uptake, it may increase incorporation of glucose into lipid. [14C]-Glucose incorporation into lipid will be determined following transfection of 3T3-L1 cells with plasmids expressing E4orf1 or Null vector. We hypothesize that E4orf1 will up-regulate de novo lipogenesis.

### 3A.4 Cell Signaling Involved in E4orf1 Induced Glucose Uptake in 3T3-L1

### 3A.4.1 Total and Isoform-specific Ras Activation by E4orf1

- **Rationale and Expected Outcome:** Ad36 requires Ras / PI3k pathway to increase glucose uptake. Also, Ad36 E4orf1 activates PI3K signaling. Therefore, E4orf1 may be sufficient to activate Ras, which is upstream of PI3K. In addition, E4orf1 protein of Ad9, which is highly homologous to that of Ad36, increases Ras activation. Identifying the specific isoform of Ras activated by E4orf1 would allow for specific elucidation and modification of the pathway with any future therapeutic agent. Activation of total Ras and its isoforms will be detected in the E4orf1 inducible stable 3T3-L1 cell line. We hypothesize that induction of E4orf1 expression will activate total Ras. Considering that siRNA against H-Ras abrogated the effect of Ad36 on glucose uptake(190), Ad36 E4orf1 is expected to specifically activate the H-Ras isoform.

### 3A.4.2 The Effect of Ad36 and E4orf1 on Cell Transformation

- **Rationale and Expected Outcome:** If E4orf1 activates Ras, a potential oncogene, its ability to oncogenically transform cells needs to be determined, considering the therapeutic potential of E4orf1. This will be determined in 3T3-L1 that constitutively express E4orf1 and in 3T3-L1 infected with Ad36 using a soft agar anchorage-independent colony formation assay. A549 bronchial carcinoma cells will be used as a positive control. Because Ad36 has not induced tumor formation in animal models, and because Ras activation alone is not always sufficient to induce tumor formation, we hypothesized that Ad36 and E4orf1 will not transform cells.

### 3A.4.3 The Effect of E4orf1 on Distal Insulin Signaling, Adiponectin, and Glut1

- **Rationale and Expected Outcome:** Ad36 up-regulates glucose uptake, PI3K activation, and Glut4, Glut1, and adiponectin expression, all of which may contribute to improved glycemic control by the virus. This experiment will determine if E4orf1 mirrors the effects of Ad36 on distal insulin signaling, adiponectin and Glut1. The E4orf1 inducible stable 3T3-L1 cell line will be used, and changes in these signaling components will be determined. We hypothesize that E4orf1 will be sufficient to increase Glut4, Glut1, and adiponectin abundance, and increase AKT phosphorylation.

#### 3A.4.4 Effect of E4orf1 on Adiponectin and Inflammatory Cytokine mRNA Expression

- **Rational and Expected Outcome:** Adenoviruses are known to acutely suppress inflammation and host cell immune response, and acute infection of Ad36 suppresses inflammatory cytokines in adipose tissue. This may be due to early adenoviral gene expression, which may be highly expressed immediately after infection. If E4orf1 is sufficient to suppress inflammatory chemokines and cytokines, that would add to its therapeutic potential in fighting insulin resistance, which is fueled by inflammation. The E4orf1 inducible expressing E4orf1 3T3-L1 cell line will be used to determine changes in inflammatory cytokines by using quantitative real-time PCR. In addition, adiponectin is known to be anti-inflammatory, so its modulation by E4orf1 will be verified at the mRNA level. Overall, we hypothesize that E4orf1 will down-regulate inflammatory cytokines and up-regulate adiponectin mRNA expression.

### 3A.5 Can E4orf1 Induce Glucose Uptake Independent of PPARγ?

- **Rationale and Expected Outcome:** Although E4orf1 is a potent stimulator of adipogenesis and PPARγ, it is unknown if E4orf1 requires PPARγ for glucose uptake. PPARγ agonists for the treatment of T2DM cause excess weight gain and may be associated with increased risk of cardiovascular events, therefore, alternative agents that improve glycemic control without upregulating PPARγ are currently under investigation. If E4orf1 is sufficient to increase glucose uptake independent of PPARγ, it would be a novel agent for determining how these two effects may be uncoupled. PPARγ knock out (KO) mouse embryonic fibroblasts will be transfected with E4orf1 or Null plasmid to determine if E4orf1 increases glucose uptake independent of PPARγ. Recent (unpublished) data from our laboratory indicated that Ad36 can increase glucose uptake in PPARγ independent manner. Therefore, it is likely that Ad36 E4orf1 may increase glucose uptake independent of PPARγ.

## 3B. The Effect of E4orf1 on Hepatic Glucose and Lipid Metabolism

### 3B.1 The Effect of E4orf1 on Glucose Output in Hepatocytes

- **Rationale and Expected Outcome:** Uncontrolled hepatic glucose output often contributes to hyperglycemia in T2DM, which could be regulated by PI3K activation. E4orf1 is sufficient to activate PI3K, and therefore may be able to suppress hepatic gluconeogenesis and glucose output. HepG2 human hepatocytes as well as murine primary hepatocytes will be transfected with Ad36 E4orf1, Ad2 E4orf1, or Null plasmid and glucose output will be measured in gluconeogenic conditions. Ad2 is not adipogenic, and does not significantly improve glycemic

control *in vivo*, and therefore will be used as a control for the presence of an adenoviral gene to ensure any effect on hepatic metabolism is specific to Ad36 E4orf1.

### 3B.2 The Effect of E4orf1 on Hepatic Lipid Accumulation

Ad36 protects mice from HFD induced hepatic steatosis. This may be an important contributor to better glycemic control observed in this model. Three key determinants of hepatic lipid stores include a) de novo lipogenesis, b) lipid oxidation, and c) lipid export. The following experiments will determine if E4orf1 modulates any of these pathways.

#### 3B.2.1 The Effect of E4orf1 on Hepatic Fatty Acid Oxidation

- **Rationale and Expected Outcome:** Ad36 reduces hepatic lipid accumulation in response to high fat diet(190), but the mechanism is unknown. Gene expression data indicated that it may be through increased fatty acid oxidation and fat export. Ad36 viral DNA and RNA expression was detected in the liver, indicating it may be a direct effect of infection on hepatocytes. Ad36 may also increase fatty acid oxidation indirectly, through an up-regulation of adiponectin in adipose tissue(190). To determine if Ad36 may have a direct effect on hepatic fatty acid oxidation through E4orf1, HepG2 [14C]-Palmitate total, complete ($CO_2$), and partial oxidation will be determined in response to Ad36 E4orf1, Ad2 E4orf1, or Null vector transfection. We hypothesize that Ad36 E4orf1 up-regulates fatty acid oxidation directly in hepatocytes, and that E4orf1 may contribute to a local effect of Ad36 infection on suppression of hepatic lipid accumulation.

#### 3B.2.2 The Effect of E4orf1 on Hepatic De Novo Lipogenesis

- **Rationale and Expected Outcome:** Genes of de novo lipogenesis (Sterol regulatory element binding protein-1c (SREBP-1c) and Forkhead Transcription factor FOXO1) were nearly significantly down regulated in Ad36 infected livers(190). Therefore, Ad36 may also reduce hepatic lipid accumulation through local suppression of hepatic de novo lipogenesis. The effect of E4orf1 on de novo lipogenesis will be tested in HepG2 cells following transfection with Ad36 E4orf1, Ad2 E4orf1, or the Null vector. We hypothesize that E4orf1 may suppress de novo lipogenesis, which may contribute to lower hepatic lipid accumulation.

### 3B.2.3 The Effect of E4orf1 on Hepatic ApoB Secretion

- **Rationale and Expected Outcome**: Ad36 may also increase lipid export, as indicated by hepatic gene expression (higher levels of microsomal triglyceride transfer protein and ApoB expression), thereby decreasing hepatic lipid stores. Excretion of ApoB-containing very low density lipoprotein will be measured in conditioned media from HepG2 cells transfected with Ad36 E4orf1, Ad2 E4orf1 or the Null vector. We hypothesize that E4orf1 may be sufficient to increase lipid export in hepatocytes, thereby decreasing hepatic lipid accumulation.

# Chapter 2. Methods

## 2.1 Research Design

### 2.1.1 Objective 1. To Determine If Ad36 Infection Is Associated with Better Glycemic Control in Children

#### 1A. Association of Ad36 Infection with Glycemic Control in Prepubertal Caucasian and African American Children

Sera given from the "Mechanisms of the Metabolic Syndrome in Prepubertal Youth" (MET) study of 45 children were screened for the presence of neutralizing antibodies to Ad36 via serum neutralization, as previously described(195). Means for fasting glucose, insulin, HOMA-IR, and intra-hepatic lipid were compared with respect to Ad36 seropositivity as described in the statistics section. These parameters had been previously measured by Dr. Melinda Sothern and her colleagues. A preliminary study, "Study of Insulin Sensitivity in Louisiana Low, high or normal weight Youth (SILLY)"(242; 244), developed the protocols for the MET study. The final protocols were approved by the Institutional Review Board, and are described in detail elsewhere(190). Briefly, DXA (Hologic QDR 4500A Bedford,MA) was used to measure body composition. Fasting glucose and insulin was assayed after a 12 hr fast, with Ortho Clinical Diagnostics VITROS® 5,1 FS (Rochester, NY) and EIA kit from ALPCO (Salem, NH), respectively. Intrahepatic lipid was determined by proton magnetic resonance spectroscopy (1H-MRS) to non-invasively evaluate lipid stores.

#### 1B. Association of Ad36 Infection with Glycemic Control in Hispanic Children

Baseline Sera from "LA VIVA FAMILIA" study of obese and nonobese Hispanic children in Texas were screened for the presence of neutralizing antibodies to Ad36 as described previously (243). Means for fasting glucose, insulin, and HOMA-IR were compared with respect to Ad36 seropositivity as described in the statistics section. These

parameters were measured by Dr. Nancy Butte and colleagues. This study was previously approved by the Institutional Review Board of Baylor College of Medicine. Fasting insulin levels were measured via radioimmunoassay kit (Linco Research Inc, St Charles, MO), and fasting glucose with a glucose oxidase assay after an overnight fast. Body composition was measured via DXA with the Hologic Delphi-A whole-body scanner (Hologic Inc, Waltham, MA).

**Statistics**

For the MET study samples, fasting insulin, HOMA IR, and intrahepatic lipid data were skewed and was therefore transformed (logarithmic). SAS 9.1 software was used to implement a general linear models approach to compare means of fasting glucose, transformed fasting insulin, HOMA IR, and intra-hepatic lipid between antibody positive and antibody negative subjects. Age, race, body fat and sex were included as covariates in the model. The least squares adjusted means were back-transformed to the original scale after analysis for skewed variables. Two-sided 95% confidence limits were calculated, and also back-transformed for the least squares means that were asymmetric about the estimated means. Significance was considered at $p<0.05$ for one directional alternative hypothesis.

For the LA VIVA FAMILIA study, two statistical methods were implemented to detect differences in fasting glucose, insulin, and HOMA-IR between antibody positive and antibody negative subjects. First a general linear models approach was used in SAS 9.1. Fasting insulin and HOMA-IR were first transformed logarithmically due to skewed distributions. Age, body fat, family and sex were included in the model initially. The least squares adjusted means were back-transformed to the original scale after analysis

for skewed variables. Two-sided 95% confidence limits were calculated, and also back-transformed for the least squares means that were asymmetric about the estimated means. Significance was considered at $p<0.05$ for one directional alternative hypothesis.

Next, logistic regression was performed using SAS 9.1. The odds ratio for parameters being below the median for Ad36 seropositive individuals relative to the odds for seronegativity were compared. Sex, adiposity, and family were included in the model, and significance was considered if $p< 0.05$ for one directional alternative hypothesis.

### 2.1.2 Objective 2. Identify the Characteristics of Adipose Tissue and Liver Associated with Ad36 Induced Improvements in Glycemic Control

#### 2A. Adipose Tissue

##### 2A.1 Adipocyte Metabolism

###### 2A.1.1 Spread of Ad36 Infection in Human Adipose Derived Stem Cells

Human adipose derived stem cells were plated in 96 well glass bottom plates and infected with Ad36 at 3.8 plaque forming units per cell (PFU/cell) or mock infected as described in techniques and assays. Day 3, 5, 7, 9, and 13 post infection, cells were fixed and stained for DAPI for visualization of nuclei, and with anti-adenoviral hexon antibody as a marker of Ad36 infection as described in techniques and assays. As expected Ad36 infected cells stained positively for Ad36 hexon, whereas Mock infected cells did not. For each well, a representative 20X picture was taken on a Zeiss Axiovert 40 CFL microscope. The percent of Ad36 infected cells was quantified by counting cells expressing Ad36 hexon protein and dividing by the total number of nuclei (DAPI staining) in the given picture. Three wells per group were counted in this manner.

### 2A.1.2 Lipid Accumulation in hASC Following Ad36 Infection with and without MDI

Human adipose derived stem cells (hASC's) were plated on 96-well glass bottom plates and Mock or Ad-36 infected at 70% confluence, and 3.8 PFU/cell. Day 3, 5, 7, or 9 post infection, cells were fixed and stained with BODIPY (lipid specific stain) and DAPI for nuclei, as described in techniques and assays. 10X and 20X images were taken on a Zeiss Axiovert 40 CFL microscope. Four biological replicates per group were quantitated. The 96-well plate was read on Molecular Devices FlexStation, and BODIPY staining was quantitated at 485/538 nm, and DAPI at 405/477 nm. Several unstained wells were quantitated for subtraction of background fluorescence. Data were then expressed as the mean BODIPY:DAPI ratio, as a reflection of lipid per cell.

### 2A.1.3 The Effect of Ad-36 Infection on Lipid Accumulation with Respect to Confluency

3T3-L1 cells were plated at sub confluence on glass bottom 96-well plates, and infected with Ad36 (1 PFU/cell) at confluence, or 1 or 2 days prior to confluence. One set of plates was fixed 9 days post confluence, and another set was fixed 9 days post infection. This allowed for cells to accumulate lipid with a constant number of days post infection or post confluence. After fixation, cells were stained with BODIPY and DAPI as described in techniques and assays, and data were expressed as ratio of BODIPY:DAPI for lipid per cell. Thirty biological replicates per group were used.

#### 2A.1.4 De Novo Lipogenesis Time Course Following Ad36 Infection in 3T3-L1

Seventy percent confluent 3T3-L1 were plated in 24 well plates and Ad36 (3.8 PFU/cell) or Mock infected. An assay to determine DNL was conducted as described in techniques and assays Day 1, 3, and 6 post infection. Six biological replicates per group were used. Lipogenesis was normalized to optical density of a bicinchoninic acid assay (BCA) (Sigma Aldrich # B9643, #C2284) assay to control for protein content of each well. .

#### 2A.1.5 Modulation of Glucose and Palmitate Oxidation in 3T3-L1 by Ad36

Seventy percent confluent 3T3-L1 plated in 24 well plates were Mock or Ad36 infected (3.8 PFU/CELL). Day 1, 3, 6, or 8 post infection, glucose oxidation and palmitate oxidation assay were conducted as described in techniques and assays. Six biological replicates per group were used for each time point, and oxidation was normalized to protein content for each well.

### 2A.2 Effect of Ad36 on Adipose Tissue Morphology

For adipose tissue morphology studies, two separate models were used (190). The first was chow fed C57BL/6J mice, infected with Mock, Ad36 or Ad2 and sacrificed 12 weeks post infection. Retroperitoneal fat pads were harvested for analysis. The second model was C57BL/6J mice on a HFD, then infected with Mock, Ad36 or Ad2, and sacrificed 20 weeks post infection. Epididymal fat pads were harvested for analysis from this model. The chow fed model was infected at 4 weeks of age, whereas the HFD mice were started on the high fat diet at 6 weeks of age and infected 8 weeks later. Adenoviral DNA and RNA was

detected in adipose tissue of mice from both models, indicating the infection was present in these tissues. Details of these animal models are described previously (190).

### 2A.2.1 Change in Adipocyte Cell size in C57BL/6J Mice on Chow and High Fat Diet

Retroperitoneal adipose tissue from chow fed C57BL/6J mice was obtained 12 weeks post infection and fixed in 4% paraformaldehyde immediately after harvesting and stored at 4ºC. Epididymal adipose tissue was obtained from mice on HFD and also fixed in 4% paraformaldehyde immediately after harvesting and stored at 4ºC. Fixed adipose tissue from both chow and HFD mice were paraffin embedded and sliced to 8 µM thickness on slides. For the HFD model, 6 mice from Mock, 5 from Ad36, and 4 from Ad2 group were processed. One slide per mouse with two specimens per slide were made and deparaffinized. Slides were then stained for macrophages as described in techniques and assays, and cells could be easily visualized after this staining. Four pictures per specimen were taken with Zeiss Axioskop 40 and analyzed for cell size (8 pictures per mouse). For the chow model, 6 mice from Mock, 3 from Ad36 and 3 from Ad2 were processed. Three specimens per mouse were placed on one slide, and three pictures per specimen were taken so 9 pictures per mouse). Slides were then fixed and stained for CD31 as described in techniques and assays, and adipocytes could be easily visualized after this staining. Pictures were taken with the Zeiss Axioskop 40. For the analysis, Image J (National Institutes of Health http://rsb.info.nih.gov/ij/download.html) software was used. The pictures were divided into four quadrants, and four cells per quadrant were measured for

adipocyte diameter, quantified by the program in pixels after manually drawing a line across the adipocyte. Adipocyte diameter means and tertiles were then compared as described in the statistics section.

### 2A.2.2 Effect of Ad36 on Macrophage Infiltration in C57BL/6J Mice on Chow and HFD

Slides were created for both chow and HFD mice as described in research design for A.2.1 (same groups, number of animals per group, and number of specimens per slide) and stained for macrophages using Mac-2 antibodies (Lifespan BioSciences, INC # LS-C62936) as described in techniques and assays. After staining, pictures were taken on Zeiss Axioskop 40. Macrophage staining was quantified by using Image J threshold analysis, where the threshold was set so that only positive staining could be seen, and quantified as pixels$^2$ by the software for each picture. For the HFD animals, larger adipose tissue sections were available, therefore 5X pictures were taken. For chow fed animals, smaller sections were available, so 10X pictures were taken for quantification of macrophage staining. Data were analyzed as described in the statistics section.

### 2A.2.3 Effect of Ad36 on Adipose Tissue Vascularization and Angiogenesis

First CD-31 staining was conducted in the chow and HFD C57BL/6J mice as described in techniques and assays. Slides were processed as described in the research design for A.2.1 (same groups, number of animals per group, and number of specimens per slide). Pictures were taken after staining on Zeiss Axioskop 40. CD-31 staining was quantified by using Image J threshold analysis, where the threshold was set so that only positive staining could be seen, and

quantified as pixels$^2$ by the software for each picture. Data were analyzed as described in the statistics section.

Next, an angiogenesis assay was conducted with human adipose tissue explants from three donors as described in techniques and assays and as previously described(245). Tissue was infected with Mock, Ad36, or Ad-2 (2 million viral particles per well), and galic acid treatment was used as a negative control. 30 replicates per group were used, and angiogenesis was scored every 2-4 days post infection for 15 days. Data were expressed as mean angiogenic index score for each group and each time point. The assay was repeated three times with tissue from three donors.

And lastly, a tube formation assay was conducted with SVEC4-10 murine endothelial cells as described in techniques and assays. Cells were infected with Mock, Ad36, or Ad2 (3.8 PFU/cell). The acute effect of infection was observed 5 hours post infection, and a 24 and 75 hr time point was also observed to test for a more long-term effect. For each time point, pictures were taken on Zeiss Axioskop 40, and three biological replicates per group were used.

## 2B. Effect of Ad36 on Hepatic Steatosis

### 2B.1 Effect of Ad36 on liver steatosis and glycogen stores in C57BL/6J mice on HFD

Livers from C57BL/6J mice on HFD were harvested 20 weeks post infection as described elsewhere (190) and immediately flash frozen in liquid nitrogen, and stored at -80ºC until processing. Adenoviral DNA and RNA was detected in these livers, which indicates successful infection of these tissues *in vivo*. Samples were thawed and soaked in 30% sucrose for 1 week at 4ºC. Samples were then

embedded in O.C.T. Compound freezing medium (TissueTek # 62550) cryomolds and cryosectioned at 8 µM thickness on positively charged slides. Slides were stained for glycogen as described in techniques and assays. Image J threshold analysis was used to quantitate lipid, and total picture area minus glycogen staining was considered an approximation of lipid, since lipid leaves the sample during the glycogen staining process, as described elsewhere(246).

**Statistics**

All cell based metabolism and lipid accumulation assays were completed with a minimum of three replicates, and a student's t-test was used to compare means. The comparison of interest was Ad36 compared to Mock, to determine if Ad36 changed parameters compared to the Mock condition. We expected Ad2 to not be significantly different from Mock, and a comparison between Ad36 and Ad2 was not of interest. One tailed tests were used for lipid accumulation and DNL experiments with hASC and 3T3-L1, since we hypothesized that Ad36 would increase lipid accumulation based on previous findings (247). For glucose and palmitate oxidation studies, a two tailed t-test was performed since no specific direction was expected for either parameter following Ad36 infection. All assays were adjusted to cell number either by DAPI staining or by estimating protein content of individual wells.

For immunohistochemistry studies of adipose tissue or liver from HFD or chow fed mice, at least three mice per group were analyzed, with 8-9 pictures taken per mouse for analysis. Student's t-test was first used to compare between groups. For adipocyte size analysis, tertiles were also calculated based on the range of cell

sizes of all groups pooled together. For each group, the percentage of cells falling in the upper and lower tertile was then calculated. A paired t-test was used to determine if within a group, more cells fell within the lower or upper tertile. A one-sided t-test was conducted for macrophage staining, with the hypothesis that infection would increase macrophage infiltration. CD-31 t-test was two sided, with no specific hypothesis. Liver glycogen and lipid content t-tests were also two sided.

### 2.1.3 Objective 3: Determine if the E4orf1 Protein of Ad36 Enhances Glucose Disposal in Adipose Tissue and Liver, and if it Alters Lipid Metabolism in Liver for Lower Lipid Stores

#### 3A. Effect of E4orf1 in Adipocytes

##### 3A.1 Is E4orf1 Necessary for Ad36 Induced Glucose Uptake?

3T3-L1 preadipocytes were plated in 12-well plates at 60% confluence and transfected with either E4orf1 siRNA (Ambion #AM16100) or non-targeting(NT) siRNA(Thermo Scientific, #D-001810-02-05) as described in techniques and assays,, then immediately after transfection the cells were infected with Ad36 (5 PFU per cell) or mock infected. The resulting groups were tested: Mock with E4orf1 siRNA, Ad36 with NT siRNA, and Ad36 with E4orf1 siRNA. Mock-infected cells with E4orf1 siRNA served as a baseline control, and Ad36 infected cells with either NT siRNA, or E4orf1 siRNA were the two experimental groups. Two days post transfection/infection, basal 2-Deoxy-D-glucose (2DG) uptake was determined as described in techniques and assays. Eight biological replicates were assayed per group. Glucose uptake was normalized to protein content, which was measured via BCA assay. This experiment was repeated three times and data are presented as fold

change relative to Mock with E4orf1 siRNA. RNA was harvested in parallel, and knockdown was verified by detection of E4orf1 mRNA levels using quantitative real time PCR as described in techniques and assays.

**3A.2 Is E4orf1 Sufficient to Increase Glucose Uptake?**

3T3-L1 preadipocytes and adipocytes were transfected with V5 tagged E4orf1 expressing pcDNA or Null pcDNA plasmids as described in techniques and assays. Two days post transfection, 2DG uptake assay was conducted under basal and insulin stimulated (100 nM) conditions as described in techniques and assays. Eight biological replicates per group were assayed, and glucose uptake was normalized to protein content. Glucose uptake assay was repeated twice for adipocytes, and once for preadipocytes in this system.

Next, to determine the dose response effect of E4orf1 on glucose uptake, Ad36 E4orf1 (E4pTRE) and empty vector (pTRE) control inducible stable 3T3-L1 cell lines were created using the TetON Advanced system (Clonetech# #630930) as described in techniques and assays. 24 hours post induction with 0, 750, or 1,000 ng/mLDoxycycline (Clonetech #631311) for different expression levels of E4orf1, a 2DG glucose uptake assay was conducted as described in techniques and assays. Eight replicates per group were used. pTRE was treated with 100 nM insulin as a positive control for the assay, and this cell line was also treated with 1,000 ng/mLDoxycycline (n=2) to ensure the induction media did not affect glucose uptake.

**3A.3 The Effect of E4orf1 on DNL in 3T3-L1 Preadipocytes**

Sixty percent confluent 3T3-L1 were plated in 12-well plates and with V5-E4orf1 and Null plasmids as described in techniques and assays. Two days post transfection, a DNL assay was conducted with and without 100 nM insulin as described in techniques and assays. Conversion of [14C]-Glucose to fatty acid was determined and normalized to protein content. Eight biological replicates per group were used.

### 3A.4 Cell Signaling Involved in E4orf1 Induced Glucose Uptake in 3T3-L1

#### 3A.4.1 Total and Isoform-specific Ras Activation by E4orf1

For determination of isoform-specific activation of Ras, the E4pTRE and pTRE cell lines were exposed to 1,000 ng/mLDoxycycline for 24 hours, and the activation was detected via a pull down assay for the Ras binding domain (RBD) of Raf as described in techniques and assays. Before pull down, 6% of the whole cell lysate was collected and loaded to SDS-PAGE to determine total Ras abundance. Activation was detected by Western Blot (WB) with isoform specific antibodies against H-Ras, N-Ras, K-Ras or total Ras (all isoforms) as described in techniques and assays. Using NIH Image J, total Ras abundance was normalized to β-actin expression, and the ratio of activated to normalized total Ras is expressed in the figures. The same densitometry approach was also used for isoform specific WB.

#### 3A.4.2 The Effect of Ad36 and E4orf1 on Cell Transformation

3T3-L1, A549 and 3T3-L1 E4orf1 constitutively expressing cell line were plated in 60 mm dishes for the soft agar assay as described in techniques and assays. Constitutive cells were created as described elsewhere (203). Cells were fixed at day 7, 14, and 21 for determination of colony formation. Four 10X images, one

per plate quadrant, were counted for viable cells and colonies. The percent of viable cells that formed colonies was calculated.

### 3A.4.3 The Effect of E4orf1 on Distal Insulin Signaling, Adiponectin, and Glut1

The E4pTRE and pTRE cell lines were treated with 1,000 ng/mLDoxycycline and harvested 24 hours later for WB. Total and phosphorylated AKT (as an indicator of PI3K activation), and Glut4, Glut1, and adiponectin abundance were determined by WB as described in techniques and assays. Proteins were normalized to β-actin expression, and Image J was used for densitometry calculations. Activated AKT was calculated as the ratio of p-AKT (ser308) to total AKT. Three biological replicates per group were used for WB.

### 3A.4.4 The Effect of E4orf1 on Adiponectin and Inflammatory Cytokine mRNA Expression

The E4pTRE and pTRE cell lines were exposed to 1,000 ng/mLDoxycycline and harvested 24 hours later for RNA. The expression of adiponectin, Monocyte chemotactic protein-1, (MCP-1), Macrophage colony stimulating factor (MCSF), Tumor necrosis factor alpha (TNF-α), Interferon-gamma (INF-γ), Interleukin-10 (IL-10), and Toll-like receptor-4 (TLR-4) was measured via quantitative real-time PCR as described in techniques and assays. Eight biological replicates per group were used.

## 3A.5 Can E4orf1 Induce Glucose Uptake Independent of PPARγ?

PPARγ knock-out Mouse embryonic fibroblasts (MEF) were obtained from Bruce Spiegelman (248) and plated for 80% confluence and transfected with V5-E4orf1 or Null plasmids using Lipofectamine 2000 (Invitrogen # 11668-019) as described in

techniques and assays. Twenty four hours post transfection, a 2DG uptake assay was conducted as described in techniques and assays. Eight replicates per group were used.

## 3B. The Effect of E4orf1 on Hepatic Glucose and Lipid Metabolism

### 3B.1 The Effect of E4orf1 on Glucose Output in Hepatocytes

HepG2 cells were transfected with V5-Ad36 E4orf1, V5-Ad2 E4orf1 or Null plasmids via electroporation as described in techniques and assays. Two days post transfection, cells were serum starved for 4 hours, washed with phosphate buffered saline (PBS) and treated with serum free, glucose free media (Invitrogen, #11966) with or without 10 nM insulin for 3 hours. Glucose content in the media was determined using a glucose oxidase assay as described in techniques and assays, and BCA assay was conducted for each well to normalize glucose output to mg protein per well. This experiment was repeated twice, with six biological replicates per group, so data of both experiments are represented as fold change relative to Null.

Next, HepG2 were again transfected with V5-Ad36 E4orf1 or Null plasmids, and treated for glucose output 2 days post transfection. Cells were serum starved for 4 hours, then washed with PBS and treated with cAMP (1 mM) and Dexamethasone (500 nM) as gluconeogenic stimulators, with or without 10 nM insulin for 3 hours. At that point a glucose oxidase assay was used to determine glucose content in the media, and glucose output was again normalized to protein content. Eight biological replicates were tested per group.

Lastly, primary hepatocytes from C57BL/6J, 129Sv, and FVB mixed background(249) were transfected with V5-Ad36 E4orf1, V5-Ad2 E4orf1, or Null

plasmids as described in techniques and assays, and a glucose output assay was conducted 2 days post transfection. In this experiment, the serum free, glucose free condition with and without 100 nM insulin was tested. A preliminary experiment with 8 replicates was conducted to standardize transfection and assay conditions, followed by another experiment where 24 replicates per group were tested.

## 3B.2 The Effect of E4orf1 on Hepatic Lipid Accumulation

### 3B.2.1 The Effect of E4orf1 on Hepatic Fatty Acid Oxidation

A series of two experiments was used to determine the effect of E4orf1 on fatty acid oxidation. First, HepG2 cells were transfected with V5-Ad36 E4orf1, V5-Ad2 E4orf1, or Null plasmids with PolyJet (SignaGen #SL100688) as described in techniques and assays. Two days post transfection, a palmitate oxidation assay was conducted as described in techniques and assays. Eight biological replicates per group were tested, and total and complete palmitate oxidation was normalized to protein content.

Next, HepG2 cells were transfected with V5-Ad36 E4orf1, V5-Ad2 E4orf1, or Null plasmids and another palmitate oxidation assay was conducted to verify the changes in the ratio of complete to partial fatty acid oxidation via E4orf1 observed in the first experiment. The assay was conducted 2 days post transfection, and again included eight biological replicates. The ratio of partial to complete oxidation, and the percent partial oxidation was calculated as fold change relative to Null of data from the first and second experiments.

### 3B.2.2 The Effect of E4orf1 on Hepatic DNL

HepG2 cells were transfected with V5-Ad36 E4orf1, V5-Ad2 E4orf1, and Null plasmids with PolyJet as described in techniques and assays. Two days post transfection, a DNL assay was conducted as described in techniques and assays. This experiment was replicated twice, each time with eight biological replicates per group, and results are expressed as fold change relative to Null.

### 3B.2.3 The Effect of E4orf1 on Hepatic ApoB Secretion

HepG2 cells were transfected with V5-Ad36 E4orf1, V5-Ad2 E4orf1, or Null plasmids with PolyJet as described in techniques and assays. Twenty four hours post transfection, cells were switched to Dulbecco's minimum essential media (DMEM) without phenol red (Invitrogen # 31053-036) plus 1.5% Bovine Serum Albumin (BSA) for the next 24 hours. The media samples were then collected and stored at -20ºC. ApoB secretion was determined via ELISA (Alerchek # A70102) according to manufacturer's instructions, and 1:50 dilution of media was used instead of the suggested 1:1000 dilution based on results from a preliminary experiment where several dilutions were tested. Protein was measured via BCA, and ApoB secretion was normalized to protein content. Eight biological replicates per group were tested.

### Statistics

All metabolic assays were conducted with at least 8 biological replicates, and student's t-test was used to determine significant differences with Bonferroni correction when more than one comparison was tested. E4orf1 siRNA experiment was repeated three times, adipocyte glucose uptake following transfection was repeated twice, HepG2 glucose output, fat oxidation, and denovo

lipogenesis assays were repeated twice. All metabolic assays were normalized to protein content. For the ApoB ELISA, two technical replicates were used for each sample.

For WB, three biological replicates were tested for each group. Student's t-test was used to determine significant differences between groups. All proteins were normalized to housekeeping protein. For Ras activation, assays were loaded to SDS-PAGE by volume, so total Ras was normalized to protein, and activation was expressed as the ratio of activated to total normalized expression. AKT is expressed as the ratio of phosphorylated to total AKT.

Quantitative real-time PCR experiments were determined for eight biological replicates per group. Student's t-test was used to test for significant differences between groups. Each gene was normalized to a housekeeping gene, and each sample was tested with two technical replicates.

## 2.2 Techniques and Assays

### 2.2.1 Cell Culture

3T3-L1 cells were obtained from American Type Culture Collection (ATCC #CCL-92-1, Manassas, VA) and maintained in high glucose Dulbecco's Modified Eagle Medium (DMEM) (Invitrogen, #11995), 10% normal calf serum (#SH30072.03, Hyclone) and an antibiotic-antimyotic agent (1%) (Sigma Aldrich #A5955). E4pTRE and pTRE clones were maintained in Tet-free fetal bovine serum (Clonetech, #631101) with 0.25 μg/mL puromycin and 0.05 μg/mL hygromycin (Invitrogen, #10687-010).

For adipogenic differentiation, two days post confluence, 3T3-L1 preadipocytes plated in 10cm dishes were induced to differentiate by adding DMEM containing 10% FBS (#SH30071.03, Lot: ASL30786, Hyclone), 20 ng/mL insulin, 115 ng/mL isobutylmethylxanthine, and 0.39 ng/mL dexamethasone. Forty-eight hours after the induction, cells were switched to maintenance media of DMEM containing 10% FBS, and 5 ng/mL insulin.

HepG2 cells were obtained from Dr. Jianping Ye at the Pennington Biomedical Research Center, LA. They were maintained in high glucose DMEM, 10% fetal calf serum, and an antibiotic-antimyotic agent (1%).

Primary mouse hepatocytes were obtained from Dr. Charlie Dong, Harvard University, Boston, MA. They were maintained in William's Medium E (Invitrogen # 12551-032) supplemented with 2 mM glutamate, 10% FBS, and primocin (Invivogen # ant-pm-1).

### 2.2.2 Viral Infection

Ad36 was obtained from American Type Culture Collection (ATCC # VR-913) and propagated in A549 cells after plaque purifying three times as described (192; 193). Ad2 was also obtained from American Type Culture Collection (ATCC#). Viral titers were determined by plaque assay and cell inoculations were expressed as plaque forming units (PFU) per cell (192; 193). Cells were generally infected at 70% confluence unless stated otherwise. The necessary amount of stock virus for a given viral dose (PFU/cell) was added to serum free DMEM, and the viral media incubated for 1 hr with cells. Cells were replenished with fresh media after the one hr incubation.

### 2.2.3 Ad36 Hexon and DAPI Staining of hASC

Cells were washed with PBS and then fixed for 20 minutes with 4% paraformaldehyde. After fixation, cells were permeabilized in 0.1% Triton PBS for 10 minutes, , blocked in 10% goat serum in 1% BSA for one hr , and then incubated with a rabbit antibody for Ad36 hexon protein overnight at 4º C. After washing in PBS 3X for 10 minutes, they were then incubated with a secondary Alexaflour goat antirabbit IgG (red) (Invitrogen # A-21245) for 1 hour. Cells were then washed 3X with PBS for 10 minutes each. DAPI (Invitrogen # D3571) was diluted 1:1000 in PBS and incubated with cells for 20 minutes at room temperature. Cells were washed 1X in PBS after DAPI staining, and images were captured.

### 2.2.4 BODIPY Staining of hASC

Cells were washed with PBS and then fixed with 4% paraformaldehyde (USB Corporation, #19943) for 20 minutes. BODIPY 493/503 (Invitrogen #D3922) was diluted to 10 ug/mL in PBS and incubated with cells after fixation for 20 minutes. Cells were then washed 1X with PBS for 10 min, and incubated with DAPI diluted 1:1000 in PBS for 10 min. Cells were then washed 2X in PBS before images were captured.

### 2.2.5 Glucose Oxidation Assay

Cells were serum starved for 1 hr in glucose free DMEM (Invitrogen #, 11966025) then incubated with 500 µL high glucose DMEM (Invitrogen # 11995081) with 1 µCi/mL [14C]-Glucose (PerkinElmer #NEC042A001MC) for 3 hours. During the incubation, plates were wrapped in parafilm to minimize $CO_2$ loss. After incubation, 400 µL of media was transferred to a well of a $CO_2$ trapper (custom made as described (250)), adjacent to 200 µL of 1 M NaOH. When all samples were loaded,

the trapper was sealed, and 40 µL of 70% perchloric acid (Sigma Aldrich # 311421) was injected into the media. After rotating the $CO_2$ trapper for 1 hour, 200 µL of NaOH containing [14C]-$CO_2$ was removed and placed in a scintillation vial with 5 mL scintillation fluid. The samples were read after 15 minutes on a Beckman scintillation counter (LS 6500). After media was harvested, cells were solubilized in 0.05% sodium dodecyl sulfate (SDS) and protein content was measured via BCA. All BCA assays were read at 595 nM on a Biorad Benchmark Plus microplate spectrophotometer. For calculations, a blank vial for background subtraction and the original media with isotope was read, and the total activity was used to calculate nmol glucose oxidized in 3 hr per mg of protein.

### 2.2.6 Palmitate Oxidation Assay

Cells were incubated with 500 µL high glucose DMEM (Invitrogen # 11995081) with 1 µCi/mL [14C]-Palmitate (PerkinElmer # NET043001MC), 100 µM palmitate (Sigma Aldrich, #P9767-10G), 0.25% Bovine serum albumin (Sigma Aldrich # A7030), 1 mM carnitine (Sigma Aldrich #C0158), 12.5 mM HEPES buffer for 3 hours. During the incubation, plates were wrapped in parafilm to minimize $CO_2$ loss. After incubation, 400 µL of media was transferred to a well of a $CO_2$ trapper, adjacent to 200 µL of 1 M NaOH. When all samples were loaded, the trapper was sealed, and 40 µL of 70% perchloric acid (Sigma Aldrich # 311421) was injected into the media. After rotating the $CO_2$ trapper for 1 hour, 200 µL of NaOH containing [14C]-$CO_2$ was removed and placed in a scintillation vial with 5 mL scintillation fluid. After media was harvested, cells were solubilized in 0.05% sodium dodecyl sulfate SDS and protein content was measured via BCA. The acidic media was collected in eppendorf tubes and stored at 4ºC over night, and spun down at 15,000 g for 10 min at 4ºC

(Eppendorf centrifuge 5417R). Two hundred µL of the supernatant was collected and placed in a scintillation vial detection of acid-soluble metabolites. The samples were read after 15 minutes on a Beckman scintillation counter. For calculations, a blank vial for background subtraction and the original media with isotope was read, and the total activity was used to calculate nmol palmitate oxidized in 3 hr per mg of protein.

### 2.2.7 De Novo Lipogenesis

Cells were treated with the same [14C]-palmitate media used in for the palmitate oxidation assay (as described in "E") for 3 hours. After the three hours treatment, media was aspirated and cells washed in cold PBS. Two hundred µL of 0.05% SDS was then used to solubilize cells, and the cell lysates were collected in 2 mL eppendorf tubes. Samples were spun down for 5 min at 4ºC, at 15,000 g. Twenty µL of sample was collected at this time for BCA protein determination. After resuspending the pellet, 1 mL of chloroform:methanol (2:1) was added to each sample. The samples were then rocked for 15 minutes at room temperature, and then 0.5 mL of $ddH_2O$ was added. The samples were then again rocked for 15 minutes, and tubes were spun for 10 min at 4ºC, at 3,000 rpm. The upper phase was discarded, and the lower organic phase was collected in scintiallation vials for reading on the Beckman scintiallation counter. Calculations were normalized to protein content.

### 2.2.8 Macrophage Immunohistochemistry

Slides were deparaffinized with two 15 minutes changes in xylene, and two 15 minutes changes in 100% ethanol. They were then placed in Methanol containing 2% $H_2O_2$ by volume for 30 minutes. Next, they were rehydrated with a series of 5 minutes changes in 95%, 70%, and 50% ethanol. Before blocking, slides were washed 3X in PBS. Blocking with 1%BSA, 5% normal horse serum at room temperature for 1

hr was followed by overnight incubation with 1:3,000 dilution of primary Mac-2 antibody (Lifespan BioSciences, INC # LS-C62936) in 1%BSA at 4ºC. The next day, slides were washed 3X in PBS and incubated with 1:222 dilution of anti-mouse secondary (Vecastain ABC kit, Vector Laboratories #PK-4004) in 1% BSA for 1 hr at room temperature. After washing 3X with PBS, the ABC solution (Vecastain ABC kit) was added to slides for 30 min. Slides were then washed 3X in PBS and diaminobensidine solution plus 1.6 μL $H_2O_2$ was added per mL was used to develop the slides for 2 min. Slides were washed 3X with PBS, then with tap water 2X, and then dehydrated in a series of alcohol (50%, 70%, 95%, and 100%) before mounting with Citifluor (Ted Pella, Inc., #19472) and coverslipping.

### 2.2.9 CD-31 Immunohistochemistry

Slides were stained with a CD31 staining kit (Biocare Medical # RT 517 SK) according to the manufacturer's protocol. The CD31primary antibody (BD Biosciences, #550274) was used at 1:50 dilution.

### 2.2.10 Adipose Tissue Explant Angiogenesis Assay

The angiogenesis assay was conducted as previously described (245). Briefly, explants were embedded in a thrombin media and infected with Ad36 or Ad2 the following day with 2 million PFU/well or Mock infected. A blinded observer scored the explants every 3-5 days for angiogenic growth as described.

### 2.2.11 Tube Formation Assay

Assay was conducted as described previously (102). Briefly, 40,000 cells per well SVEC4-10 were plated in 96 well plates coated with basement membrane extract (BD Biosciences, #354230), and tube formation was observed 5 hours post plating and images were captured. For an acute effect of infection, Ad36 or Ad2 were added

directly as cells were plated. For Day 1 and Day 3 post infection time points, SVEC4-10 were infected on 10 cm plates, and trypsinized and plated for tube formation either Day 1 or Day 3 post infection. A viral dose of 5 PFU/cell was used for all time points, with 5 replicates per group.

### 2.2.12 Glycogen Staining

Slides of liver sections were fixed with Carnoy's fixative for 15 minutes (6 parts ethanol, 3 parts chloroform, and 1 part glacial acetic acid), then washed in distilled water for several minutes. Periodic acid solution (1%) (Sigma 395132-1L) was then added for 5 minutes before adding Schiff's reagent for 8 minutes (Sigma 3952016-500ml). Samples were then washed in running tap water for 10 minutes, and dehydrated in a series of increasing concentrations of alcohol (50, 70, 85, and 100% ethanol). The slides were then air dried and mounted with Permount (Fisher Scientific # SP15) and coverslipped.

### 2.2.13 [3H]-2-Deoxyglucose Uptake Assay

Cells in 12 well plates were serum starved for 2 hours, and then washed 2X with PBS before adding 450 µL KRP (136 mM NaCl, 4.7 mM KCl, 10 mM $NaPO_4$, 0.9 mM $CaCl_2$, 0.9 mM $MgSO_4$) with or without 100 nM insulin (Sigma Aldrich, #15500), depending on the experiment, for 15 minutes. Two to three wells were treated with KRP plus 100 nM cytochalasin (Sigma Aldrich, #C6762) for subtraction of nonspecific glucose uptake. Fifty µL of 10X isotope solution was then added to each well for a final concentration of 100 nM cold 2-deoxy glucose and 0.5 µCi/mL [3H]-2-Deoxyglucose (PerkinElmer #NEC720A250UC) for 5 minutes. Immediately after the 5 minute incubation, cells were washed in ice-cold PBS. 500 µL of 0.05% SDS was then added to each well, and after incubation of cells for 30 min at 37ºC, 450 µL of

lysate was added to a scintiallation vial and the remaining 50 µL was used for protein determination via BCA assay. Samples were read on a Beckman scintillation counter the following day.

### 2.2.14 E4orf1 siRNA Transfection

3T3-L1 preadipocytes were plated into 12-well plates (80,000 cells/well) and transfected the next day with Lipofectamine (Invitrogen #18324-012). A ratio of 2 µL Lipofectamine and 100 pmol Ad36 E4orf1 siRNA or NT siRNA was used for transfection, which produced 60% knockdown of E4orf1 expression as determined by quantitative real-time PCR. Knockdown was confirmed two days post transfection by harvesting RNA and detecting E4orf1 mRNA via quantitative real time PCR. The following E4or1 siRNA sequence was custom designed by Ambion (#AM16100) :

Sense siRNA Strand (5'→3'): GAGAGUGAUUUUUCCUUCATT

Antisense siRNA Strand (5'→3'): UGAAGGAAAAAUCACUCUCTC

### 2.2.15 Quantitative Real-time PCR for Detection of E4orf1

E4orf1 was detected using quantitative real time PCR. RNA was harvested and isolated using a RNA Mini Easy Kit (Qiagen, #74104), and cDNA was synthesized via RT PCR (Applied Biosystems # 4368814) according to manufacturer's instructions. An Ad36 E4orf1 FAM nonflourescent primer-probe was custom designed and synthesized (Integrated DNA Technologies). The E4orf1 primer probe is as follows:

Probe 5'-/56-FAM/TGC TGC TCT /ZEN/TTA ACC ACA CGG ACC G/3IABkFQ/-3'

Primer 1 5'-CCC TCG CGG ACATAC AAA A-3'

Primer 2 5'-GCC GGG AGA AGA CAT GAT CTC-3'

100 ng of cDNA was loaded per well in duplicate for detection of E4orf1. GAPDH primer probe was used as a housekeeping gene (Applied Biosystems, assay ID#

Mm99999915_g1), and 2 ng per well was loaded in duplicate for each sample. Taqman Universal PCR Mix was used for both genes according to manufacturer's instructions (Applied Biosystems #4304437). Expression was detected with the Applied Biosystems 7900 Sequence Detection System and the $\Delta\Delta^{Ct}$ method.

**2.2.16 Plasmid Preparation and Transfection**

The plasmid pcDNA-V5-E4orf1 was cloned using Invitrogen GateWay system that included two steps. 1) Direct TOPO cloning of Ad36 E4ORF1 cDNA and Ad2 E4ORF1 into pENTR-D TOPO vector (Invitrogen #K2400-20) according to manufacturers manuals. 2) pENTR-E4ORF1 vectors from first step was used for recombination with pcDNA-V5 vector (Invitrogen #12489-019) using LR Clonase enzyme (Invitrogen # 11791-019) to obtain pcDNA-V5-E4orf1 which was used for cell transfection.

3T3-L1 preadipocytes were transfected with Lipofectamine. Cells were plated into 12 well plates (80,000 cells/well), and transfected the next day with a 3:1 ratio of Lipofectamine to plasmid DNA according to the manufacturer's instructions. Transfection was verified via protein harvest and WB for the detection of V5-tagged E4orf1 using V5 antibodies.

3T3-L1 adipocytes were transfected on day 6 post adipogenic induction. After trypsinizing with 0.25% trypsin, cells were counted and transfected by electroporation with AMAXA kit nucleofection solution L (Lonza, #VCA-1005) according to the manufacturer's protocol except that each cuvette contained 2.5 million cells and was plated to two wells of a 12 well plate. The AMAXA Nucleofector II Device was used for electroporation. The next day after the cells had settled on the plate, media was gently

removed and replaced with fresh media to remove any remaining transfection solution and the cells that did not survive transfection. Transfection was verified via protein harvest and WB for the detection of V5- tagged E4orf1 with V5 antibodies.

### 2.2.17 Generation of Ad-36 E4orf-1 Stable Inducible 3T3-L1 Cell Lines

#### 2.2.17a Outline

1. Transfection standardization of 3T3-L1 with Lipofectamine and TetON plasmid.
2. Puromycin kill curve to determine selection concentration
3. pTetON transfection and stable selection
    a. pTetON transfection
    b. Selection process
4. Screening of TetON Clones
    a. pTIGHT-Luc transfection and Luciferase assay standardization
    b. Screening of clones
5. pTRE TIGHT and pTRE TIGHT-E4orf1 selection and screening
    a. pTRE TIGHT and pTRE TIGHT E4orf1 transfection selection
    b. E4orf1 clone screening.
6. E4 clone characterization

#### 2.2.17b Detailed Procedure

Clontech's TetON Advanced system (Clonetech, #630930) was used to create an inducible 3T3-L1 Ad36 E4orf-1 expressing cell line. This system was chosen for tightly controlled, robust expression of E4orf1. 3T3-L1 were first transfected with the pTet-On Advanced vector and selected for stable transfectants using Lipofectamine. This vector contains a tetracycline responsive transcriptional transactivator, which in

the presence of Doxycycline, binds to a pTIGHT inducible promoter and activates transcription of a downstream gene of interest. After selecting for the best pTet-On clone by luciferase assay following transient transfection with pTRE-TIGHT-Luc, that clone was expanded and transfected with either pTRE-TIGHT (empty vector control) or pTRE-E4orf1-TIGHT. Stable transfectants were then selected, expanded, and screened for E4orf1 expression by quantitative real-time PCR. Each step is described in detail below.

1. **Transfection Standardization**

   3T3-L1 were plated in 12-well plates for 50, 70 and 80 percent confluence and transfected the next day with pMAX-GFP (green fluorescent protein) (Lonza) at 3:1, 6:1 and 6:2 ratio of μL Lipofectamine: mg plasmid DNA per well according to manufacturer's instructions. Cells were fixed for 15 minutes with 10% formalin at 48 hours post transfection and stained with DAPI for nuclei staining for a total cell count. Three 10X pictures were taken with the Zeiss Axioskop 40 per condition, and percent of cells expressing GFP was calculated. The 3:1 ratio at 50% confluence was selected as the best condition, with 86% transfection efficiency.

2. **Puromycin and Hygromycin Kill Curve**

   To determine the dose for selection of transfected 3T3-L1, a dose and duration experiment was conducted. 3T3-L1 were plated for 50% confluence and treated the next day with 0.25, 0.5, 1, 2, 3, 5 or 10 μg/mL of puromycin (Clonetech # 631306). For hygromycin, doses of 0.01, 0.05, 0.15, 0.2, and 0.5 μg/mL were chosen. Every three days, a set of cells for each dose was

trypsinized, viable cells were counted with a hemocytometer after staining with trypan blue, and fresh media was replaced on the remaining time points. Based on the resulting kill curves, 1 μg/mL was chosen as an optimal dose for puromycin selection, and 0.1 μg/mL was chosen as an optimal dose for hygromycin selection.

**3. pTetOn Advanced Transfection and Stable Selection**

a. 3T3-L1 were plated in 12 well plates at 50% confluency and transfected the following day with 3:1, 6:2, or 12:4 ratio of μL Lipofectamine to μg plasmid DNA, and each condition was also co-transfected with a linear puromycin marker (Clonetech #ST0207) (with 1:20 marker to plasmid DNA ratio). 48 hours post transfection, cells were observed with Zeiss Axioskop 40 for transfection efficiency, since the pTetOn plasmid expresses GFP. The 3:1 condition of pTetOn Advanced showed approximately 20% efficiency, 6:2 showed 40% efficiency, and 12:4 showed 80% efficiency. Cells were stressed, however, with increasing amount of Lipofectamine. After verifying successful transfection, cells were trypsinized and each well was replated in a 10 cm dish so that cells would spread out to single cells for the development of colonies after selection.

b. Doses of 1 μg/ml, 2 μg/mL, and 3 μg/mL of puromycin were used for selection. Two methods were applied for selection: either the selection dose was applied immediately after transfer to the 10 cm plates ("immediate dosing"), or it was applied gradually ("gradual dosing") with

0.25X at 2 days, 0.5X at 4 days, 0.75X at 6 days, and 1X at 8 days post transfer to the 10 cm plate. The 3:1 condition stopped expressing GFP after transfer to the 10 cm plate, and all plates of this condition were discarded. The 6:2 condition and 12:4 condition continued to express GFP well. Immediately treating the plates with 2 ug/mL and 3 ug/mL puromycin resulted in cell death, and these plates were discarded. The 1 μg/mL "gradual" and 1 μg/mL "immediate" plates, and the 2 μg/mL "gradual" plates survived well and after selection grew colonies.

After 15 days post transfer to 10 cm plates, isolated clones were selected visually, and marked with a permanent marker using an inverted microscope. Each clone was scraped manually using a de-tipped 200 μL pipette tip and placed in a 96-well plate. Then, as each clone grew to confluence, it was trypsinized and expanded to a 48-well, 24-well, 12-well, 6-well and finally a 10 cm plate. At the 10 cm stage, each clone was frozen down in 80% Tetracycline free fetal bovine serum (FBS) (Clonetech, #631101) 10% DMEM, and 10% dimethyl sulfoxide freezing media so that all clones could be screened together, since all clones were growing at different rates. A total of 22 clones were selected and expanded for screening.

**4. TetOn Advanced Clone Screening**

a. The first three clones (named 3a, 1b, and 1c) isolated were used to standardize the luciferase assay for screening clones. All clones were plated for 50% confluence in 12 well plates and transfected the next day

with a 6:2 ratio of Lipofectamine to pTre TIGHT-Luc plasmid DNA. 48 hours post transfection, cells were treated with 0, 0.1, 1, 10, 100, or 1,000ng/mL of Doxycycline. In addition, to test if the Hyclone FBS contains Tetracycline, which can cause high background induction in this system, Tetracycline free FBS from Clonetech was used as another condition with 0 and 1,000 ng/mL Doxycycline. Twenty four hours post treatment, the luciferase assay (Promega #1531) was carried out. Cells were washed with cold PBS, and cells were lysed using 70 μL per well of the lysis buffer. After vortexing, samples were spun down at 12,000 g for two minutes and the supernatant was transferred to a new 1.5 mL Eppendorf. Twenty μL of the sample was loaded in duplicate into a 96 well plate. After addition of the Luciferase assay buffer, the plate was read using a Luminescense plate reader (Berthold Technologies, MicroLumat Plus). Normal FBS showed no dose response or clear indication of luciferase activity, however, clone 3a showed a 3-fold induction of luciferase activity with Tet-free FBS with 1,000 ng/mL Doxycycline compared to 0 ng/mL Doxycycline. This indicated the FBS may have some tetracycline contamination, which can induce a similar effect to Doxycycline treatment in this system. Therefore, from then on, all clones were maintained in Tet-free FBS.

To determine the best time point post Doxycycline treatment and to determine the effect of a wider range of Doxycycline treatments for screening the clones, clone 3a was then plated and again transfected with

pTre TIGHT-Luc, and treated with 0, 100, 1,000, or 10,000 ng/mL Doxycycline in duplicate two days post transfection. The luciferase assay was then conducted as described above at 1 hr, 6 hr, 12, hr, 24, and 48 hours, and an untransfected group was added in order to subtract luciferase assay background (Figure 1). The resulting data is displayed in the figure below, and 12 hours was selected as the best time point with 1,000 ng/mL Doxycycline as the optimal dose for screening. This time point demonstrated the clearest dose response, and 1,000 ng/mL dose had the highest luciferase expression.

b. Next, all clones were screened by first transfecting with pTre TIGHT-Luc, treating each clone in duplicate 48 hours post transfection with either 0 or 1,000 ng/mL Doxycycline, and conducting a luciferase assay 16

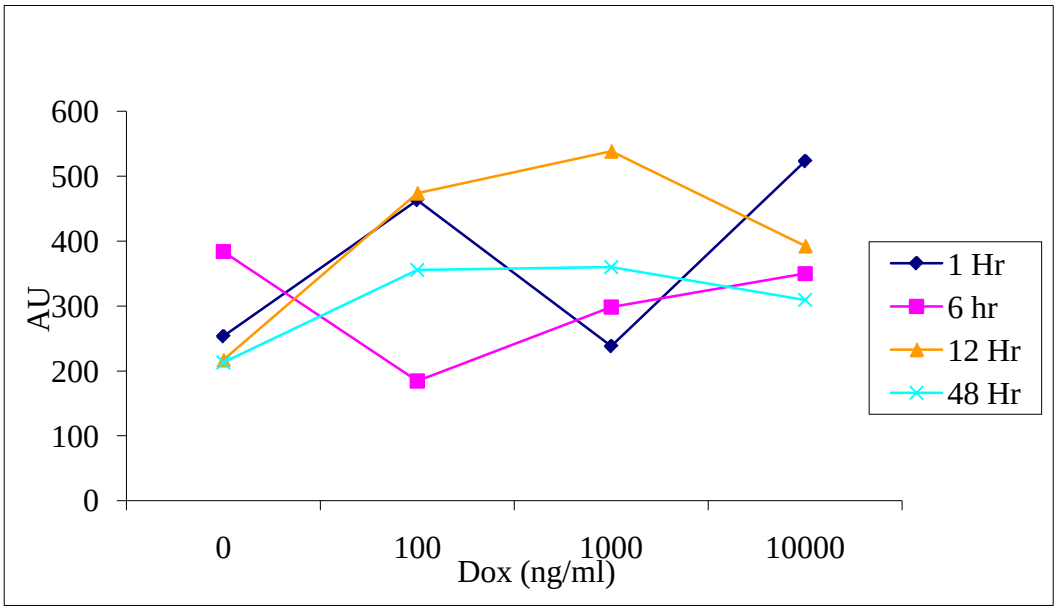


**Figure 1. Luciferase Assay Standardization.** 3T3 TetON Clone 3a was treated with several doses of Doxycycline for 1, 6, 12, and 48 hours, and a luciferase assay was conducted to determine the optimal dose and time point for screening all clones.

hours post Doxycycline treatment. The 22 TetOn Advanced clones were screened in two batches. If luciferase activity was induced by at least 1.5 fold with 1,000 ng/mL Doxycycline exposure, it was expanded and frozen down. The two best clones showed approximately 2.5 fold induction of luciferase with Doxycycline treatment.

**5. pTRE TIGHT and pTRE TIGHT-E4orf1 Selection and Screening**

a. The TetOn Advanced clone with the highest luciferase expression was split into 12-well plates for 50% confluency and transfected the next day with a 6:2 ratio of µL Lipofectamine to mg of either pTRE TIGHT or pTRE TIGHT-E4orf1 plasmid DNA. The linear hygromycin marker (Clonetech, #ST0206) was co-transfected with 0.1 mg per well. Two days post transfection cells were trypsinized and reseeded in a 10 cm plate, hygromycin treatment was started for selection. Doses of 0.05, 0.15, and 0.25 µg/mL of hygromycin were used either immediately, or gradually, similar to the way TetOn Advanced clones were selected. The 0.15 and 0.25 “immediate” and “gradual” doses were very toxic following transfection, so another transfection was conducted and doses of 0.05, 0.1, and 0.15 “gradual” µg/mL hygromycin were used. The TetON/pTRE clones grew extremely slowly and were switched to 20% Tet-free FBS with maintenance 0.05 ug/mL hygromycin after the 15 day selection period. Then, three rounds of harvesting over the next 10 days were conducted, visually marking the clones with a marker and manually

scraping with a de-tipped 200G tip. Clones were expanded over one month to the 10 cm stage for freezing and screening.

b. Once the clones had grown to the 10 cm plate stage, each clone was trypsinized and distributed into four wells of a 6-well plate, and one 10 cm plate. The 10 cm plate was frozen down and stored at -80º C, and the 6-well plate was treated with either 0 or 1,000 ng/mL Doxycycline and harvested for RNA after 16 hours.

Once RNA had been collected from all clones, two step quantitative real-time PCR was used to detect E4orf1 expression. The Teton/pTRE empty vector control clone with and without Doxycycline was used as the calibrator for the delta delta Ct calculation. The best clone was chosen with 6.5 fold increase in E4orf-1 expression for expansion and further characterization.

**6. E4orf1 Clone Characterization**

The pTRE TIGHT-E4orf1 clone with the highest expression during screening was plated in 6 well plates and treated with either 0, 500, 1,000, 5,000, or 10,000 ng/mL Doxycycline and harvested for RNA at either 16 hr, 24 hr, or 48 hr post treatment. Two passages were treated with these conditions, one that was frozen at -80º C right after selection (maintenance passage 1) and one that was passage 14 post selection (maintenance passage 14). E4orf1 expression at all conditions was detected via quantitative real-time PCR, and expressed as fold expression relative to pTRE empty vector control cell line (Figure 2). A loss of controlled dose response of E4orf1 expression to Doxycycline treatment occurs by passage

14 of the cell line. Early passages of the E4orf1 clone were therefore used for experiments.

### 2.2.18 Ras Activation Assay

Ras activation assay (#17-218, Upstate) was conducted according to manufacturer's protocol. After the Ras activation assay, four separate gels were loaded with 6% of the whole cell lysate for determination of total Ras and the slurry for determination of activated Ras. Each WB was probed with either 1:200 dilution of H-, N-, or K-Ras antibodies (Santa Cruz # sc-520, sc-519, and sc-30, respectively) for the detection of each isoform, or the Anti-Ras CLONE10 antibody provided with the activation kit for determination of total Ras activation.

### 2.2.19 Western Blotting

Cells were harvested in RIPA buffer complete with anti-protease (Sigma Aldrich, #P8340) and anti phosphatase inhibitor cocktail (Thermo Scientific #78420). Protein concentration was determined with a BCA assay, and samples were prepared with 5X lane marker reducing buffer (Thermo Scientific #39000) and ddH2O so the sample

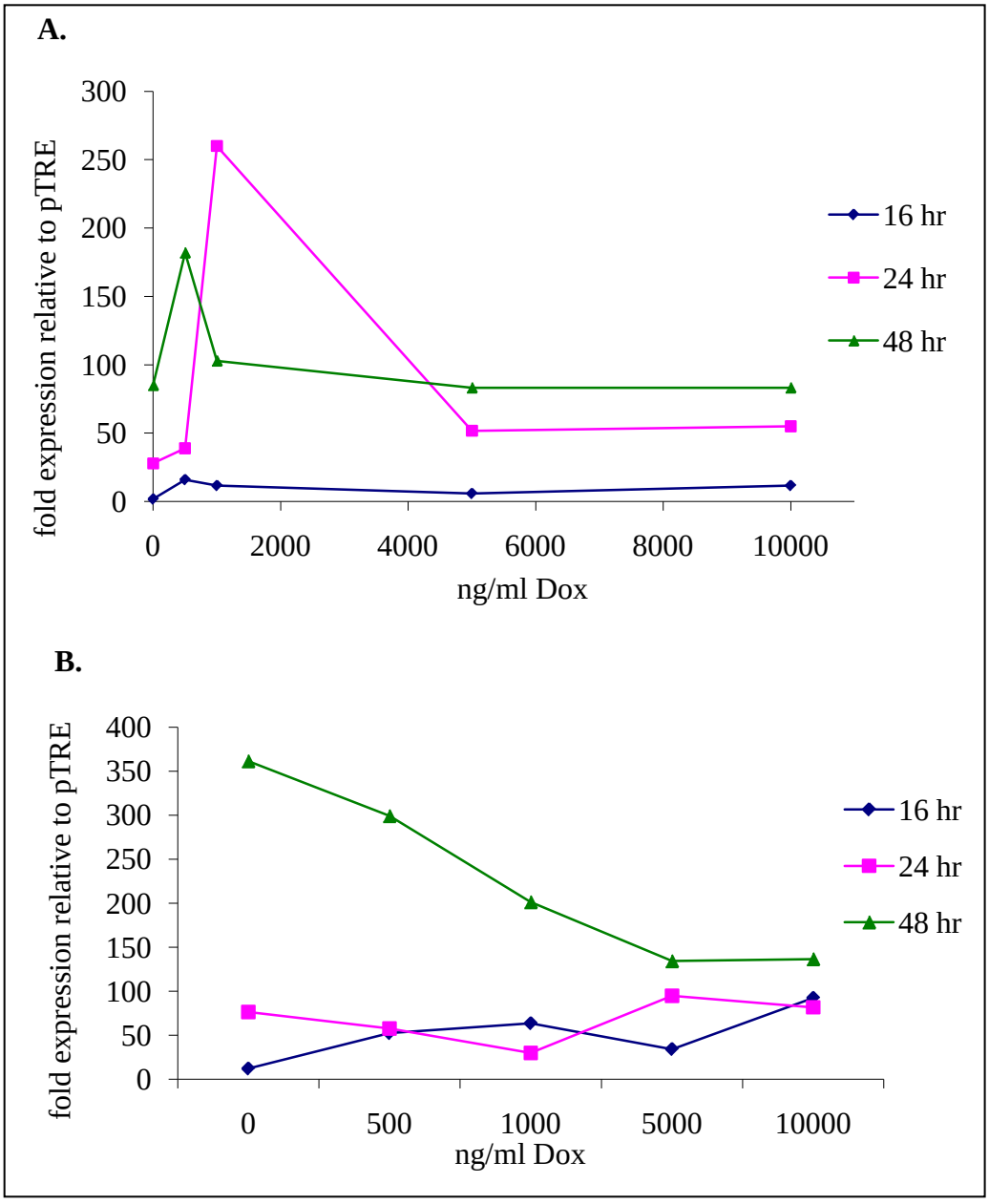


**Figure 2. Characterization of E4orf1 Expression in E4pTRE Cell Line.** E4orf1 expression standardization for pTRE TIGHT-E4orf1 clone. A) Maintenance passage 1 E4orf1 expression, expressed as mean expression relative to pTRE empty vector clone. B) Maintenance passage 14 of same clone, expressed as mean expression relative to pTRE empty vector clone.

volume was constant for loading. SDS-PAGE was performed and proteins were transferred to PVDF membrane. For detection of activated Ras, the slurry and 6% of whole cell lysate was loaded in a 15% gel, and isoform specific antibodies for H-, N-, and K-Ras (Santa Cruz #(Santa Cruz # sc-520, sc-519, and sc-30, respectively) were used at

1:200 dilution. Twenty μg protein was loaded in a 7% gel for detection of Glut4 with monoclonal antibody (RandD Systems # MAB1262) at 1:1,000 dilution. Fifteen μg protein was loaded in to a 10% gel for determination of Ras (Cell Signaling #3965S) at 1:1,000 dilution. Fifteen μg protein was loaded in to a 10% gel for determination of adiponectin at 1:1,000 dilution (Millipore #MAB3608). Fifteen μg protein was loaded in to a 10% gel for determination of Glut1 at 1:200 dilution (Santa Cruz Biotechnologies #sc-7903). For detection of successful transfection of V5-tagged E4orf-1, V5 antibodies (Invitrogen #46-0705) were used at 1:1000 dilution. Lastly, 10% gels were loaded with 15 μg and probed for p-AKT and total AKT (1:1000) (Cell Signaling #'s 9271 and 9271, respectively). For all proteins, β-actin was used as a loading control (Santa Cruz #sc-69879)(1:500 dilution). Densitometry was conducted using Image J software by the National Institutes of Health, and all graphs are represented as the ratio of the protein of interest to β-actin.

### 2.2.20 Soft Agar Assay

Briefly, 2 mL per plate of minimal essential medium (MEM) 10% FBS, 0.6 % agar was allowed to solidify at room temperature. Then, 0.5 mL of 80,000 cells/mL suspended in MEM 10% FBS, 0.3% agar was added. After the agar solidified at room temperature, another 2 mL of MEM 10% FBS, 0.6 % agar was added as a top layer. Cells were re-fed with 0.5 mL of 2X MEM, 20% FBS every seven days. Cells were fixed at day 7, 14, or 21 with 1 mL 0.01% crystal violet in 10% formalin overnight at $4^{o}$ C.

### 2.2.21 Quantitative Real-time PCR for Detection of Adiponectin and Inflammatory Cytokines

RNA was harvested and isolated using a RNA Mini Easy Kit (Qiagen, #74104), and cDNA was synthesized via RT PCR (Applied Biosystems # 4368814) according to

manufacturer's instructions. GAPDH primer probe was used as a housekeeping gene (Applied Biosystems, assay ID# Mm99999915_g1), and all inflammatory cytokines were detected with Applied Biosystems Gene Expression Primer Probe Assays (Applied Biosystems, INFγ #Mm99999071_m1, TLR-4 # Mm00445274_m1, MCP-1 #Mm00441243_g1, TNF-α #Mm00443259_g1, MCSF#00432688_m1, IL-10 #Mm00439615_g1). Two 2 ng per well was loaded in duplicate for each sample. Taqman Universal PCR Mix was used according to manufacturer's instructions(Applied Biosystems #4304437). For adiponectin mRNA detection, a primer was designed, and β-actin was used as a housekeeping gene. Both primers were ordered from IDT. The primers are as follows:

Adiponectin:

Forward: 5'-AAG GAC AAG GCC GTT CTC T -3'

Reverse: 5'- TAT GGGTAGTTG CAGTCA GTT GG -3'

β-Actin:

Forward: 5'-ACG TTG ACA TCC GTA AAG AC-3'

Reverse: 5'-GAT CTT CAT GGT GCT AGG AG-3'

SYBR green master mix (Biorad #170-8884) was used according to manufacturer's instructions for detection of adiponectin and β-actin. Expression of all genes was detected with the Applied Biosystems 7900 Sequence Detection System and using the standard curve method.

### 2.2.22 Mouse Embryonic Fibroblast Transfection

Cells were plated for 90% confluence without antibiotic and transfected the next day with Lipofectamine 2000 (Invitrogen # 11668-019) according to manufacturer's instructions. Briefly, 1.6 μg plasmid DNA and 4 μL of Lipofectamine 2000 per well were allowed to

complex for 15 minutes in Opti-MEM (Invitrogen #51985-091). Meanwhile, 800 µL of fresh serum free DMEM was added to each well. After complexation, 200 µL of transfection complex was added to each well and incubated for 6 hours before transfection media was replaced with fresh DMEM + 10% FBS.

### 2.2.23 HepG2 Plasmid Transfection

HepG2 cells were transfected for glucose output assays using the AMAXA Nucleofector II device, Cell Line Nucleofector Kit V (Lonza #VACA-1003) with either pcDNA-V5-AD36-E4orf1 or pcDNA-V5-DEST plasmids and plated in 96-well plates. Nearly confluent HepG2 cells were trypsinized, counted, and 2 µg of plasmid and 2 million cells were used per cuvette. Nucleofector program T-028 was used for transfection, and after resuspension 40,000 cells per well were plated on 96-well plates for the glucose output assay. Transfection was verified via protein harvest and WB for the detection of V5-tagged E4orf1 with V5 antibodies.

For HepG2 lipid oxidation, DNL, and ApoB secretion studies, PolyJet (SignaGen #SL100688) was used for transfection according to manufacturer's instructions. For each well, 4.5 µL plasmid and 1.5 mg plasmid was complexed, and transfection complex was left on cells overnight for 14-16 hours.

### 2.2.24 Glucose Oxidase Assay

A colorimetric assay was used for determination of glucose output into media (Raichem, #R80038). Manufacturer's instructions were followed, and 10 µL of media was loaded into each well, and a standard curve starting from 5 mM glucose diluted in serum free, glucose free media was used to determine exact molar concentration of glucose for unknown samples. Glucose output was adjusted to protein concentration as measured by BCA (Sigma Aldrich # B9643, #C2284) after solubilization of cells with 0.05% SDS.

Primary hepatocytes were solubilized in RIPA buffer, and were subjected to several rapid freeze-thaw cycles before lysing. Each sample was removed and spun down at 14,000 rpm for 10 minutes at 4 ºC, and the supernatant was taken for BCA assay.

# Chapter 3. Results

## 3.1 Objective 1. To Determine If Ad36 Infection Is Associated with Better Glycemic Control in Children

### 1A. Association of Ad36 Infection with Glycemic Control in Prepubertal Caucasian and African American Children

To determine an association of previous Ad36 infection with improved glycemic control, sera from 45 children from a previously characterized cohort, the MET study (32 Caucasian (71%), 10 Black(22%), 3 other races (6%), 22 males (48%), 23 females (52%), age 7-9 years), were screened for the presence of Ad36 neutralizing antibodies. Ad36 seropositivity is significantly associated with lower fasting glucose (p=0.04) and insulin (p=0.04), lower HOMA IR (p=0.03), and less intra-hepatic lipid (p=0.04) (Table 1).

**Table 1**. **Association of Glycemic Control with Ad36 in MET Study**. Prepubertal boys and girls (n=45; Black/White/other: 10/32/3). Mean[a] (95%CI) adjusted for sex and body fat mass. Intra-hepatic lipid normalized to spleen density. Higher HU value equates to lower lipid content. Krishnapuram et al, American Journal of Physiology Endocrinology and Metabolism, 2011, Am Physiol Soc, used with permission. (190)

| | Ad36 - | Ad36 + | P |
|---|---|---|---|
| N=42 | N=35 | N=10 | |
| Fasting glucose (mg/dL) | 74.5 (71.6-77.4) | 68.7 (62.9-74.6) | 0.04 |
| Fasting Insulin (μU/ml) | 3.1 (2.4-4.1) | 1.8 (1.1-3.0) | 0.04 |
| HOMA IR | 0.51 (0.39-0.69) | 0.28 (0.16-0.48) | 0.03 |
| Intra-hepatic lipid (% water peak) | 0.005 (0.002-.006) | 0.003 (0.004-0.008) | 0.04 |
| [a] Arithmetic mean for glucose; Geometric mean for insulin, HOMA-IR and intra-hepatic lipid | | | |

### 1B. Association of Ad36 Infection with Glycemic Control in Hispanic Children

Sera of 585 Hispanic children from the VIVA LA FAMILIA study were screened for the presence of neutralizing antibodies to Ad36. Out of 585, 42 subjects tested seropositive

to Ad36 (7%). Prevalence of Ad36 infection in this cohort is lower than other populations previously tested. Several subjects were related in this cohort, therefore fasting blood glucose, insulin, and HOMA IR were adjusted for family and body fat mass. Fasting blood glucose was significantly lower for Ad36 seropositive subjects (p=0.04). In addition, Ad36 seropositive subjects had a significantly greater odds ratio for fasting glucose, fasting insulin, and HOMA IR to fall below the median of the overall group (p=0.02, 0.04, and 0.02, respectively)(Table 2). Thus, Ad36 seropositivity is associated with improvements in glycemic control in Hispanic, Caucasian, and African American children.

## 3.2 Objective 2. Identify the Characteristics of Adipose Tissue and Liver Associated with Ad36 Induced Improvements in Glycemic Control

### 2A. Adipose Tissue

#### 2A.1 Adipocyte Metabolism

##### 2A.1.1 Spread of Ad36 Infection in Human Adipose Derived Stem Cells

The spread of Ad-36 infection in hASC's was determined. A time course of Ad36 infection was tracked by staining of nuclei and Ad36 hexon protein to determine of the percent of cells infected with Ad-36 (Figure 3). Spread of infection in hASC's was initially slow, but progresses quickly after Day 5 post infection. A 3-fold increase in the percent of infected cells occurred between Day 3 and Day 5 post infection, while a nearly 6-fold increase in the percent of infected cells occurred between Day 5 and Day 7, and a 2.5-fold increase between Day 7 and Day 9 (Figure 3B). This indicates that Ad-36 infection of hASC's is replicative, that it spreads well in this cell type, and they provide an excellent model for the study of Ad36 and lipid metabolism.

**Table 2. Association of Glycemic Control with Ad36 in VIVA LA FAMILIA Study.** Hispanic boys and girls (n=585). Odds ratio adjusted for sex, body fat mass and family. Mean[a] (95% CI), adjusted for adiposity and family[b] . NS: p>0.05. Krishnapuram et al, American Journal of Physiology Endocrinology and Metabolism, 2011, Am Physiol Soc, used with permission. (190)

| | Ad36 - | Ad36 + | P |
|---|---|---|---|
| N=585 | N=543 | N=42 | |
| Fasting glucose (mg/dL) | 92.2 (91.3-93.0) | 89.1 (85.8-92.4) | 0.04 |
| Fasting Insulin (μU/ml) | 15.9 (15.2-16.6) | 16.6 (13.9-19.8) | NS |
| HOMA IR | 3.58 (3.42-3.76) | 3.65 (3.03-4.40) | NS |
| **OR for Ad36+ to be below the median of the overall group** | | | |
| | OR | 95% CI | P |
| Fasting glucose | 2.5 | 1.1 – 5.7 | 0.02 |
| Fasting Insulin | 1.8 | 0.9 – 3.4 | 0.04 |
| HOMA IR | 2.4 | 1.1 – 5.3 | 0.02 |

[a] Arithmetic mean for glucose; Geometric means for Insulin and HOMA IR. [b]Initial models included age and sex but neither was a significant predictor so both were excluded from the final analytical model; however, the resulting p-values were unchanged.

### 2A.1.2 Lipid Accumulation in hASC Following Ad36 Infection with and without MDI

Next, a lipid accumulation time course of hASC's with and without differentiation inducer MDI revealed that lipid accumulation is increased by Ad36 infection. In the presence of MDI, both Mock and Ad36 infected groups accumulated lipid at a similar rate initially, and lipid accumulation in Ad36 group surpassed Mock after Day 7, with significantly more lipid per cell Day 9 post infection (Figure 4) (p=0.003). Without induction by MDI, Ad-36 alone was sufficient to increase

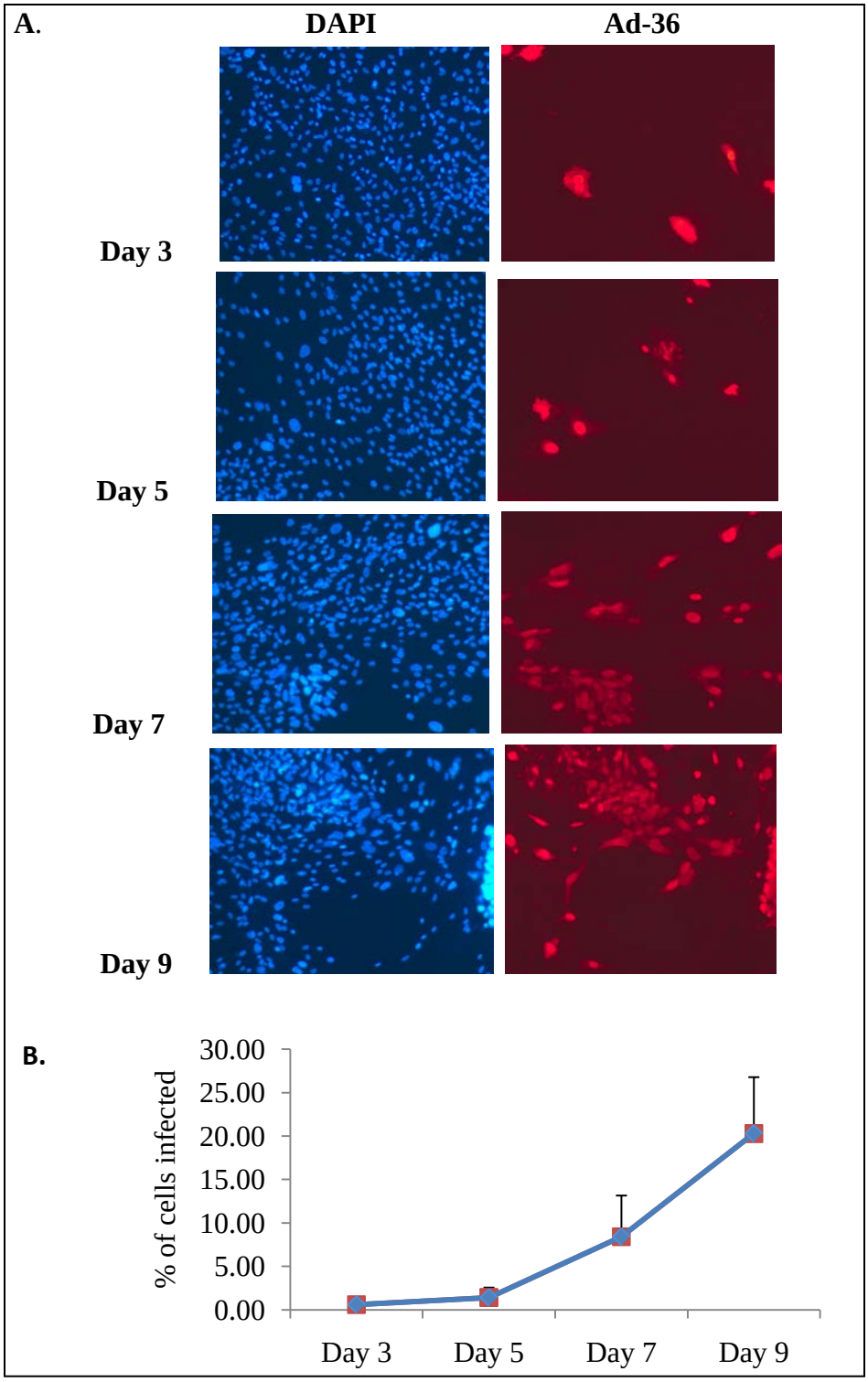


**Figure 3. Ad36 Hexon and DAPI Staining Time Course in hASC.** Time course of Ad36 infection in hASC, post infection with 3.8 PFU/cell. A) Representative

20X pictures of DAPI and Ad36 Hexon staining for various time points. B) Percent of cells infected for each time point, expressed as mean percent ± SD.

lipid accumulation compared to Mock (p=0.01 for Day 3, Day 5, Day 7, p=0.06 for Day 9)(Figure 4). Ad-36 increases lipoprotein lipase (LPL) expression and translocation (202), which may explain the increased lipid accumulation here.

### 2A.1.3 The Effect of Ad-36 Infection on Lipid Accumulation with Respect to Confluency

The effect of Ad-36 on 3T3-L1 lipid accumulation is well documented (200; 247), but the effect of confluency at the time of infection is unknown. 3T3-L1 cells are a particularly good model for this as infection is not replicative in these cells (200). How confluency of 3T3-L1 effects Ad36 induced lipid accumulation was determined in 3T3-L1. 3T3-L1 infected at confluence accumulate significantly more lipid than those infected 2 days prior to confluence (Figure 5). In the first experiment, cells were incubated with virus for the same amount of time regardless of the time of infection relative to confluency (Figure 5A). In the second experiment, cells were incubated for the same amount of time post confluence (Figure 5B). In both experiments, cells have greater lipid accumulation when infected at confluence compared to those infected 2 days prior (p=0.00001 and 0.0003, respectively). Therefore, regardless of incubation time with the virus or time post confluence, Ad36 infection demonstrated a synergistic effect with confluence.

### 2A.1.4 De Novo Lipogenesis Time Course Following Ad36 Infection in 3T3-L1

Although Ad36 increases glucose uptake in adipose tissue, the fate of intracellular glucose and if it contributes to lipid accumulation is unknown. Ad36 significantly increases de novo lipogenesis in 3T3-L1 ($p<0.05$ Day 6 post infection) (Figure 6).

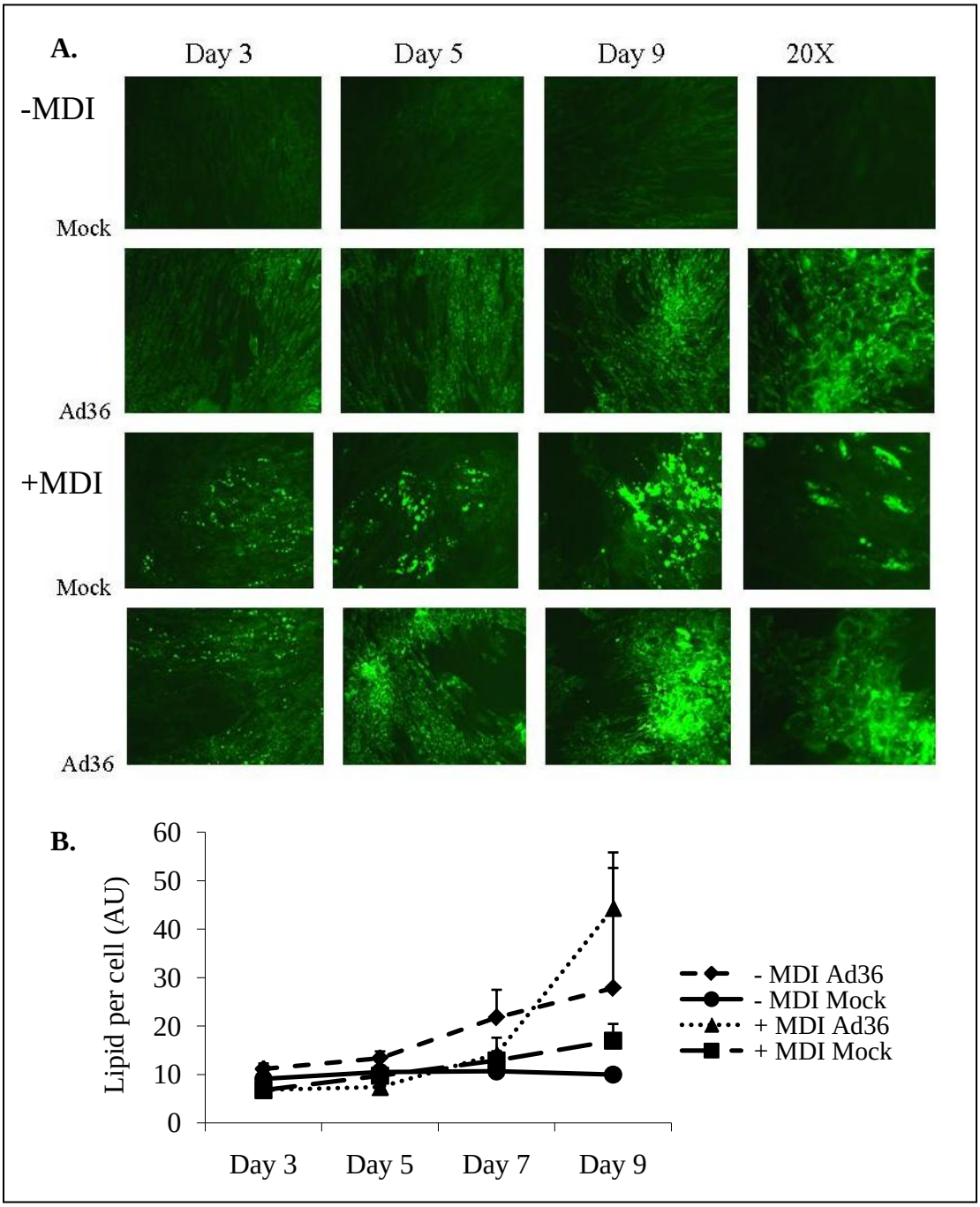


**Figure 4. Time Course of Lipid Accumulation Following Ad36 Infection.** Lipid accumulation in hASC after Mock or Ad36 infection (3.8 PFU/cell), with or without MDI. A) Representative images of BODIPY staining in hASC's following Ad-36

infection w or w/o MDI. Published first elsewhere (Pasarica et al., Stem Cells, Issue 26, p.19, AlphaMed Press)(202) B) BODIPY fluorescence quantified and normalized to DAPI florescence for quantification of lipid per cell, expressed as mean ± SD for each condition and time point.

Specifically, between Day 3 and Day 6 post infection, DNL is up-regulated. This time period post confluence and post infection is when preadipocytes are rapidly accumulating lipid, becoming mature adipocytes. Therefore, as cells infected with Ad-36 differentiate, they may accumulate lipid through increased conversion of glucose to lipid. This may result in concomitant glucose clearance from circulation and lipid accumulation in cells.

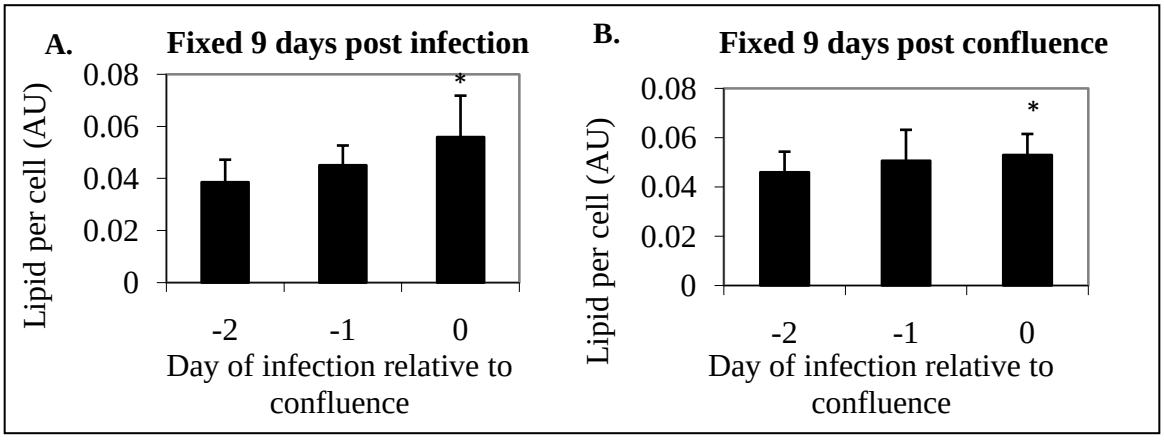


**Figure 5. Lipid Accumulation Per Cell in Ad36 Infected 3T3-L1.** Lipid accumulation in 3T3-L1 infected with 1 PFU/cell different days relative to confluence. **A**) Mean lipid per cell ± SD in 3T3-L1 infected at -2, -1, and 0 days relative to confluence, fixed and quantitated 9 days post infection. Cells accumulate more lipid if infected at confluence ($p=0.00001$). B) Mean lipid per cell ± SD in 3T3-L1 infected at -2, -1, and 0 days relative ton confluence, fixed and quantitated 9 days post confluence. Cells accumulate more lipid if infected at confluence ($p=0.0003$). These data were first published elsewhere(247).

### 2A.1.5 Modulation of Glucose and Palmitate Oxidation in 3T3-L1 by Ad36

Oxidation of glucose and palmitate were monitored in 3T3-L1 infected with Mock, Ad36, or Ad-2. A time course following infection (Figure 7) indicated that Ad36 consistently reduces glucose oxidation (Figure 7A) ($p<0.05$ for Day 3, 6

and 8) , and up-regulates palmitate oxidation (Figure 7B)($p<0.05$ for Day 8) compared to Mock- infected cells, and Ad2 infection did not have a similar effect on 3T3-L1 substrate utilization. The ratio of palmitate to glucose oxidation is consistently higher following Ad36 infection compared to Mock (Figure 7C), indicating the Ad36 infected cells preferentially oxidize fatty acids.

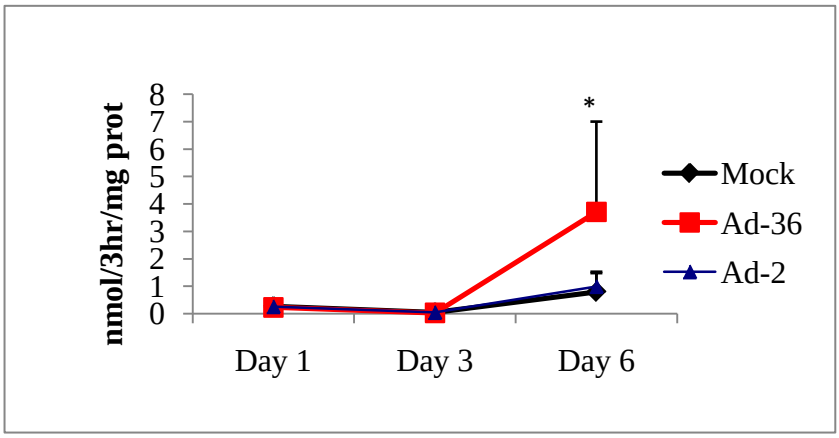


**Figure 6. DNL Following Mock, Ad36, and Ad2 Infection of 3T3-L1.** DNL Expressed as mean nmol glucose/3 hr/ mg protein ± SD. Ad36 has significantly greater lipid accumulation than Mock infected cells by Day 6 post infection ($p=0.05$).

## 2A.2 Effect of Ad36 on Adipose Tissue Morphology

### 2A.2.1 Change in Adipocyte Cell Size in C57BL/6J Mice on Chow and High Fat Diet

Adipocyte size in healthy, chow fed C57BL/6J mice was determined in Mock, Ad36, or Ad2 infected animals. Animals were sacrificed 12 weeks post infection, and epididymal adipose tissue was stained for either CD68 (macrophage marker) or CD31 endothelial cell marker) as described in methods. From this staining, 10X or 5X images were taken, to measure adipocyte diameter as described in methods. Mean adipocyte diameter of Ad36 infected mice was significantly smaller compared to Mock-infected mice (77.9 ± 4.3 vs. 101.3 ± 15.14 pixels,

respectively, p=0.04), whereas Ad2 infected mice adipocyte diameter is not significantly different than Mock (Figure 8A). The percent of adipocytes in Ad36 infected adipose tissue in the "small" category, which fall in the bottom tertile (as defined by the range adipocyte sizes of all groups) is significantly higher than the percent in the "large" category, which fall within the upper tertile (63% ± 3.8% vs. 12.4% ± 2.5% , respectively, p=0.005) (Figure 8B). This indicates that Ad-36 shifts the adipocyte cell size distribution to smaller adipocytes (Figure 8C).

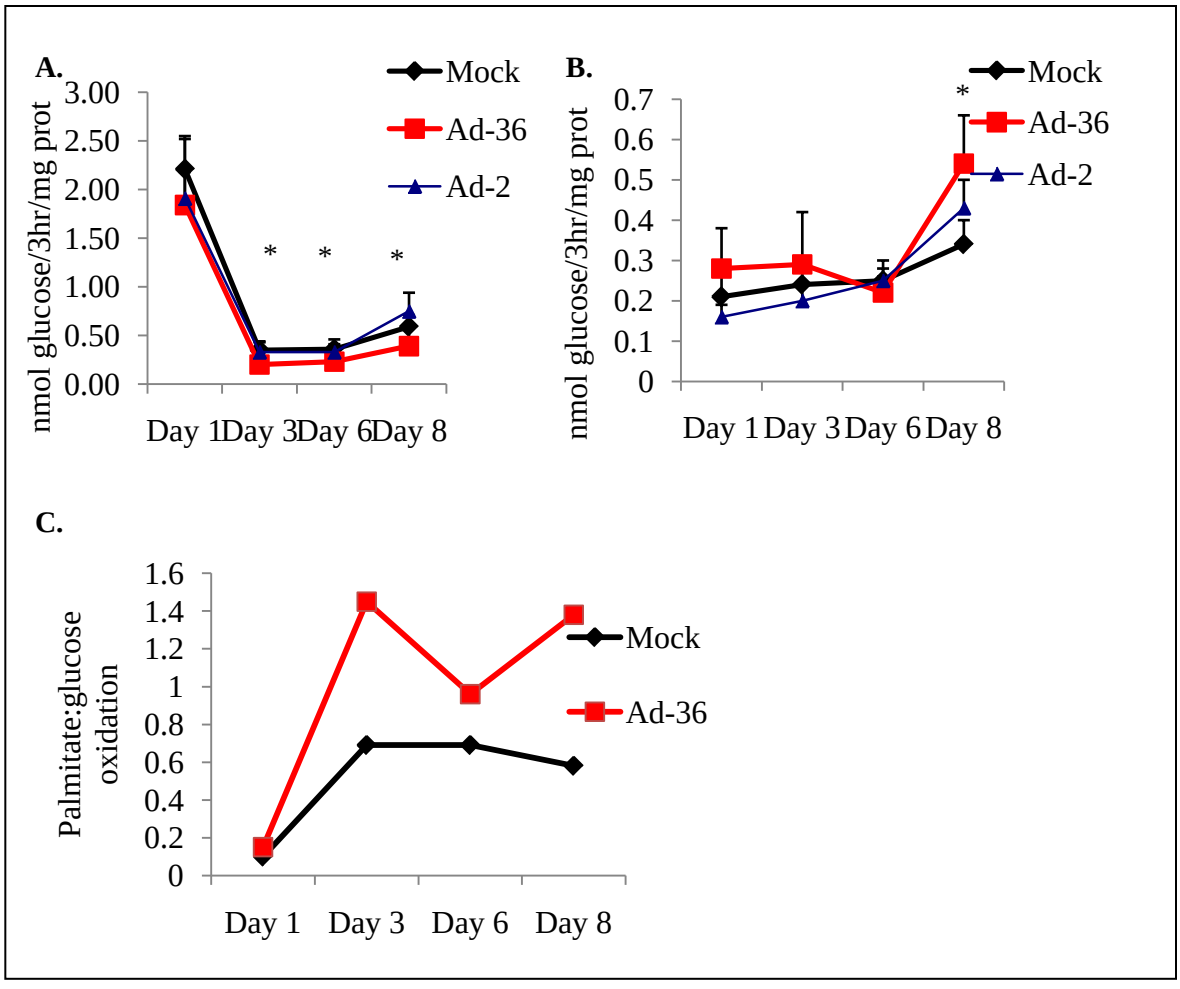


**Figure 7. Time Course of [14C]-Glucose Oxidation and [14C]-Palmitate Oxidation.** Time course glucose and lipid oxidation in 3T3-L1 Mock, Ad2 or Ad36 infected (3.8 PFU/cell). A) [14C]-Glucose oxidation in Mock, Ad36, and Ad2 infected cells. Ad36 decreases glucose oxidation ($p<0.05$ for Day 3, 6 and 8) B) [14C]-palmitate oxidation, in Mock, Ad36, and Ad2 infected 3T3-L1. Ad36 increases fat oxidation in 3T3-L1) ($p<0.05$

for Day 8) C) The ratio of palmitate: glucose oxidation, which is consistently higher in Ad36 group compared to Mock.

Adipocyte diameter is also altered by Ad36 infection in C57BL/6J mice on a high fat diet. The mean adipocyte diameters for Mock, Ad36, and Ad2 infected mice are not significantly different, however, the distribution of adipocyte sizes differs between groups. A larger percentage of Ad36 infected adipocytes falls in the "large" category (upper tertile of Mock range of adipocyte diameters) than the "small" category (42.5 $\pm$ 9.1 vs. 21.6% $\pm$ 7.8%, respectively, p=0.04) (Figure 9A). The opposite trend is apparent in Ad-2 infected adipose tissue, with more adipocytes falling in the "small" category than the "large" category (43% $\pm$ 7.8% vs. 23.3% $\pm$ 3.9%, respectively, p=0.008). These changes in cell size distribution are presented in the box plot graph of all three groups (Figure 9B).

**2A.2.2 Effect of Ad36 on macrophage infiltration in C57BL/6J mice on chow and HFD.**

Macrophage infiltration into adipose tissue is considered a marker of inflammation and insulin resistance, and can occur with a high fat diet. Because Ad36 improves glycemic control, we hypothesized that it may modulate macrophage infiltration. Immunohistochemistry staining of macrophages in both chow fed and HFD fed C57BL/6J mice was quantified using Image J. In the chow fed model Ad2 infection increased macrophage infiltration (p=0.01) compared to Mock infected animals (Figure 10). While Ad36 infection shares a similar trend, this relationship is not statistically significant when compared to

Mock in this model. Variation in macrophage staining is especially high in Ad36 infected chow fed mice, suggesting that in this condition, another variable factor

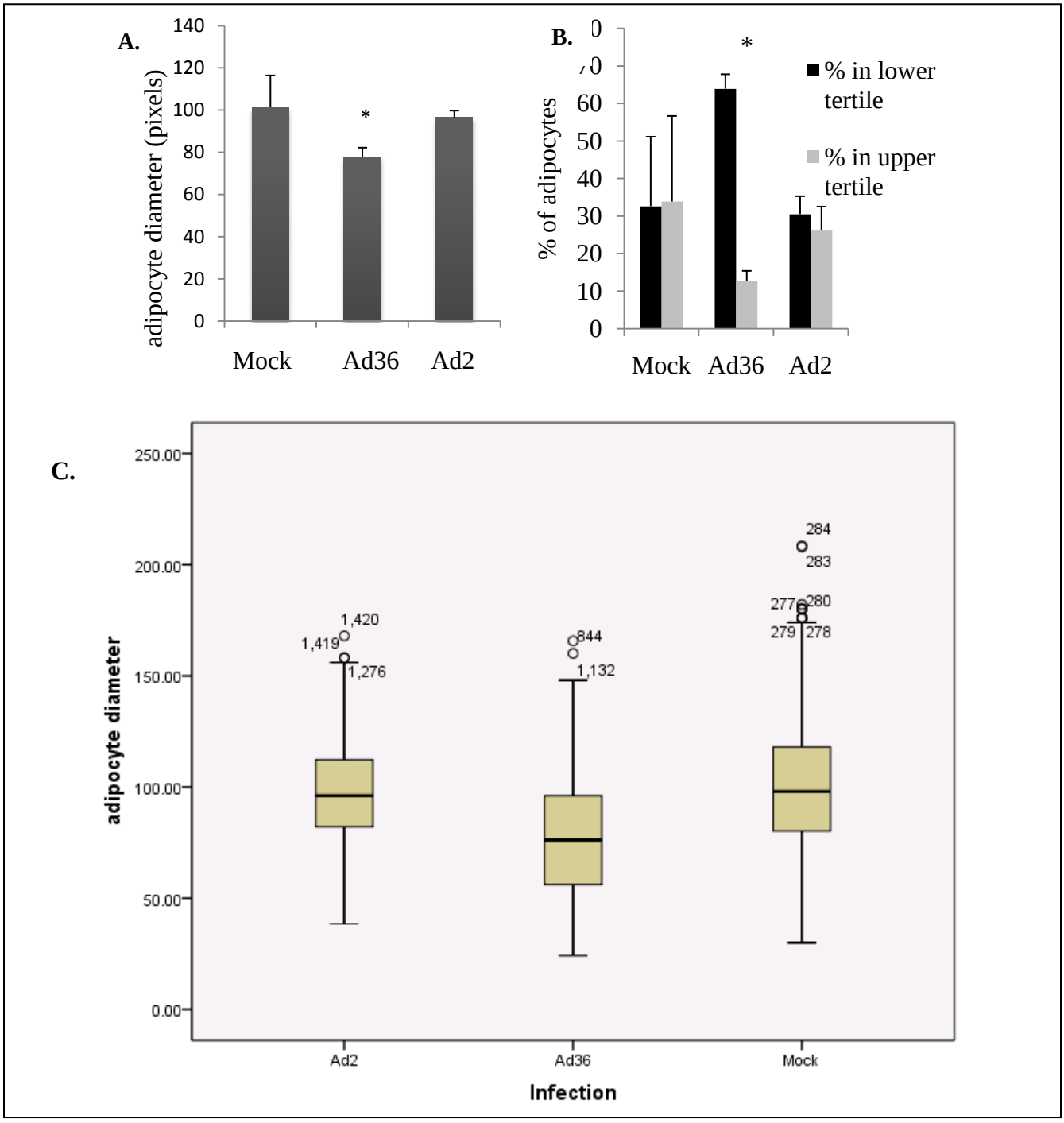


**Figure 8. The Effect of Ad-36 on Adipocyte Size in Chow Fed C57BL/6J Mice.** Adipocyte diameter in Mock, Ad36 and Ad2 infected C57BL/6J mice on chow diet. A) Mean adipocyte diameter ± standard deviation. Ad-36 infected adipose tissue has a lower mean adipocyte size than Mock infected adipose tissue (p*=0.04). B). Percent of total adipocytes falling in the lower

or upper tertile, as defined by the range of adipocyte diameter measurements pooled from all groups. Percentage was calculated for each mouse and averaged, mean ± SD for each group. Ad36 has a greater number of adipocytes in the lower tertile compared to the upper tertile($p=0.005$), whereas Mock and Ad2 does not. C) Box plot of all adipocyte diameter measurements pooled for each group. Outliers are labeled by measurement number.

such as the level of local Ad36 infection in adipose tissue may be impacting macrophage levels.

In the HFD model, no significant differences in macrophage infiltration were detected by this method (Figure 10B). This may be due macrophage infiltration induced by the high fat diet, which may be overwhelming any effect of infection.

**2A.2.3 Effect of Ad36 on Adipose Tissue Vascularization and Angiogenesis**

Adipose tissue growth without adequate angiogenesis can lead to poor adipose tissue vascularization and consequently hypoxia, inflammation, and insulin resistance(113). To determine how Ad36 modulates vascularization, adipose tissue of chow and HFD C57BL/6J mice was stained for CD-31 as a marker of endothelial cells and thus vascularization. In both models, Ad36 and Ad2 significantly increased adipose tissue CD31 staining compared to Mock infected mice (Figure 11, $p<0.05$), indicating this may be a general effect of adenoviral infection.

Next, to determine if Ad36 and Ad2 may increase adipose tissue vascularization through induction of angiogenesis, an assay that specifically measures angiogenesis in human adipose tissue explants was used(245). The assay was repeated three times. Overall, Ad36 inhibits angiogenesis, much like the negative

control (galic acid treatment), while Ad2 levels of angiogenesis are very similar to the baseline Mock-infected control group (Figure 12). For the third trial

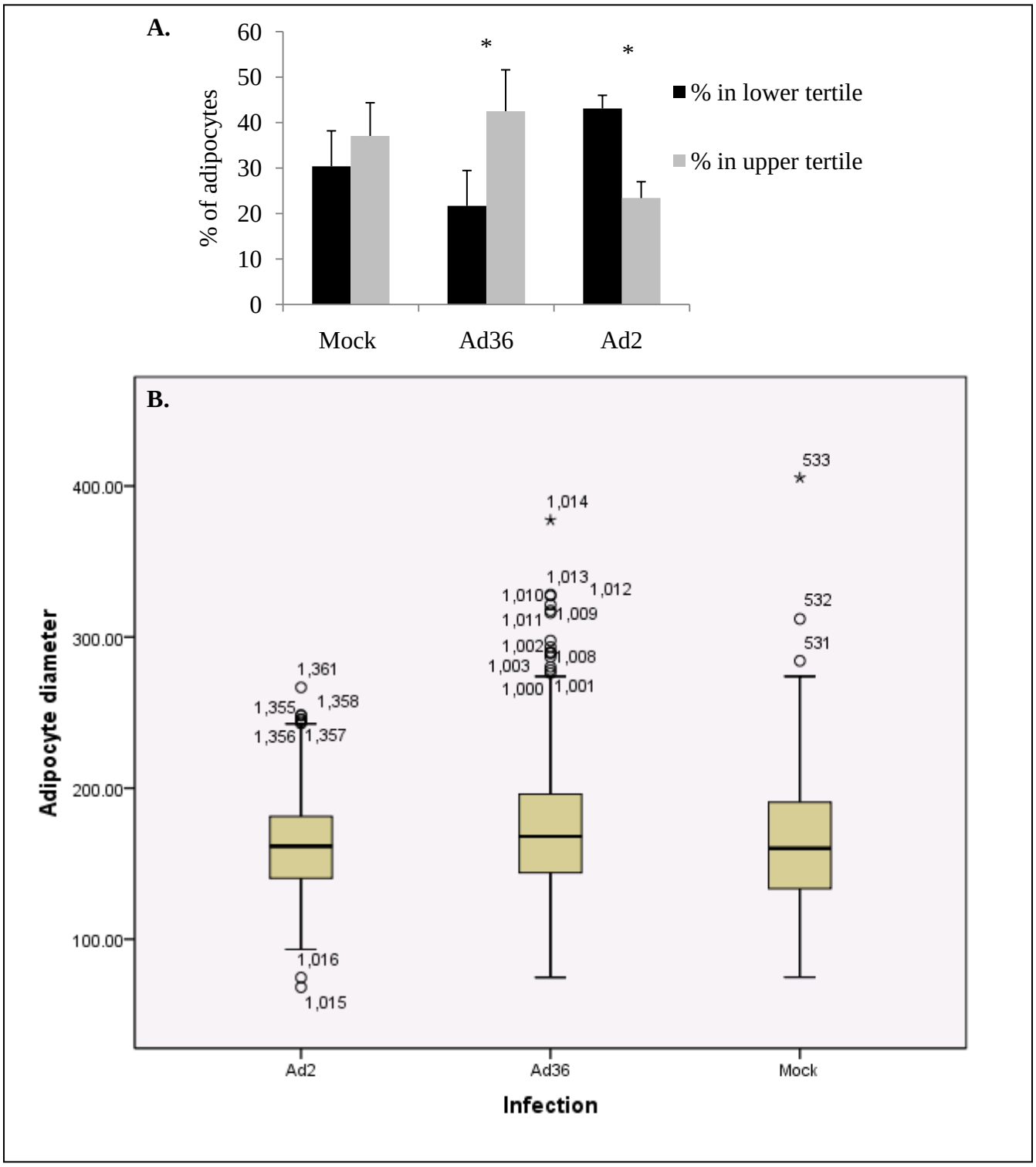


**Figure 9. The Effect of Ad-36 on Adipocyte Size in HFD C57BL/6J Mice.** Adipocyte diameter in C57BL/6J mice on HFD. There is no significant difference between mean diameters

of Ad-36, Ad2, or Mock infected adipocytes. A) Percent of total adipocytes falling in the lower or upper tertile, as defined by the range of adipocyte diameter measurements pooled from all groups. Percentage was calculated for each mouse and averaged, mean $\pm$ SD for each group. Ad36 has a greater number of adipocytes in the upper tertile compared to the bottom tertile($p=0.04$), whereas Ad2 has significantly more falling into the smaller category compared to the large category ($p=0.008$). C) Box plot of all adipocyte diameter measurements pooled for each group. Outliers are labeled by measurement number.

conducted, the adipose tissue did not respond as well, with very low levels of angiogenesis and the Mock group had very similar levels of angiogenesis to the negative control (GA) until Day 15 of the assay (data not shown). Similar trends were seen, however, with the infected groups in this third assay. Neither viruses, therefore, are strongly angiogenic in human adipose tissue ex vivo.

Lastly, the effect of Ad2 and Ad36 on induction of tube formation in SVEC4-10 murine endothelial cells plated on basement membrane extract was determined. A tube formation assay measuring the acute (5 hr post infection) and long-term response of SVEC4-10 cells (Days 1 and 3 post infection) was conducted with Mock, Ad36, and Ad2 infected cells. Five hours post infection, neither adenovirus enhanced the length of tubes formed by SVEC4-10 cells (Figure 13). One day post infection, Ad36 caused a different morphology all together, with cells stacking on top of each other, while Ad2 allowed cells to align but not create complete networks of tubes. By Day 3 post infection, Ad2 infected cells had died, and Ad36 continued to inhibit tube formation by SVEC4-10 endothelial cells. Thus both adenoviruses impaired tube formation, and Ad2 was particularly virulent in this cell type.

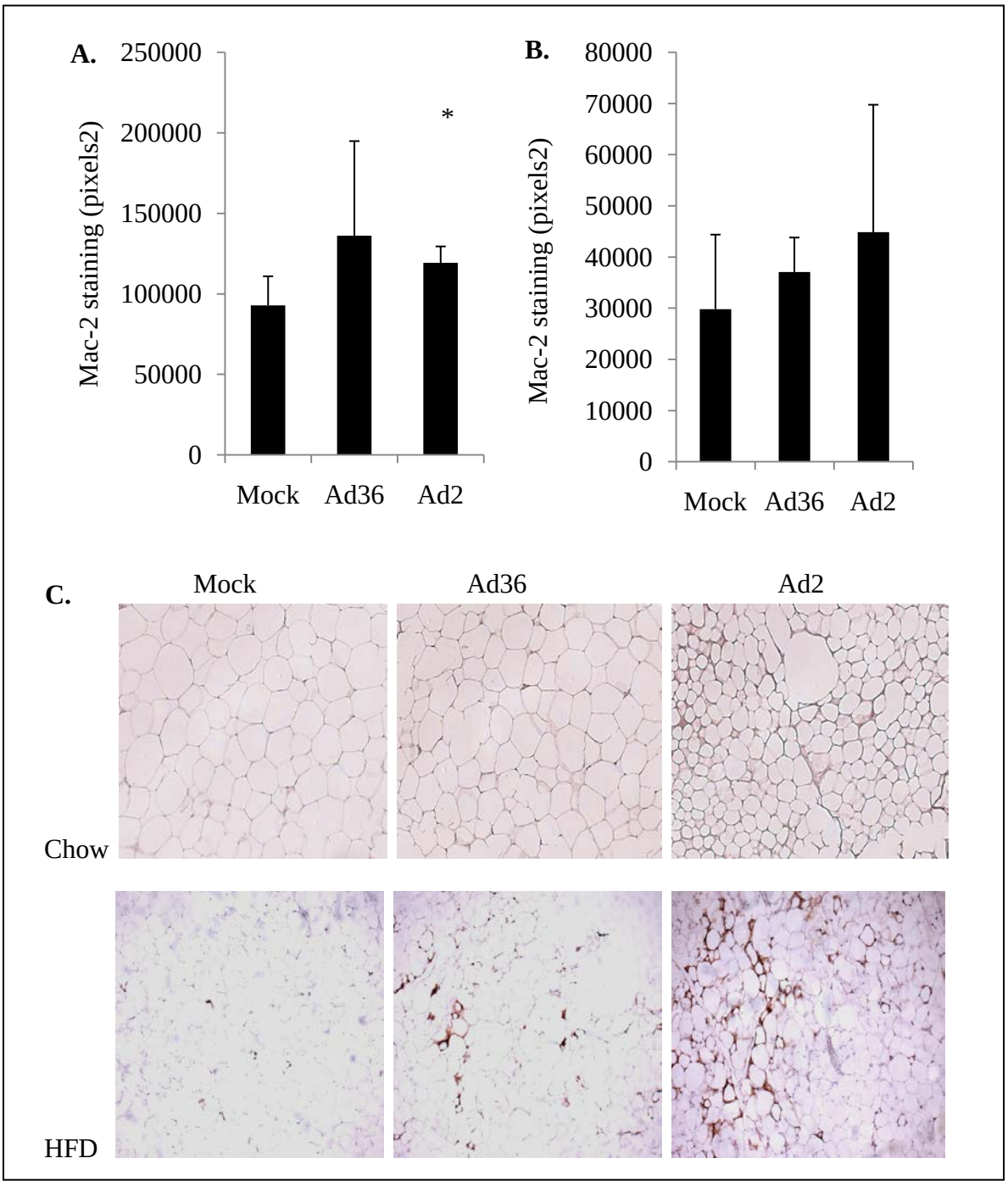


**Figure 10. Macrophage Infiltration in Adipose Tissue of C57BL/6J Mice on Chow and HFD.** A) Macrophage staining of chow fed mouse adipose tissue, quantified by Image J. Mean $\pm$ SD. Ad2 has significantly more macrophage staining than Mock ($p=0.01$). B) Quantification of macrophage staining of HFD mice adipose tissue. Mean $\pm$ SD. There were no significant differences macrophage staining for this model. C) Representative images of macrophage staining, which appear as a dark brown stain. Chow fed are 10X (top), HFD are 5X (bottom).

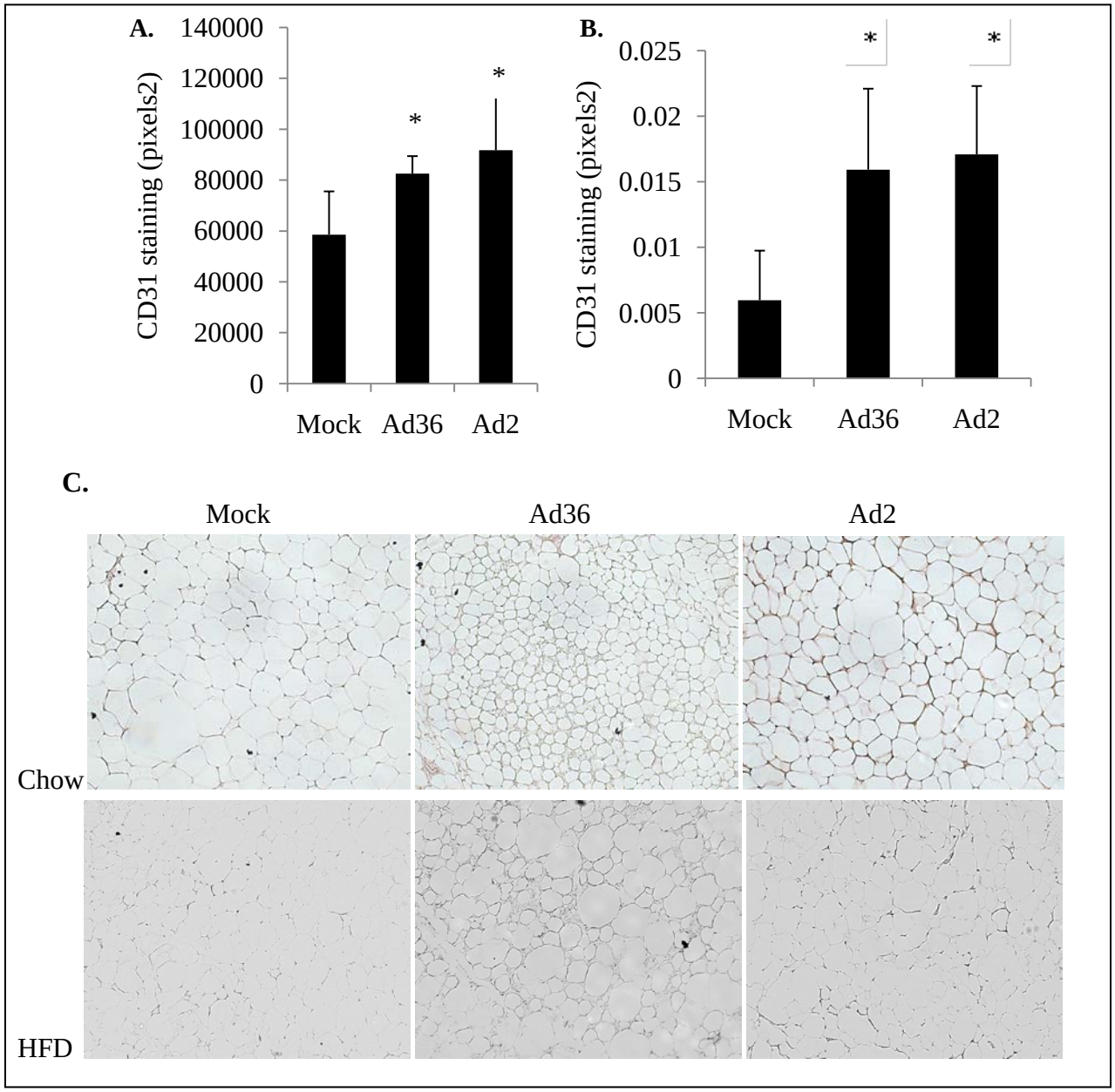


**Figure 11. CD-31 Staining of Adipose Tissue from Mice on Chow Diet and HFD.** Adipose tissue vascularization in C57BL/6J mice on chow or HFD. A) Image J quantification of CD31 staining in chow fed C57BL/6J mice adipose tissue. Expressed as Mean $\pm$ SD. Ad36 and Ad2 infected mice have significantly higher CD31 staining compared to Mock infected mice ($p=0.003$ and 0.04, respectively). B) Quantification of CD31 staining in HFD fed C57BL/6J mice adipose tissue. Expressed as Mean $\pm$ SD. Ad36 and Ad2 infected mice have significantly higher CD31 staining compared to Mock ($p=0.03$ and 0.02, respectively). C) Representative 10X images of CD31 staining. CD-31 staining appears as a dark brown color.

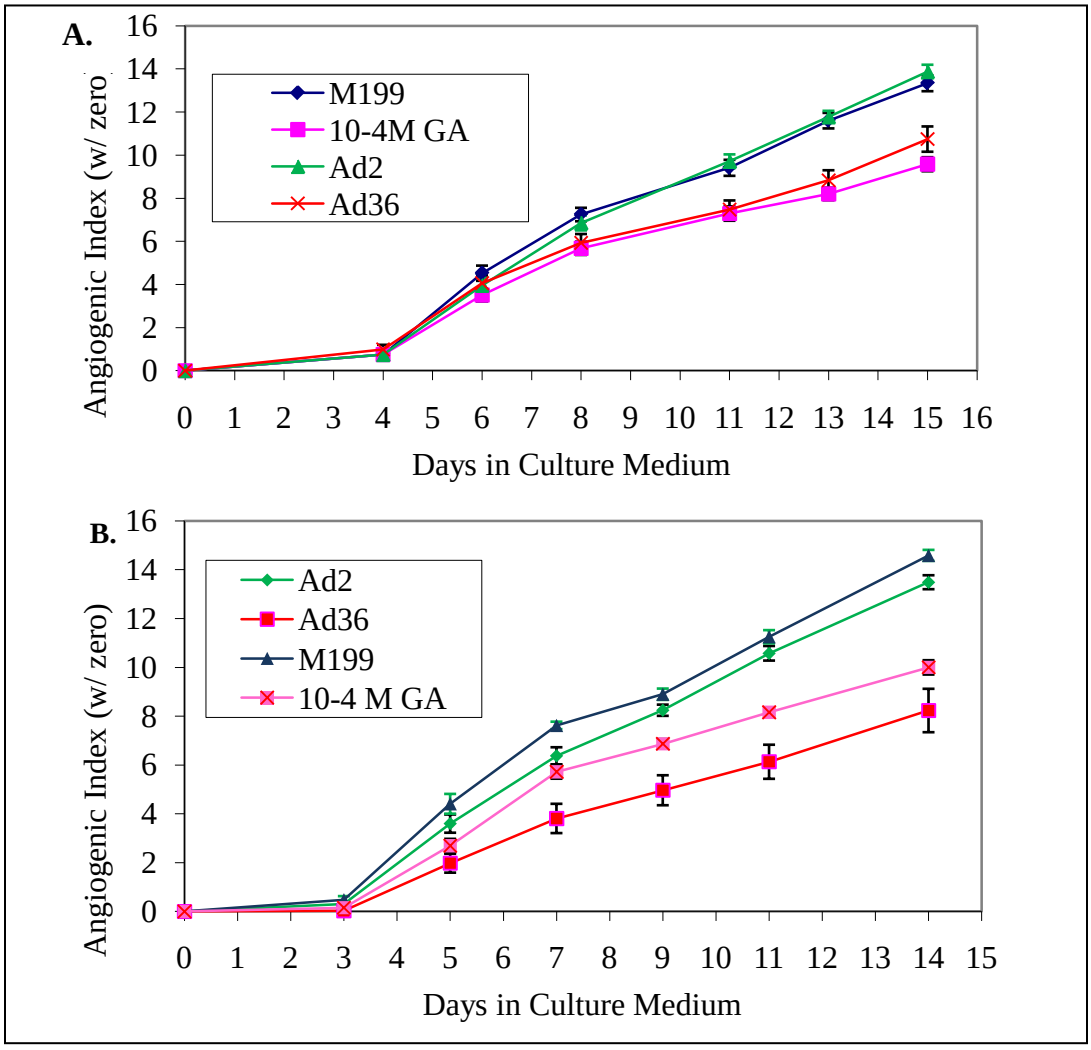


**Figure 12. Human Adipose Tissue Angiogenesis Assay.** Human adipose tissue angiogenesis in response to Mock, Ad2 and Ad36 infection. Mean angiogenesis index ± SD. Galic acid treatment inhibits angiogenesis and is a negative control, whereas M199 is the media + Mock infection as a baseline control. Adipose tissue from A) 42 years old, female, Caucasian, BMI=24.7) B) A 34 year old female, Caucasian, BMI=26.2.

## 2B. Effect of Ad36 on Hepatic Steatosis

### 2B.1 Effect of Ad36 on Liver Steatosis and Glycogen Stores in C57BL/6J Mice on HFD

To determine if Ad36 may improve glycemic control by preventing hepatic steatosis and improving glycogen stores, liver sections from Mock, Ad36, and Ad2 infected C57BL/6J

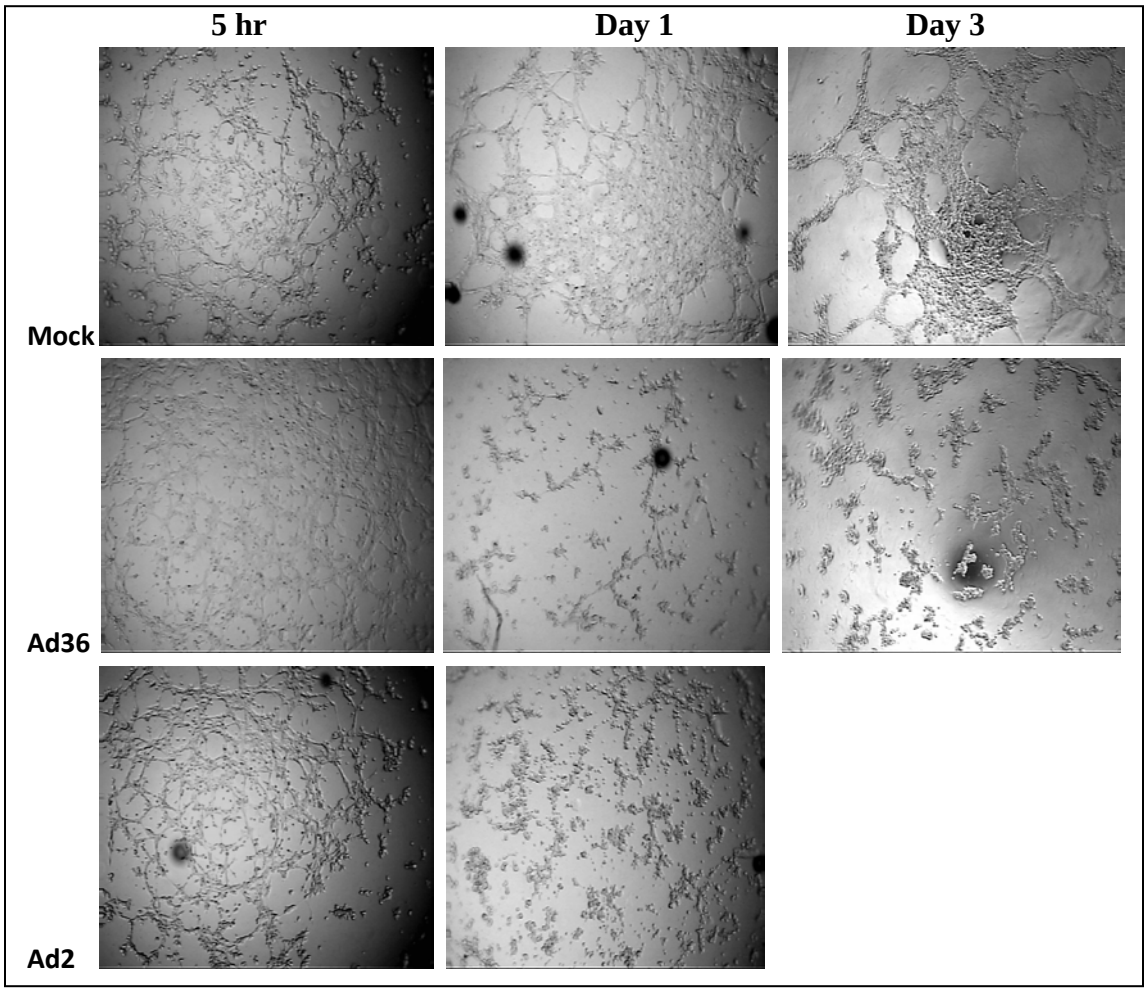


**Figure 13. Tube Formation Assay Following Mock, Ad36 and Ad2 Infection.** 5X images of tube formation assay of SVEC4-10 murine endothelial cells and various time points post infection with Mock, Ad36, or Ad2. Normally, SVEC4-10 cells align and form networks as seen Mock infected images. Ad36 and Ad2 infection inhibits the formation of these tubes.

mice on a HFD were stained for glycogen. Throughout processing, lipid leaves the sample and leaves white space in the tissue. Therefore, both approximate lipid and glycogen content can be quantified using Image J software. Interestingly, Ad36 significantly reduced hepatic lipid accumulation and increased glycogen stores, even in the presence of a HFD ($p=0.02$)(Figure 14). Ad2 infection, on the other hand, increases high fat diet induced steatosis and decreases hepatic glycogen stores. The prevention of steatosis by Ad36 may be a strong contributor to its attenuation of dysglycemia.

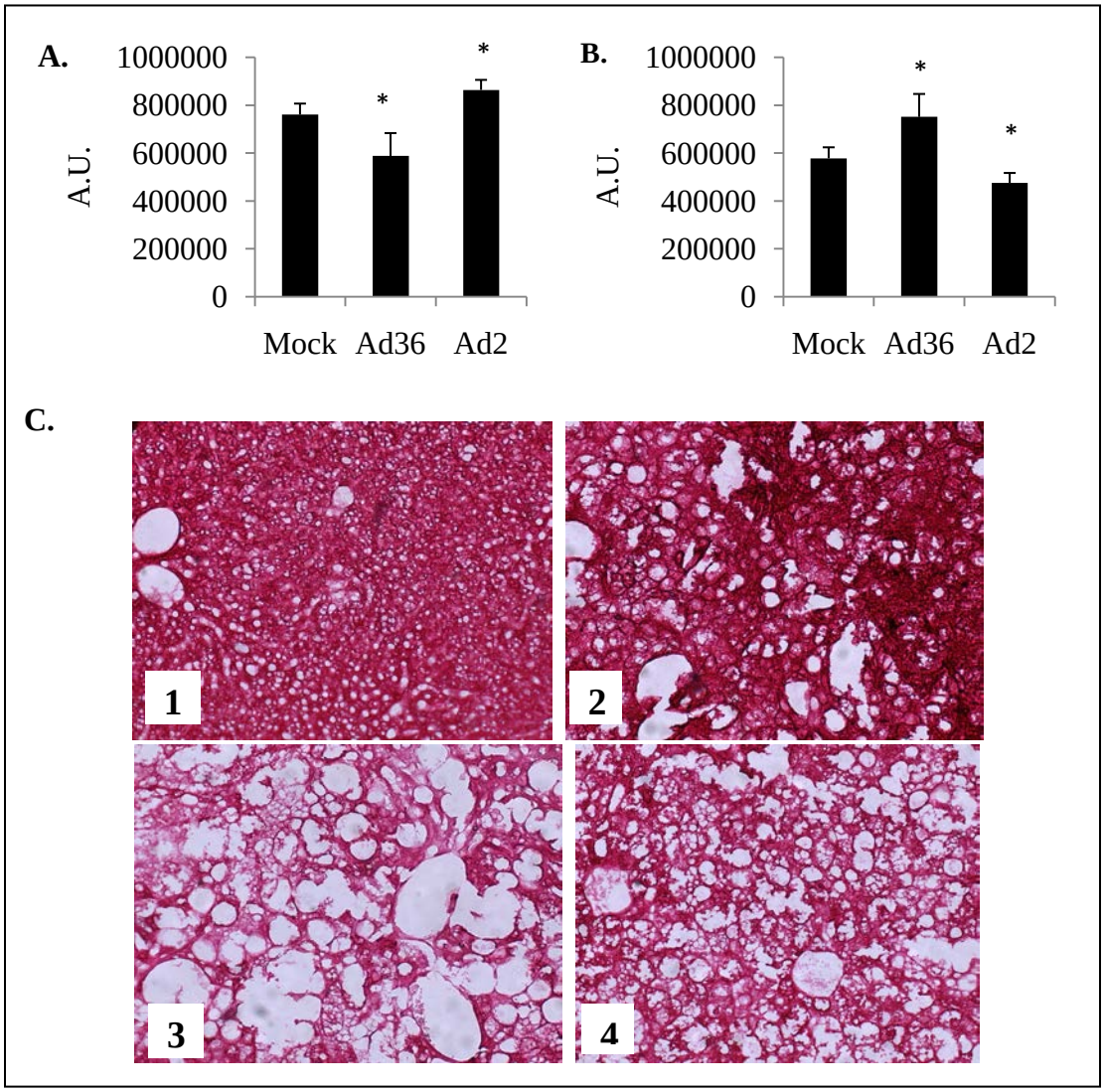


**Figure 14. Glycogen and Lipid Quantitation in Liver of Mice on a HFD.** Liver glycogen and lipid quantification in C57BL/6J mice on HFD. A) Quantification of hepatic lipid content, measured as glycogen staining-total pixel area of 10X photo. Mean ± SD. Ad36 has significantly less lipid than Mock, whereas Ad2 has significantly more lipid than Mock (p=0.02 and 0.02, respectively). B) Quantification of hepatic glycogen content, Mean ± SD. Compared to the Mock group, glycogen content was greater in Ad36 group (p=0.02), and lesser for Ad2 group (p=0.02). C) Representative 10X images of liver section stained for glycogen. Pink color is glycogen, white is lipid. 1. Liver of mouse on chow diet, 2. Ad36 HFD, 3. Ad2 HFD, and 4. Mock HFD. Krishnapuram et al, American Journal of Physiology Endocrinology and Metabolism, 2011, Am Physiol Soc, used with permission. (190)

### 3.3 Objective 3. Determine if the E4orf1 Protein of Ad36 Enhances Glucose Disposal in Adipose Tissue and Liver, and If It Alters Lipid Metabolism in Liver for Lower Lipid Stores

#### 3A. Effect of E4orf1 in Adipocytes

##### 3A.1 Is E4orf1 Necessary for Ad36 Induced Glucose Uptake?

To determine if E4orf1 is necessary for Ad36 induced glucose uptake, E4orf1 siRNA was used to knock down E4orf1 expression following Ad36 infection in 3T3-L1 adipocytes, and a glucose uptake assay was conducted the next day. As expected, Ad36 transfected with nontargeting siRNA has a 70% increase in glucose uptake compared to Mock infected cells transfected with E4orf1 siRNA (p=0.05). Knockdown of E4orf1 in Ad36 infected cells, however, abrogated glucose uptake increased by Ad36 (Figure 15). E4orf1 therefore is necessary for Ad36 induced glucose uptake.

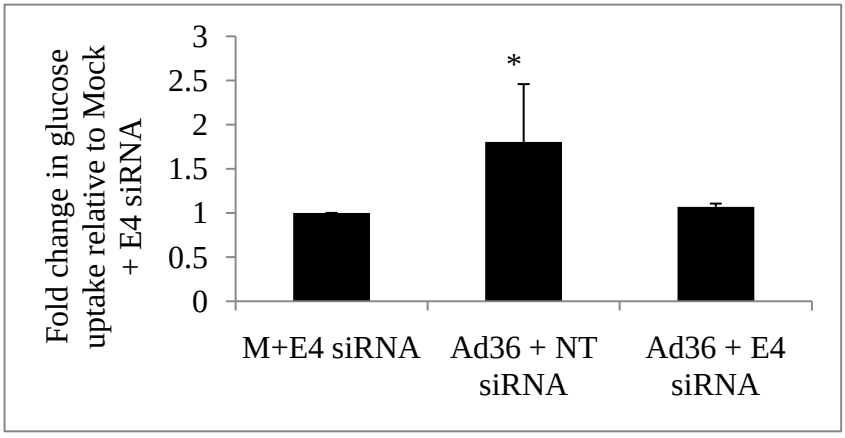


**Figure 15. Glucose Uptake in 3T3-L1 with E4orf1 Knock Down.** Glucose uptake in 3T3-L1 cells, three groups: Mock cells transfected with E4siRNA, Ad36 infected cells transfected with nontargeting siRNA and Ad36 infected cells transfected with E4orf1 siRNA. Expressed as fold change relative to M+E4siRNA $\pm$ SD because three separate experiments with statistically significant results are combined. Ad36 + NT siRNA has significantly greater glucose uptake than Mock + E4 siRNA group (p=0.05).

### 3A.2 Is E4orf1 Sufficient to Increase Glucose Uptake?

The ability of E4orf1 expression alone, without Ad36 infection, to increase glucose uptake was determined in 3T3-L1 preadipocytes and adipocytes. V5-Ad36 E4orf1 or Null plasmids were transfected into preadipocytes and differentiated adipocytes, and a 2DG uptake assay was conducted. In preadipocytes, basal glucose uptake was

greater in E4orf1 transfected cells compared to cells transfected with Null vector by about 2-fold ($p<0.0001$) (Figure 16A), and E4orf1 did not add to the effect of insulin in preadipocytes. In adipocytes, on the other hand, glucose uptake was significantly more in the basal and insulin stimulated conditions ($p<0.0001$ and $= 0.003$, respectively)(Figure 16B). This is perhaps because adipocytes are more responsive to respond to insulin than preadipocytes.

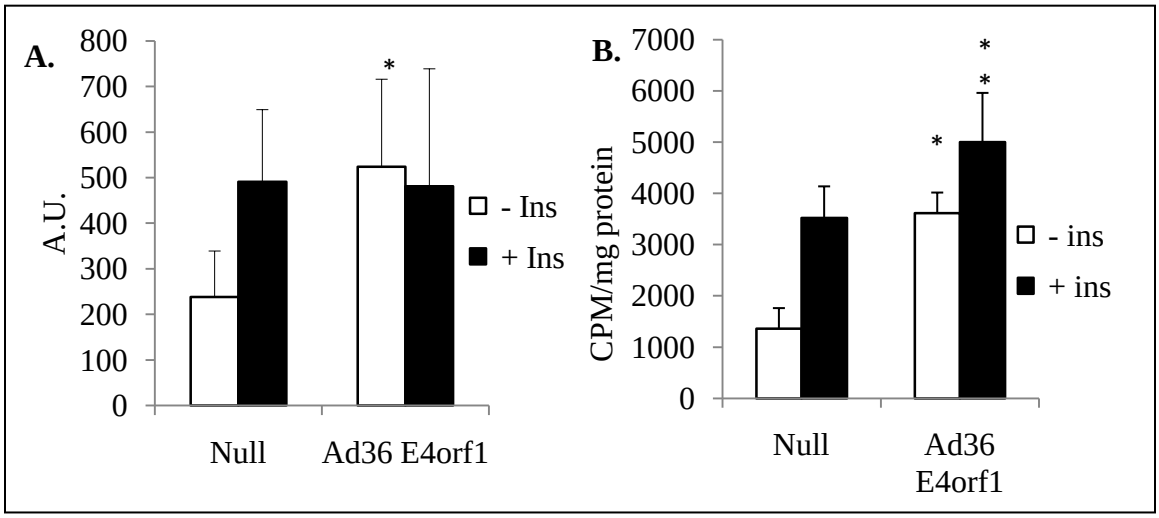


**Figure 16. Glucose Uptake in 3T3-L1 After E4orf1 Transfection.** 2DG uptake in 3T3-L1 after transfection with V5-Ad36 E4orf1 or Null plasmids**.** A) 2DG glucose uptake in 3T3-L1 preadipocytes transfected with either V5-Ad36 E4orf1 or Null vector, treated with or without 100 nM insulin. E4orf1 transfection increased basal glucose uptake compared to the Null vector transfected group ($p=0.0001$). Data expressed as mean $\pm$ SD. B) 2DG glucose uptake in 3T3-L1 adipocytes transfected with either V5-Ad36 E4orf1 or Null vector, treated with or without 100 nM insulin. E4orf1 transfection increased basal and insulin stimulated glucose uptake compared to the Null vector transfected group ($p=0.0001$ and 0.003, respectively). Data expressed as mean $\pm$ SD.

The ability of E4orf1 to increase cellular glucose uptake in a dose dependent manner was next determined. The E4pTRE cell line was exposed to varying levels of E4orf1 expression in response to 0, 750, or 1,000 ng/mL Doxycycline for 24 hr and glucose uptake was determined. Compared to the E4orf1 cell line without Doxycycline

treatment, treatment with both 750 and 1,000 ng/mL Doxycycline for 2 levels of E4orf1 expression induces greater glucose uptake ($p=0.05$ and $p=1.8*10^{-6}$, respectively), although this relationship is only statistically significant for E4orf1 with 1,000ng/mL Doxycycline after a Bonferroni correction for multiple comparisons (Figure 17). Glucose uptake in E4orf1 with 1,000 ng/mL Doxycycline is also significantly more than in the pTRE empty vector cell line ($p=2.6*10^{-7}$). Therefore, a trend in glucose uptake in response to E4orf1 expression is evident, and E4orf1 is able to induce glucose uptake in two different systems (transfection and inducible).

### 3A.3 The Effect of E4orf1 on DNL in 3T3-L1 Preadipocytes

DNL was determined in 3T3-L1 transfected with V5-Ad36 E4orf1 and Null plasmids. Compared to transfection with Null vector, E4orf1 transfection significantly increased DNL from [14C]-Glucose in the basal and insulin stimulated conditions. ($p=0.038$ for both) (Figure 18). Thus not only does E4orf1 increase glucose uptake, but it also promotes conversion of that glucose to lipids.

### 3A.4 Cell Signaling Involved in E4orf1 Induced Glucose Uptake in 3T3-L1

#### 3A.4.1 Total and Isoform-specific Ras Activation by E4orf1

Ad36 activates Ras, and requires Ras for increasing cellular glucose uptake (188). We therefore hypothesized that E4orf1 may be sufficient to activate Ras. The E4pTRE cell line was used to determine Ras activation, after 24 hours of E4orf1 expression in response to 1,000 ng/mL Doxycycline. The E4pTRE cell line had significantly more total and activated Ras compared to pTRE exposed to 1,000 ng/mL Doxycycline ($p=0.04$ and 0.01, respectively)(Figure 19), and specifically

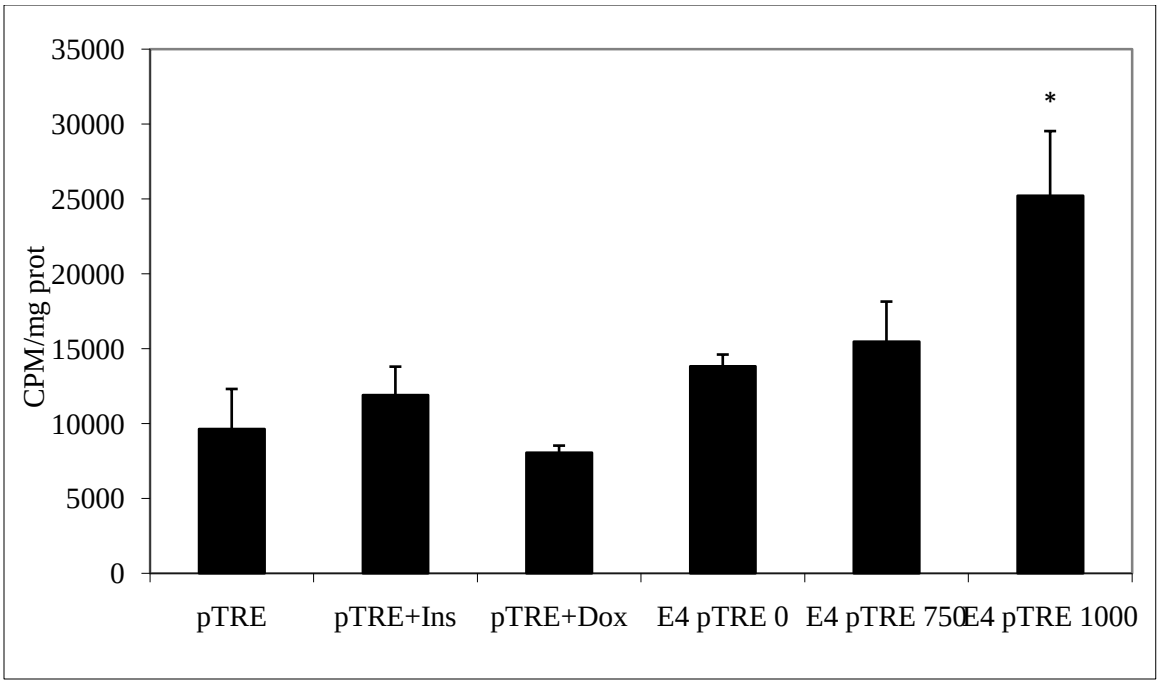


**Figure 17. Glucose Uptake in E4pTRE or pTRE Cell Lines.** Dose response in 2DG uptake in E4pTRE and pTRE cell lines. pTRE cell line was used as a baseline control, and the E4pTRE cell line was exposed to varying levels of E4orf1 expression in response to 0, 750, or 1,000 ng/mL Doxycycline treatment for 24 hr. pTRE was also treated with 100 nM insulin as a positive control for the assay, and 1,000 ng/mL Doxycycline (n=2) as a control for Doxycycline treatment. E4pTRE exposed to 1,000 ng/mL Doxycycline had significantly greater glucose uptake compared to E4pTRE exposed to 0 ng/mL Doxycycline, and compared to the pTRE cell line ($p=1.8*10^{-6}$ and $2.6*10^{-7}$). Data expressed as Mean $\pm$ SD.

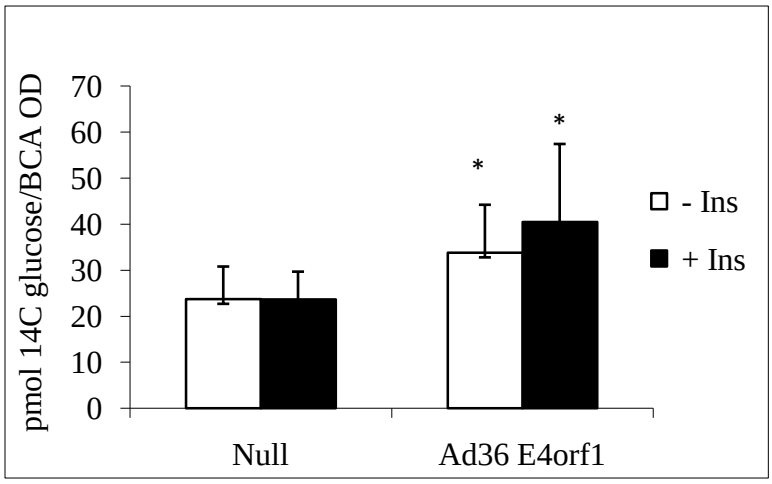


**Figure 18. DNL in 3T3-L1 Following E4orf1 Transfection.** DNL following transfection of 3T3-L1 preadipocytes with V5-Ad36 E4orf1 or Null plasmids, with or without 100 nM insulin. Data expressed as pmol [14C]-glucose in the lipid fraction divided by protein content, Mean $\pm$ SD. DNL is significantly

greater with E4orf1 transfection in the basal and insulin stimulated condition (p=0.04 for both).

the H-Ras isoform was activated (p=0.01). While the total N-Ras isoform abundance was up-regulated by E4orf1 (p=0.0001), N-Ras was not significantly activated by E4orf1. The K-Ras isoform was not easily detectable in 3T3-L1, and no change in abundance or activation was apparent (data not shown). Therefore, H-Ras may be the predominant form activated by E4orf1 for its downstream actions.

### 3A.4.2 The Effect of Ad36 and E4orf1 on Cell Transformation

Ras, an oncogene in certain cases, is activated by Ad36 and E4orf1. Therefore, to determine if Ad36 or E4orf1 induce cell transformation, a soft agar anchorage-independent growth assay was performed for E4orf1 constitutive expressing and Ad36 infected 3T3-L1. A549 bronchial carcinoma cells served as a positive control, and formed colonies within the agar as expected. Neither Ad36 infection or constitutive E4orf1 expressing cells developed colonies, even 21 days post plating, indicating both are unable to transform 3T3-L1 (Figure 20).

### 3A.4.3 The Effect of E4orf1 on Distal Insulin Signaling, Adiponectin, and Glut1

Ad36 can up-regulate distal insulin signaling (PI3K and Glut4) despite impaired proximal IR and IRS-1/2 signaling(188). Because E4orf1 is sufficient to increase glucose uptake, we hypothesized that it may be sufficient to up-regulate distal insulin signaling. The inducible E4orf1 expressing 3T3-L1 cell line was exposed

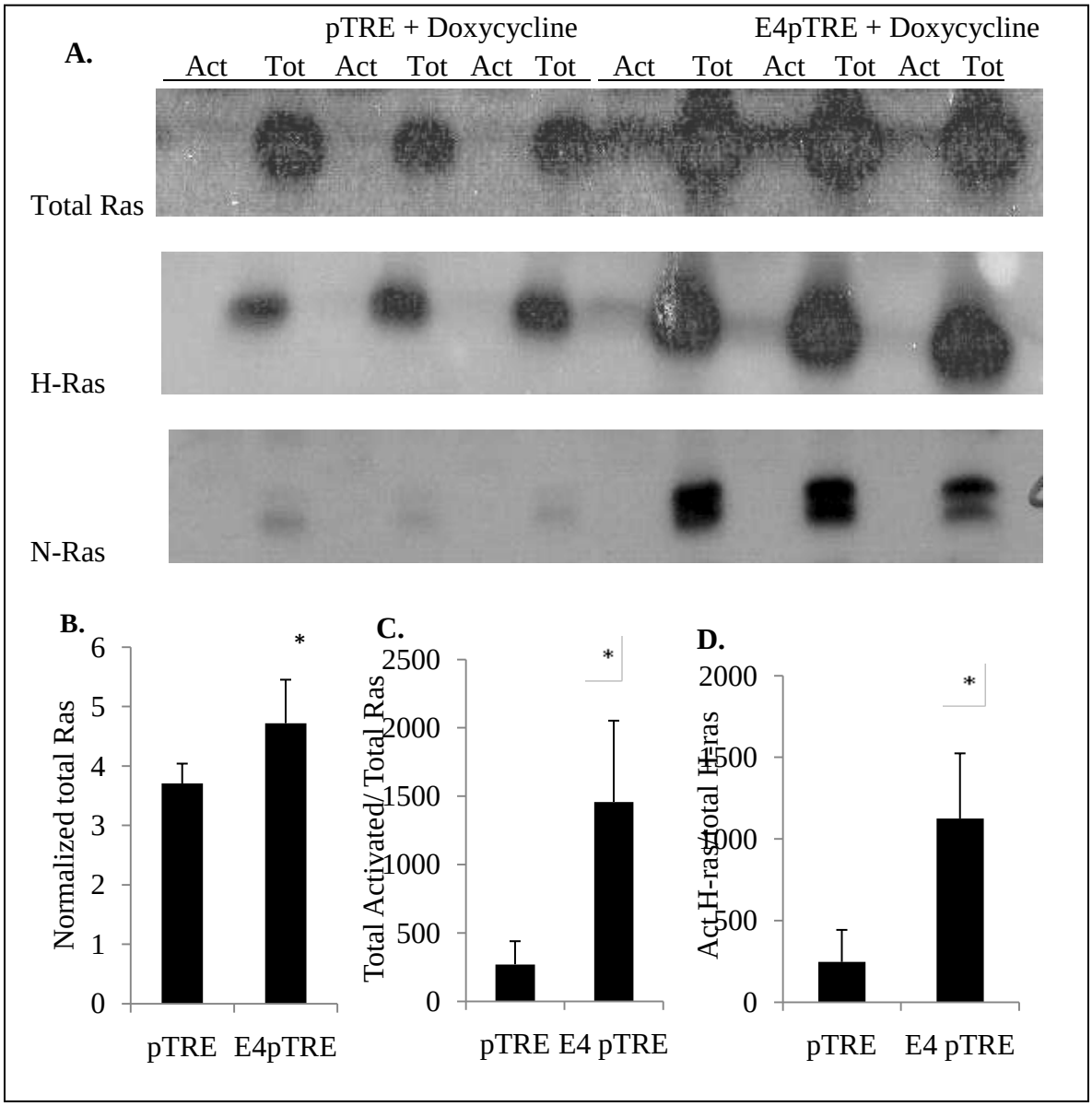


**Figure 19. Ras Activation by E4orf1.** E4pTRE or pTRE cell lines were exposed to E4orf1 for 24 hr in response to 1,000 ng/mL Doxycycline. A pull down for the Ras binding domain of Raf was conducted for the detection of activated Ras (Act) and before the pull down, 6% of the total lysate was loaded for normalization to total Ras (Tot). A) WB of Total, H-Ras, and N-Ras. B) Densitometry data for total Ras normalized to β-actin, expressed as Mean ± SD. E4pTRE clone has significantly more total Ras than pTRE (p=0.04) C) Densitometry for activated Ras, expressed as the ratio of activated to normalized total Ras, Mean ± SD. E4pTRE clone has significantly more total Ras activation than pTRE (p=0.01)D) Densitometry for activated H-Ras, expressed as the ratio of activated H-Ras to normalized total H-Ras. E4pTRE clone has significantly more H-Ras activation than pTRE (p=0.01)

to 1,000 ng/mL Doxycycline, and protein was harvested 24 hours later to determine AKT activation and Glut4 abundance. E4orf1 expression increases both AKT phosphorylation ($p=3.5*10^{-5}$), which is indicative of PI3K activity, and Glut4 abundance ($p=0.05$) (Figure 21). This may be the pathway by which E4orf1 increases glucose uptake, and this is especially likely since this pathway is required for Ad36-induced increase in cellular glucose disposal.

### 3A.4.4 Effect of E4orf1 on Adiponectin and Inflammatory Cytokine mRNA Expression

Ad36 may also mediate its favorable effects on systemic glucose metabolism through adiponectin(190). Adiponectin, in addition to its favorable effects on glucose metabolism, is anti-inflammatory in adipose tissue (68). Early genes of adenoviruses are also known to be anti-inflammatory. If E4orf1 is sufficient to increase adiponectin levels and decrease inflammatory cytokine expression in adipose tissue, this may benefit the metabolic profile of adipose tissue. To determine the effect of E4orf1 on adiponectin and inflammatory cytokines, the E4pTRE and pTRE cell lines were exposed to 1,000 ng/mL Doxycycline and RNA was harvested 24 hours later. Real-time PCR was used to quantitate adiponectin and inflammatory cytokine mRNA expression levels. E4orf1 significantly increased adiponectin expression ($p=0.05$), and suppressed MCP-1, MCSF, and TLR-4 expression ($p=4.9*10^{-4}$, $1.43*10^{-7}$, and $7.5*10^{-5}$, respectively) (Figure 22). These data suggest that E4orf1 may increase adipose tissue adiponectin levels and suppress inflammation.

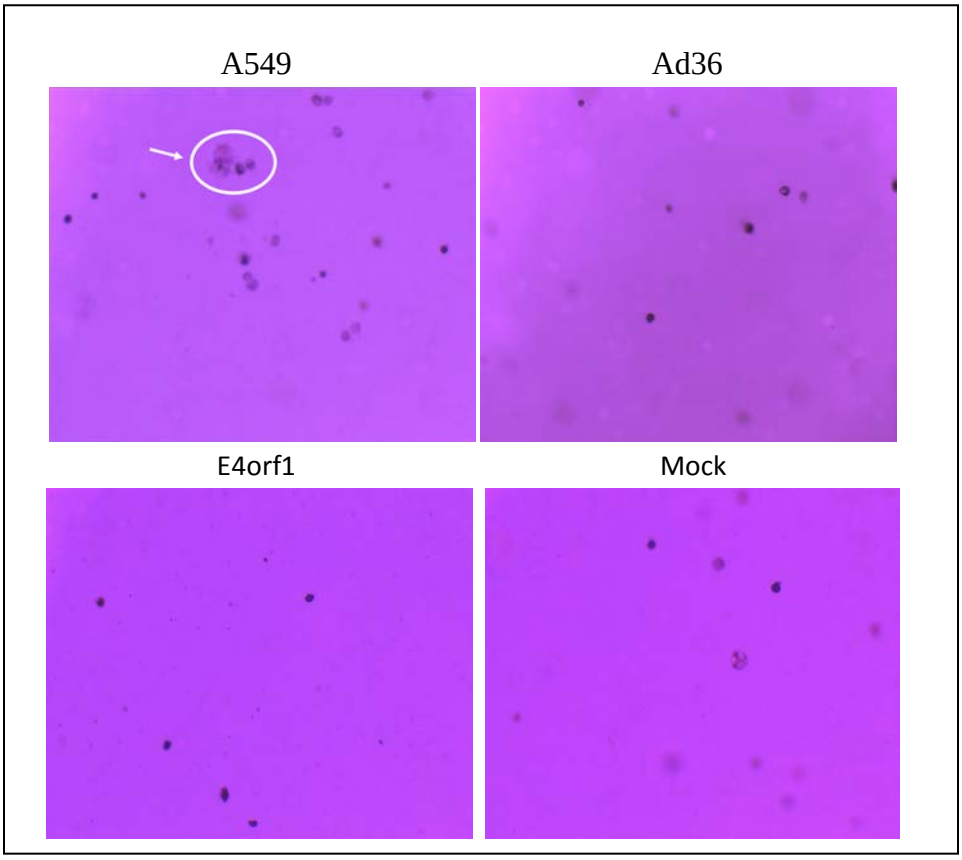


**Figure 20. Soft Agar Anchorage Independent Growth Assay.** Soft agar colony formation. Representative 10X images of colony formation, Day 21 post plating. A549 developed colonies, whereas Ad36, E4orf1 constitutives, and Mock infected 3T3-L1 did not.

**Table 3.** Percent of Viable Cells that Formed Colonies in Soft Agar Assay. Mean ± SD.

| | Day 7 | Day 14 | Day 21 |
|---|---|---|---|
| A549 | 11.3±9.1 | 9.2±2.1 | 9.9±8.6 |
| Ad36 | 0 | 0 | 0 |
| Mock | 0 | 0 | 0 |
| E4orf1 | 0 | 0 | 0 |

### 3A.5 Can E4orf1 Induce Glucose uptake Independent of PPARγ?

E4orf1 induces adipogenesis and up-regulates PPARγ similar to the action of TZDs. We therefore determined if glucose uptake induced by E4orf1 requires PPARγ. MEF PPARγ KO cells were transfected with V5-E4orf1 and Null-V5 plasmids. Even in the absence of PPARγ, E4orf1increased glucose uptake by nearly 2-fold ($p=2.5*10^{-5}$) (Figure 23). Considering PPARγ is required for preadipocyte differentiation, this indicates that E4orf1 does not require adipocyte differentiation for increasing glucose uptake, and that the two effects may be uncoupled if the molecular mechanism can be further elucidated.

## 3B. The Effect of E4orf1 on Hepatic Glucose and Lipid Metabolism

### 3B.1 The Effect of E4orf1 on Glucose Output in Hepatocytes

Uncontrolled hepatic glucose output contributes to hyperglycemia in insulin resistance. If E4orf1 is able to suppress glucose output, that may explain improved glycemic control in Ad36 infected animals. Glucose output by HepG2 cells was determined following transfection with V5-Ad36 E4orf1, V5-Ad2 E4orf1, and Null plasmid. In serum free, glucose free conditions, insulin suppressed glucose output as expected. Ad36 E4orf1 markedly suppressed glucose output in both the basal and insulin stimulated condition ($p=7.3*10^{-7}$ and 0.002, respectively) (Figure 24A), whereas Ad2 E4orf1 did not. Interestingly, E4orf1 also suppresses glucose output in the presence of cAMP and dexamethasone (gluconeogenic stimulators), in basal and insulin stimulated conditions (p=0.00001 and 0.003, respectively) (Figure 24B). Glucose output was also determined in primary mouse hepatocytes transfected with V5-E4orf1 or Null plasmids in serum starved condition, and when challenged with

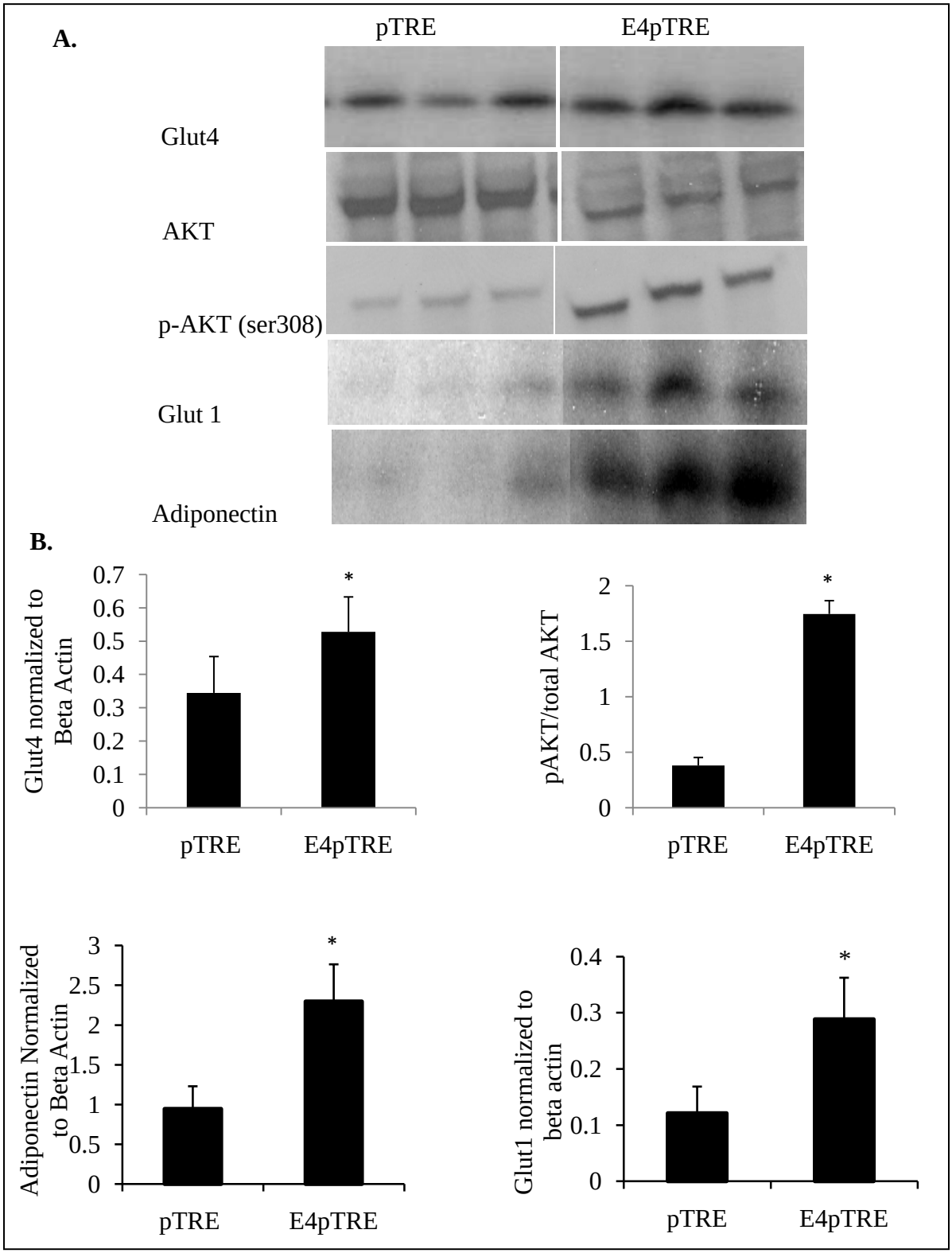


**Figure 21. Effect of E4orf1 on Distal Insulin Signaling, Glut1 and Adiponectin.** Signaling in E4pTRE and pTRE cell lines. A) WB of Glut4, total and phosphorylated AKT, adiponectin, and Glut1 in E4pTRE and pTRE cell lines, both treated with 1,000 ng/mL Doxycycline. B) Densitometry for Glut4, AKT, Glut1, and adiponectin. Glut4,

Glut1, and adiponectin are normalized to β-actin, and AKT activation is expressed as the ratio of phosphorylated AKT to total AKT. Expressed as the Mean ± SD. The E4orf1 expressing cell line had significantly greater abundance of Glut4 (p=0.05), Glut1 (p=0.01), adiponectin (p=0.006) and phosphorylated AKT ($3.5*10^{-5}$) compared to the pTRE empty vector control.

100 nM glucagon. In the serum and glucose starved condition, Ad36 E4orf1 and Ad2 E4orf1 both suppressed glucose output compared to the Null vector (p=0.0001 and 0.0003, respectively) (Figure 25A). When treated with glucagon, however, only Ad36 E4orf1 was sufficient to suppress glucose output from primary hepatocytes (p=0.02) (Figure 25B). Ad2 E4orf1 was not able to suppress glucose output from human HepG2 cells; therefore, E4orf1 of Ad36 may be a stronger suppressor of glucose output compared to Ad2 E4orf1.

### 3B.2 The Effect of E4orf1 on Hepatic Lipid Accumulation

#### 3B.2.1 The Effect of E4orf1 on Hepatic Fatty Acid Oxidation

Ad36 attenuates high fat diet induced steatosis, but the mechanism is unknown. We hypothesized that E4orf1 may alter hepatic lipid metabolism, resulting in less hepatic lipid storage. First, palmitate oxidation was measured in HepG2 transfected with Ad36 E4orf1, Ad2 E4orf1, or Null plasmid. Both complete oxidation and partial [14C]- palmitate were measured. Although total (complete + partial) oxidation did not differ between the Null and E4orf1 transfected cells (Figure 26A), the amount of completely oxidized palmitate was significantly higher in Ad36 E4orf1 and Ad2 E4orf1 transfected cells (p=0.004 and 0.01, respectively) (Figure 26B). Because total oxidation is not significantly altered by E4orf1, we hypothesized that the ratio of complete to partial oxidation may differ. After Ad36 E4orf1, Ad2 E4orf1, and null vector transfection, complete ($CO_2$) and partial (acid soluble metabolites) were

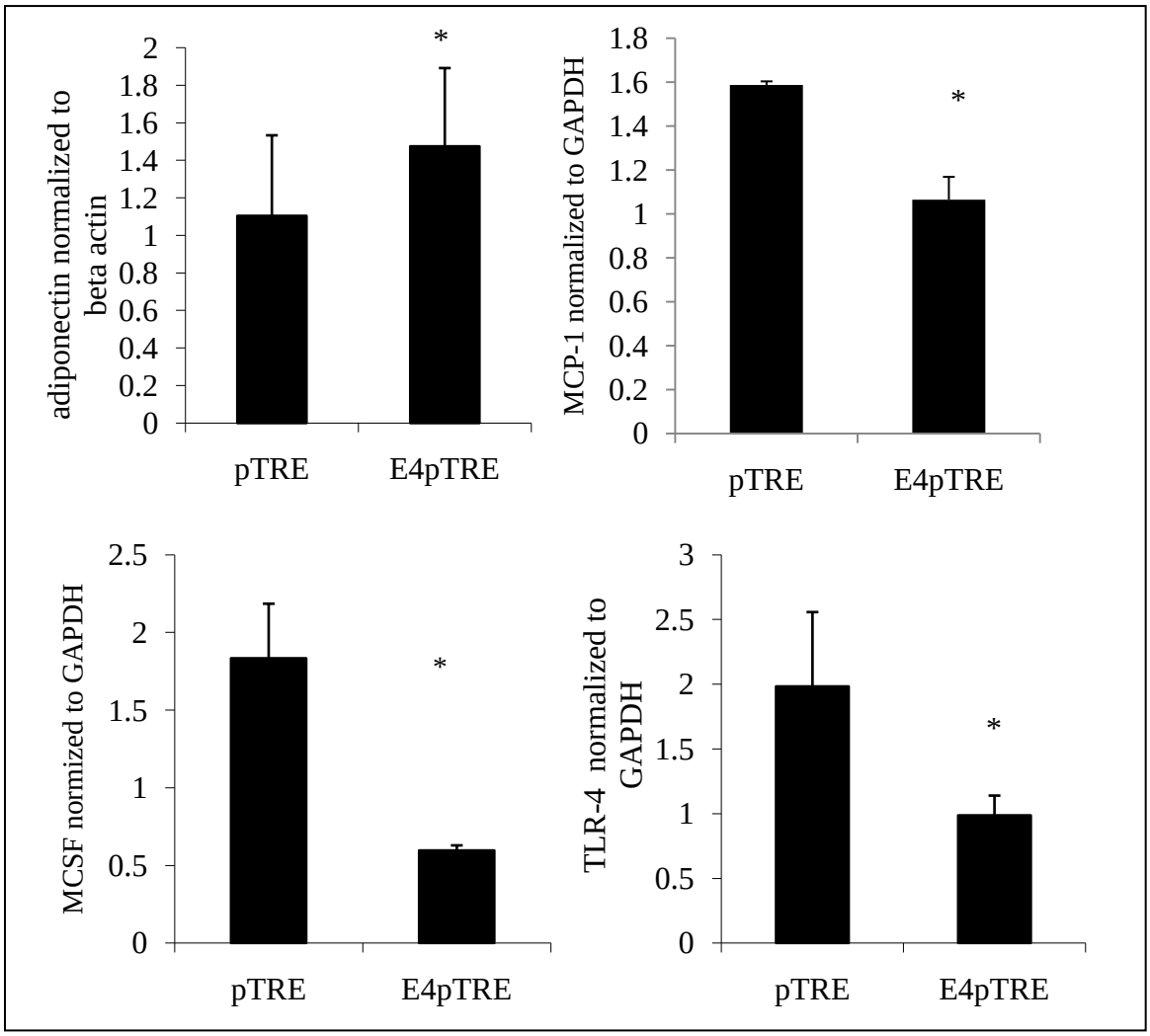


**Figure 22. Effect of E4orf1 on Adiponectin and Inflammatory Cytokine mRNA Expression.** Inflammatory cytokine and adiponectin mRNA expression in E4pTRE and pTRE cell lines. E4pTRE and pTRE cell lines were exposed to 24 hr E4orf1 expression in response to 1,000 ng/mL Doxycycline. Normalized mRNA expression in E4orf1pTRE and pTRE empty vector control inducible stable cell lines, Mean $\pm$ SD. A) Adiponectin expression is greater in E4pTRE than pTRE cell line (p=0.05), B) MCP-1 ( $p=4.9*10^{-}4$), C)MCSF, ($p=1.43*10^{-7}$, and D) TLR-4 ($p=7.5*10^{-5)}$ had lower expression in E4pTRE compared to pTRE.

measured. The percent partial oxidation was significantly lower in Ad36 E4orf1 and Ad2 E4orf1 transfected cells compared to the Null vector (p=0.002 for both) (Figure 27A). In addition, E4orf1of both viruses significantly decreases the ratio of incomplete to complete oxidation (p=0.003 and 0.007, respectively) (Figure 27B).

This indicates that E4orf1 of Ad36 and Ad2 may up-regulate mitochondrial oxidation, and minimize partial oxidation that can lead to the buildup of intermediate metabolites.

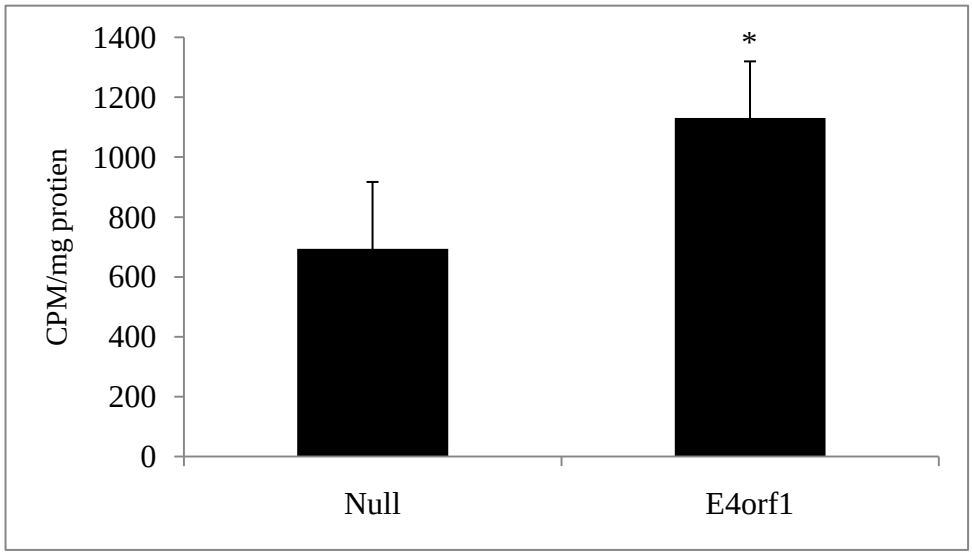


**Figure 23. Glucose Uptake in MEF PPARγ KO Cells Following E4orf1 Transfection.** Glucose uptake in MEF PPARγ KO cells following E4orf1 transfection. E4orf1 significantly increases glucose uptake ($p=2.5*10^{-5}$), even without PPARγ. Mean ± SD.

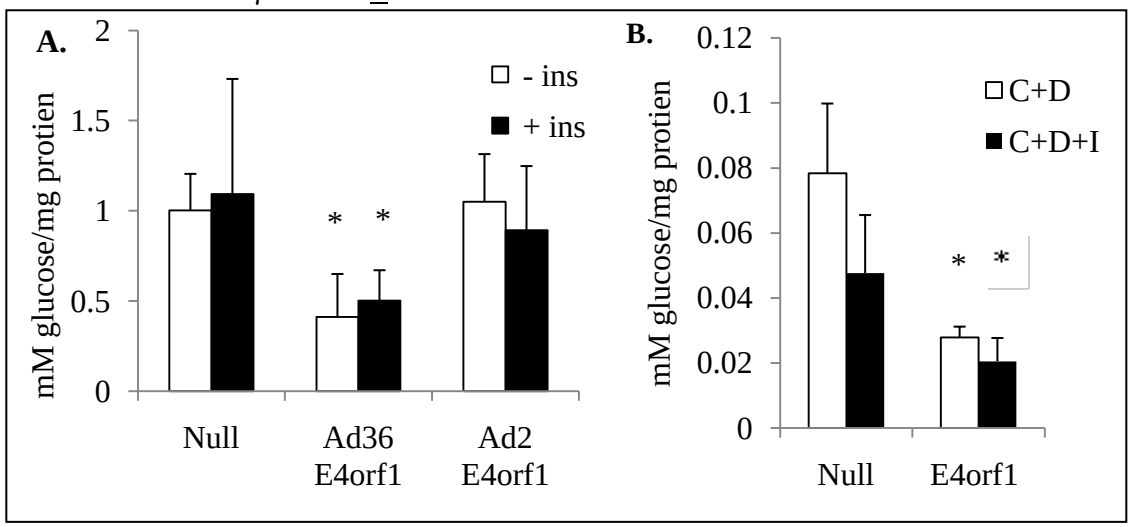


**Figure 24. Glucose Output by HepG2 Transfected with E4orf1.** Glucose output by HepG2 cells following Ad36 E4orf1, Ad2 E4orf1, or Null Vector transfection. A) Glucose output in serum and glucose starved condition, w/ and w/o 10 nM insulin, expressed as fold change relative to Null. Mean ± SD (fold change because data from two separate experiments are combined). Ad36 E4orf1 suppresses glucose output compared to basal and insulin stimulated Null transfected cells ($p=7.3*10^{-7}$ and 0.002, respectively), whereas Ad2 E4orf1 does not. B) Glucose output in HepG2

stimulated with gluconeogenic cAMP (1 mM) (C) and Dexamethasone (500 nM) (D) in the absence or presence of insulin (I). Expressed as Mean mM glucose per mg of protein, ± SD.

### 3B.2.2 The Effect of E4orf1 on Hepatic De Novo Lipogenesis

A DNL assay determined if E4orf1 suppresses synthesis of lipid from glucose in HepG2. HepG2 were transfected with Ad36 E4orf1, Ad2 E4orf1, or Null plasmid and exposed to [14C]-glucose for determination of conversion of glucose to lipid. Ad-36 E4orf1, but not Ad2 E4orf1, significantly suppressed DNL in HepG2 cells ($p=0.01$) (Figure 28).

### 3B.2.3 The Effect of E4orf1 on Hepatic ApoB Secretion

Lipid export was determined in HepG2 cells transfected with Ad36 E4orf1, Ad2 E4orf1, or Null vector. We hypothesized that E4orf1 may up-regulate export of

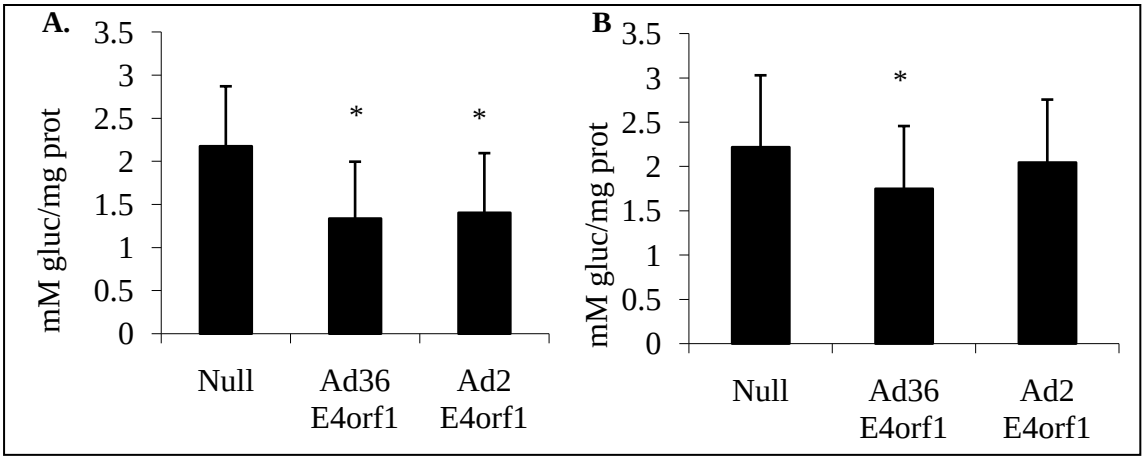


**Figure 25. Glucose Output from Primary Hepatocytes Transfected with E4orf1.** Glucose output in primary mouse hepatocytes after transfection with Ad36 E4orf1, Ad2 E4orf1, or Null vector. A) Glucose output by primary hepatocytes serum and glucose starved for 1.5 hours, expressed as mean mM glucose per mg protein + SD. Ad36 E4orf1 and Ad2 E4orf1 suppressed glucose output compared to Null vector ($p=0.0001$ and 0.0003, respectively). B) Glucose output in primary hepatocytes treated with 100 nM glucagon in serum free, glucose free media for 1.5 hr. Only

Ad36 E4orf1 suppressed glucose output in this condition (p=0.02). Expressed as mean mM glucose per mg protein, ± SD.

lipid, which may contribute to lower hepatic lipid storage observed in Ad36 infected mice. ApoB secretion is indicative of VLDL export, therefore, an ELISA determined ApoB levels in conditioned media following transfection. Ad36 E4orf1 significantly up-regulated ApoB secretion into media (p=0.01) (Figure 29), whereas Ad2 E4orf1 does not.

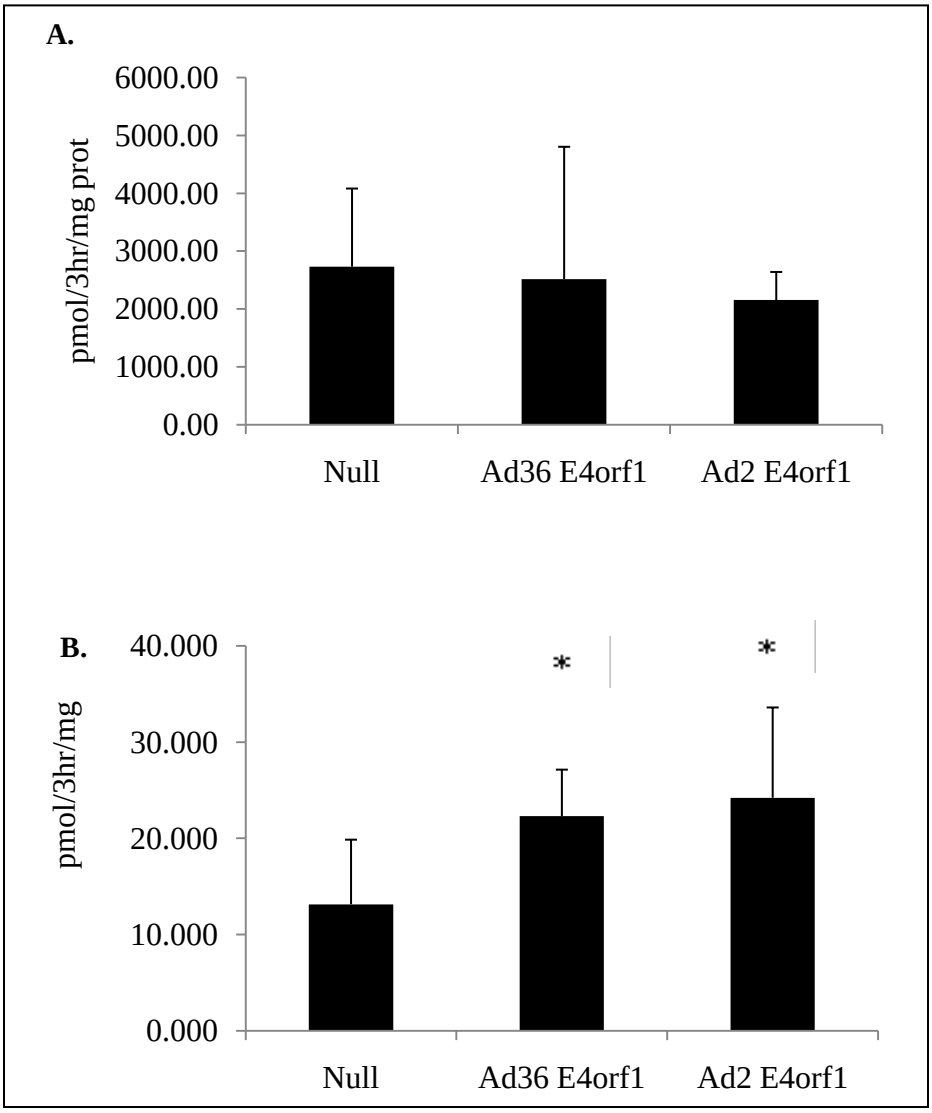


**Figure 26. Fatty Acid Oxidation in HepG2 Transfected with E4orf1.** HepG2 fat oxidation after E4orf1 transfection. HepG2 [14C]- palmitate oxidation following Ad36 E4orf, Ad2 E4orf, or Null vector. A) Total

palmitate oxidation (complete + partial), expressed as pmol palmitate/3hr/mg protein, Mean ± SD. No significant differences. B).Complete palmitate oxidation, expressed as pmol palmitate/3hr/mg protein mean ± SD. Ad36 E4orf1 and Ad2 E4orf1 have significantly greater complete oxidation of palmitate than Null (p=0.004 and 0.01, respectively.

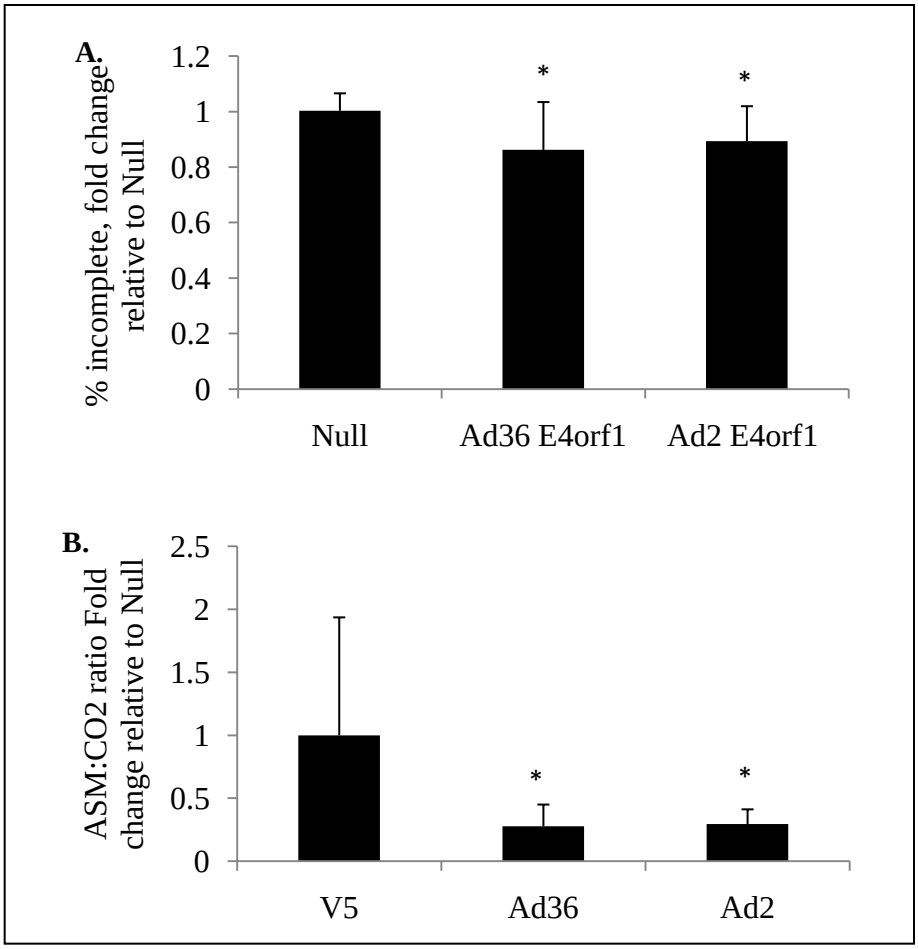


**Figure 27. Partial and Complete Fat Oxidation in HepG2 Transfected with E4orf1.** HepG2 complete and partial fat oxidation after E4orf1 transfection After Ad36 E4orf1, Ad2 E4orf1, or Null transfection, change in percentage of complete and partial [14C]-palmitate oxidation. A) Percent partial palmitate oxidation, expressed as fold change in percent, mean ± SD, compared to Null. Ad36 E4orf1 and Ad2 E4orf1 have significantly lower percent partial oxidation (p=0.002, respectively). B) Ratio of acid soluble metabolites (incomplete oxidation) to $CO_2$ (complete oxidation), expressed as mean fold change relative to null ± SD. Ad36 E4orf1 and Ad2 E4orf1 have significantly lower ratios compared to Null (p=0.003 and 0.007, respectively).

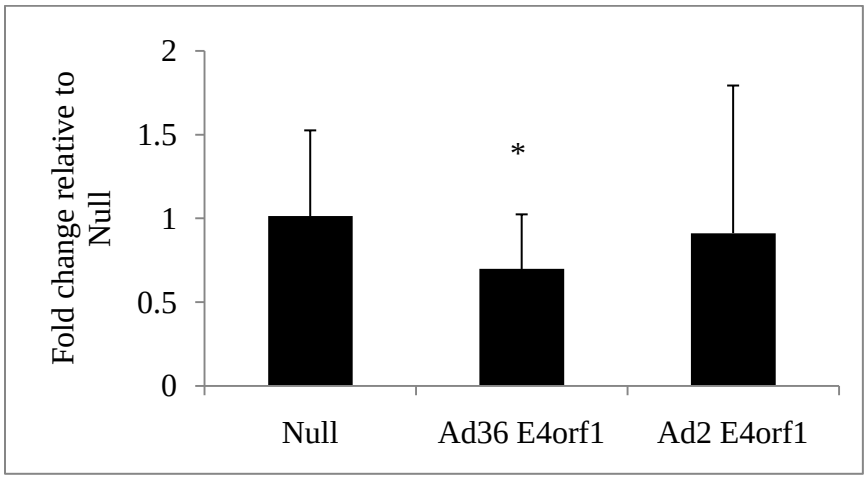


**Figure 28. DNL in HepG2 Transfected with E4orf1.** DNL in HepG2 following E4orf1 transfection. HepG2 cells were transfected with Ad36 E4orf1, Ad2 E4orf1, or Null vector. Expressed as mean fold change in pmol [14-C]-glucose/mg protein relative to Null, ± SD. Two separate experiments were combined. Ad36 E4orf1, but not Ad2 E4orf1, significantly decreases DNL compared to Null (p=0.01).

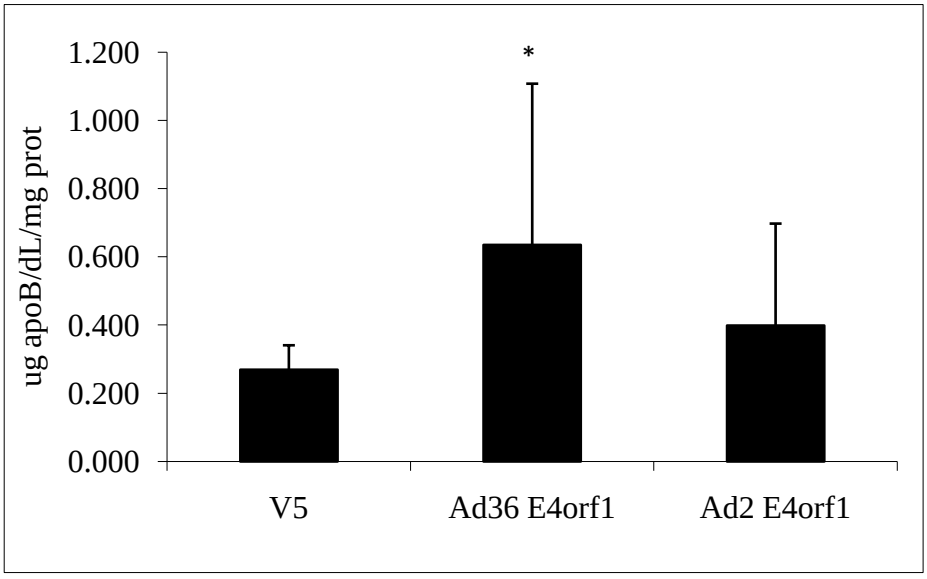


**Figure 29. ApoB Secretion from HepG2 Transfected with E4orf1**. HepG2 ApoB secretion following Null vector (V5), Ad36 E4orf1, and Ad2 E4orf1 transfection. ApoB secretion in conditioned media from HepG2 transfected with Ad36 E4orf1, Ad2 E4orf1, or Null vector. Expressed as mean µg ApoB/dL/mg protein, ± SD. Ad36 E4orf1 increased ApoB secretion into media compared to the Null vector (p=0.01).

# Chapter 4. Discussion

## 4.1 Overview of Findings

Ad36 infection is an excellent tool for the study of metabolically healthy obesity, and its anti-diabetic effects were demonstrated through three separate approaches. First, an association of Ad36 with better glycemic control in humans was established. In Caucasian, African American, and Hispanic children and adolescents, Ad36 seropositivity is associated with better glycemic control compared to the uninfected population. Next, to determine the potential mechanism, several *in vitro* experiments were conducted. Also, adipose tissue and liver from Ad36 infected C57BL/6J mice on chow and HFD were analyzed for changes in morphology following Ad36 induced improvement of glycemic control. Ad36 clearly up-regulates adipogenesis in hASC, and induces DNL and preferential fat oxidation in 3T3-L1. Ad36 increased the proportion of small adipocytes in chow fed mice and the proportion of larger adipocytes in mice on HFD. In both animal models, Ad36 did not affect macrophage infiltration. Both Ad36 and Ad2 increased adipose tissue vascularization in both mouse models, however, neither virus was able to induce angiogenesis in human adipose tissue or directly in endothelial cells. Finally, the E4orf1 protein of Ad36 was identified as necessary and sufficient for enhancing glucose disposal. Changes in glucose and lipid metabolism by viral protein E4orf1 were determined in 3T3-L1 preadipocytes and adipocytes, and HepG2 hepatocytes. In 3T3-L1, E4orf1 was sufficient and necessary to induce glucose uptake, and was sufficient to activate the same Ras-PI3K-Glut4 pathway employed by Ad36 for glucose uptake. Glucose uptake induced by E4orf1 was not dependent on PPARγ. In addition, E4orf1 up-regulated adiponectin and suppressed inflammatory cytokine production. In hepatocytes, E4orf1 suppressed glucose output and up-regulated fatty acid oxidation, lipid export, and suppressed DNL. Therefore, Ad36 is

likely to implement its favorable effect on glucose and lipid metabolism through its E4orf1 protein, which is a promising candidate for anti-diabetic therapy. These findings are discussed more in detail herein.

**4.2 Ad36 Seropositivity and Improved Glycemic Control in Humans**

Identifying an association between Ad36 seropositivity and glycemic control is an imperative first step towards harnessing any beneficial effect of the virus, since the phenomenon must be relevant in humans. It is noted that an association does not necessarily imply causation. Nevertheless, as reported in adults(188; 190), it is encouraging that seroprevalence of Ad36 in children and adolescents from several ethnicities is associated with lower fasting glucose, insulin, and HOMA IR independent of body fatness, gender, and familial relationship. Ad36 is therefore associated with improved glycemic control in a diverse range of genetic backgrounds. Hispanic children and adolescents are especially prone to developing insulin resistance (251; 252) and may have a stronger genetic predisposition towards metabolic complications. Despite this, Ad36 infection still demonstrates improved glycemic control in this population.

Ad36 seropositivity was also associated with lower intrahepatic lipid content in prepubertal children. This finding parallels the observation that Ad36 is associated with lower prevalence of NAFLD in adults (190; 253). Ad36 is therefore likely to prevent hepatic lipid accumulation in humans, which may contribute to the prevention of insulin resistance despite increased adiposity associated with infection. Specifically, hepatic lipid is associated with insulin resistance independent of body fatness (159; 171-175), therefore, the effect of Ad36 on hepatic lipid accumulation may improve glycemic control despite its effects on adiposity.

This association of improved glycemic control in Ad36 seropositive children and adolescents parallels what has been demonstrated in adults (188; 190). Antibody prevalence

does not indicate the time of infection, so the dynamics of improvement in glycemic control following infection are unknown. It is possible Ad36 infects and induces a lasting change in metabolism before clearance by the immune system, which is referred to as a "hit and run" effect. For example, gammaherpesvirus induces oncogenesis which persists long after infection is cleared (254). Alternatively, active Ad36 infection may persist at low level or remain latent and intermittently reappear to induce a change in glycemic control over time. Because adenoviral infections are common in childhood, however, and the effect of Ad36 is consistent from childhood to adulthood, it is likely that changes in glycemic control may be long-term following initial infection. Longitudinal studies following Ad36 infection are needed in the future to determine these dynamics.

Many infections have been linked to insulin resistance. "Pathogen load', a score based on presence of herpes simplex virus (HSV)-1, HSV-2, enteroviruses, and Chlamydia pneumonia, is associated with insulin resistance after controlling for age and BMI (255). This relationship was especially evident with Chlamydia pneumonia infection and enterovirus infection, and the authors suggest infection of multiple pathogens may lead to consistent low-grade inflammation that induces insulin resistance(255). Hepatitis C virus (HCV) is also associated with insulin resistance (256). Certain genotypes of HCV impair hepatic lipid export (257) and change hepatic lipid metabolism to promote viral replication(258). Parasitic *Trypanosoma cruzi* has a high tropism for adipose tissue, and alters inflammation and adipokine secretion, resulting in insulin resistance (259). Alternatively, lymphocytic choriomeningitis virus infection improves diabetes in mice (260; 261). Certain infections are evidently sufficient to alter inflammation, adipose tissue, and hepatic factors and in turn induce insulin resistance. It is therefore feasible that infectious agents may be capable of long-term changes in metabolism. In the case of Ad36

infection, adipose tissue and hepatic metabolism may be altered favorably for improvement of insulin sensitivity.

Because adipose tissue plays a critical role in mediating inflammation and response to infection, it is not surprising that infection may alter adipose tissue metabolism and insulin sensitivity. Several adipokines, especially adiponectin and leptin, mediate the immune response to infection (262). The function of macrophages and preadipocytes is so closely related that preadipocytes can convert to macrophage-like cells (263; 264). Adipose tissue has demonstrated antimicrobial activity, and the stromal vascular fraction of adipose tissue, which includes preadipocytes and macrophages, displays phagocytic activity(265). Macrophage number generally increases in response to infection. Therefore, if preadipocytes have macrophage function, it can be hypothesized their number may increase in response to infection as well, resulting in expansion of adipose tissue mass.

Although associations have been established, it is unclear if infections such as Ad36 play a causative role in improving glycemic control in humans. While establishing an association is an important first step, it is difficult to unequivocally establish causation. Several challenges are presented in the study of such a phenomenon. First, obesity and insulin resistance have insidious onset, and can develop over time. Linking a given factor to a causative role during this process can be challenging as a result. Also, many factors influence glycemic control. If an agent such as Ad36 is protective against the development of insulin resistance, controlling for all factors that may influence glycemic control is difficult. Identifying a perfect control group is therefore, challenging, since the glycemic control of the uninfected population could be influenced by many other factors. Lastly, definitively establishing a causative role of Ad36 in protection from

insulin resistance is not possible in humans because ethically, humans cannot be experimentally infected.

An alternative approach must be taken to establish a relationship between Ad36 and glycemic control in humans. Epidemiological associations, followed by prospective epidemiological studies, must first demonstrate the relevance of a particular phenomenon. The mechanism can be established through animal studies, and congruence between human and animal data can serve as confirmation of the mechanism. For instance, establishing the relationship between smoking and lung cancer, was accomplished in this manner. The Center for Disease Control (http://www.cdc.gov/cancer/lung/basic_info/risk_factors.htm#1) and National Cancer Institute (http://www.cancer.gov/cancertopics/factsheet/Tobacco/cessation#r1) state that smoking causes cancer, although all human studies on this topic are epidemiological. Extensive albeit indirect evidence has made a compelling argument in favor of a causative role for smoking in lung cancer. A similar approach will be needed to unequivocally determine any protective effect of Ad36 infection against obesity induced insulin resistance.

### 4.3 Adipose Tissue and Hepatic Determinants of Ad36 Induced Insulin Sensitivity

To determine how Ad36 may improve glycemic control, a series of *in vitro* and post-hoc studies of tissue from previous animal experiments were conducted. Changes in adipocyte metabolism, and adipose tissue and liver morphology were determined in response to Ad36 infection.

#### 4.3.1 Ad36 and Adipocyte Metabolism- *In vitro* Experiments

First, hASC were established as a model for the study of Ad36 induced differentiation of human preadipocytes. Ad36 successfully infected and spread in hASC, suggesting Ad36 may establish an active infection in human adipose tissue. Ad36 up-regulated differentiation and lipid

accumulation in hASC (202), even in the absence of adipogenic inducers, and therefore may induce preadipocytes to differentiate independent of mechanisms that normally regulate adipocyte differentiation such as nutrient and hormonal signals. Even with adipogenic induction, Ad36 infected hASC accumulated more lipid at a faster rate than uninfected control cells. Agents that induce adipocyte differentiation, such as TZDs, improve insulin sensitivity (130). The effect of Ad36 on adipogenesis has now been elucidated in 3T3-L1 and hASC (200; 247). Adipogenesis is one potential mechanism for Ad36 induced improvement in insulin sensitivity, in a manner similar to TZD treatment.

In 3T3-L1, Ad36 infection is not replicative, yet has an effect on adipogenesis(200). Signaling changes induced by Ad36 following cell entry in 3T3-L1 may act synergistically with those induced by confluence, since Ad36 induced greater lipid accumulation when cells were infected at confluence(247). Normally, confluence initiates 3T3-L1 cell cycle arrest, followed by 1-2 days of clonal expansion consisting of at least one mitotic division, which is then followed by an unusual state of growth arrest called $G_D$ that defines terminal cell differentiation, and begins the differentiation process (266; 267). Growth arrest is mediated by cAMP and PPARγ (267; 268), and Ad36 E4orf1 increases cAMP and PPARγ(203). Although Ad36 infection is not replicative in 3T3-L1, early viral genes are still expressed, and viral gene expression peaks 2-4 days post infection and only persists at very low levels up to day 7 post infection (200). Therefore, infection of 3T3-L1 at confluence probably results in peak E4orf1 expression, and thus peak activation of PPARγ and cAMP, may coincide just as cells are undergoing $G_D$ phase and initiating differentiation. This would explain the synergistic effect of infection and confluence and maximal lipid accumulation. Infecting cells 1-2 days prior to

confluence, on the other hand, may cause peak E4orf1 expression to be induced before this critical phase, and hence yield relatively lower lipid accumulation.

Adequate adipose tissue expansion can promote clearance of glucose and lipid during positive energy balance, and this process is important to prevent increased systemic free fatty acids and hyperglycemia (119). Ad36 increases LPL expression and translocation in hASC (202), suggesting it increases lipid clearance from circulation. In addition, Ad36 up-regulates glucose uptake in adipose tissue (188). Up-regulation of DNL in 3T3-L1 by Ad36 indicates glucose taken in cells may be converted into lipid, perhaps during the conversion of preadipocytes to adipocytes. This process would explain improved glucose clearance despite increased adiposity following Ad36 infection. Previous *in vivo* animal studies have also suggested Ad36 induces greater adipogenesis and DNL in response to infection (197). Although the contribution of adipose tissue DNL to lipid stores has been unclear in humans, it has been recently demonstrated that human adipocytes have the capacity for DNL, even if the overall contribution to lipid stores is minor (269; 270). Over a 9 week period, DNL can account for 20% of newly deposited triglyceride in human adipose tissue (270). Because human adipose tissue has the capacity for DNL, Ad36 should be tested in the future as an agent which may increase glucose clearance through up-regulation of adipogenesis and DNL in humans.

Adipocyte substrate oxidation was also altered by Ad36 infection, which induced preferential fatty acid oxidation in 3T3-L1. Interestingly, TZD treatment also increases fatty acid oxidation in adipocytes (271). Increased fatty acid oxidation may improve systemic clearance of free fatty acids, which is one proposed mechanism for the effect of TZD(272). In general, TZDs increase whole body fatty acid oxidation(126) and seem to improve mitochondrial dysfunction that is characteristic of insulin resistance. In fact, TZD treatment increases

mitochondrial biogenesis and uncoupling protein-1 expression in white adipose tissue (273), both of which promote fatty acid oxidation. Ad36 may have a similar effect on fatty acid oxidation due to upregulation of PPARγ and adipocyte differentiation, and energy requirements for viral replication.

Of note, Ad36 induces these phenomena despite only partial infection of cells in a given group, which biases against the virus for any given effect. Only a certain percentage of hASC and 3T3-L1 are infected by Ad36, and an effect is observed even though the remaining uninfected cells are theoretically similar to those of the control group. Overall, *in vitro* studies indicate Ad36 increased adipogenesis, DNL, and fatty acid oxidation, which may collectively improve adipose tissue expansion and lipid and glucose clearance, thereby improving glycemic control.

### 4.3.2 Ad36 Modulation of Adipose Tissue and Liver Morphology

*In vivo*, Ad36 may also alter adipose tissue morphology and the response of adipose tissue to a high fat diet. Cell size, macrophage infiltration, and vascularization were determined in response to infection in both C57BL/6J chow and high fat fed models through histochemical techniques.

Changes in adipocyte cell size are an indication of adipose tissue remodeling. Small adipocytes are usually a sign of hyperplasic adipose tissue expansion, and thus a larger capacity for adipogenesis and improved insulin sensitivity(122; 129). Larger adipocytes are usually indicative of adipocyte hypertrophy, which is associated with insulin resistance (151-156). However, both hyperplasia and hypertrophy can occur at the same time in response to positive energy balance, and the range of adipocyte size distribution is subsequently increased (274).

Interestingly, the hyperplastic response of adipose tissue to a high fat diet is strain dependent in mice, and an interaction between genes and diet on the hyperplastic response to positive energy balance is apparent (274). Therefore, other factors may also influence the relationship between cell size distribution and insulin resistance. While in some models small adipocyte size is associated with insulin sensitivity (68; 275), in others models large adipocytes are associated with insulin sensitivity(130; 276) as discussed in detail below.

In chow fed C57BL/6J mice, Ad36 increased glycemic control and the proportion of small adipocytes compared to Mock and Ad2 infected mice in retroperitoneal fat pads. Small adipocytes are a marker of adipogenesis, and characterize adipose tissue of several transgenic animal models of insulin sensitive adiposity (68; 122; 125). Small adipocytes have greater adiponectin secretion (122; 158), and this is congruent with previous observations that Ad36 increases adiponectin abundance in human adipose tissue. Therefore in normal healthy mice, Ad36 may improve adipose tissue metabolic profile by enriching the population of small, adiponectin secreting adipocytes.

In mice on HFD, on the other hand, Ad36 attenuate dysglycemia and increased the proportion of large adipocytes in epididymal fat compared to Mock and Ad2 infected animals. Normally large adipocytes are associated with inflammation, decreased secretion of adiponectin, increased insulin resistance, impaired glucose uptake and increased lipolysis (151-156). Some but not all parameters associated with large adipocyte size were apparent in Ad36 infected adipose tissue. Proximal insulin signaling is impaired in adipose tissue of infected mice, suggesting adipose tissue is more insulin resistant than Mock and Ad2 infected mice(190). In addition, Ad36 increased TNF-α expression in adipose tissue, suggesting inflammation is increases in adipose tissue (unpublished observations). Distal insulin signaling is not impaired,

however, and increased AKT phosphorylation, Glut 1 and Glut4 abundance suggest glucose uptake is not impaired in Ad36 infected adipose tissue. In addition, adiponectin abundance is higher in Ad36 infected tissue. Also, considering Ad36 activates LPL and lipid uptake, it is unlikely that lipolysis is increased in Ad36 infected tissue. This suggests that despite large adipocyte size, Ad36 may increase glucose uptake, inhibit lipolysis, adiponectin secretion. The differences in responses to Ad36 in the two mice models may also be due to differences in adipose tissue depots or durations post infection.

Although the hypertrophic response of adipose tissue to Ad36 is somewhat counterintuitive, considering most insulin sensitive models have smaller adipocytes, it is similar to the response of Collagen VI knockout mice on a high fat diet, which have enlarged adipocytes but markedly improved insulin sensitivity (130). In addition, adequate storage of lipid prevented systemic insulin resistance in Collagen VI knockout mice (130). Similarly, adipose tissue expansion in this model may accommodate large adipocytes and prevent hypoxia and inflammation that otherwise act as a signal for remodeling when storage capacity reaches an upper threshold storage capacity (130).

Exposure to TZDs for a short term period of 8 days is sufficient to induce adipocyte hypertrophy and improve lipid storage and insulin resistance, and it has been proposed that one short term dose may be sufficient to induce lasting change in insulin sensitivity (276). This approach to TZD treatment mirrors the idea of a “hit and run” hypothesis of Ad36 infection. Adipocyte hypertrophy induced by Ad36 despite a high fat diet therefore may improve insulin sensitivity in a similar manner, and increased LPL and lipid uptake by Ad36 may simply increase adipocyte threshold size. This would improve systemic fatty acid clearance. Alternatively, Ad36 infection may resist normal insulin resistance mechanisms associated with adipocyte

hypertrophy through an alternative Ras mediated glucose uptake pathway. Regardless, Ad36 seems to be a factor that alters the relationship between insulin sensitivity and adipocyte size in combination with a high fat diet.

The role of adipose tissue macrophage infiltration and inflammation in Ad36 induced improvement in glycemic control is less clear. In chow fed C57BL/6J mice, macrophage infiltration is not significantly different in Ad36 compared to Mock infected mice, whereas macrophage infiltration is increased in Ad2 infected tissue. In the HFD model, groups show no significant differences in macrophage infiltration, suggesting a high fat diet may overwhelm any effect of either virus on macrophage infiltration. Suppression of macrophage infiltration does not appear to be a major contributor to improved insulin sensitivity following infection in these mouse models. In fact, chronic infection of Ad36 in combination with high fat diet increased TNF-α expression in adipose tissue. TNF-α expression inhibits proximal insulin signaling through serine phosphorylation of IRS-1 (86; 277). This may explain the inhibition of proximal insulin signaling induced by Ad36 which may be due to up-regulation of TNF-α (190). It is both interesting and of potential therapeutic value that Ad36 improves glycemic control and glucose clearance in adipose tissue despite inflammation and inhibition of proximal insulin signaling.

Lastly, the effect of Ad36 on adipose tissue vascularization was determined in C57BL/6J mice. In both the chow fed and high fat fed mice, Ad36 and Ad2 infection increased adipose tissue vascularization relative to Mock, but only Ad36 improved glycemic control. An increase in vascularization is therefore likely to be an effect of infection, and may not contribute to glycemic control in this model. HIF-1α mRNA expression is up-regulated by both viruses in adipose tissue in the chow fed mice (unpublished observations). Ad36 increases H-Ras

activation, and H-Ras is known to mediate HIF1α activation and its downstream effectors independent of hypoxia (278). Therefore, adenoviral infection may increase HIF-1α through Ras activation or other unknown mechanisms. Regardless, an increase in HIF-1α and subsequent angiogenesis may therefore be an effect of adenoviral infection. In fact, adenoviral E4orf1 induces angiogenesis and is sufficient to establish a vascular niche (279). Anti-angiogenic factors are often added to adenoviral vectors so that the vector does not induce angiogenesis and promote tumor growth (280-282). Because both viruses increase angiogenesis and Ad36 significantly improves glycemic control in mice, and Ad2 does not, adipose tissue vascularization is not likely to play a role in Ad36 induced improvements in glycemic control.

To verify the effect of Ad36 on adipose tissue angiogenesis, an angiogenesis assay was conducted in human adipose tissue. Surprisingly, adipose tissue explants from two donors showed no induction of angiogenesis by Ad36 or Ad2, and Ad36 in fact inhibited angiogenesis in a manner similar to the negative control. This showed a lack of direct angiogenic effect of adenoviruses on adipose tissue. Instead, the increase in vascularization observed in the animal models may therefore be an *in vivo* phenomenon, or, may be a reaction of adenoviral infection that is specific to rodent tissue. It is possible that *in vivo* adenoviral infection up-regulates hypoxia and thus angiogenesis, but cultured explants are not susceptible to hypoxia due to controlled conditions.

Finally, a tube formation assay was conducted in murine endothelial cells to determine a direct angiogenic effect of Ad36 or Ad2 infection on endothelial cells. Ad36 did not improve tube formation acutely or 1-3 days post infection and actually inhibited the process. Ad2 had a similar effect, and was especially virulent in this cell type, killing cells by day 2 post infection.

Therefore, any effect of these two adenoviruses on angiogenesis in mice is probably not likely to be direct effect of infection on endothelial cells or adipose tissue.

Based on this morphological analysis of adipose tissue of C57BL/6J mice, it can be hypothesized that if Ad36 exerts any effect on glycemic control through changes in adipose tissue, it is most likely through changes in adipocyte metabolism and cell size, which are indicative of adipocyte recruitment and adipose tissue expandability. Ad36 increased glucose clearance in adipose tissue despite unchanged macrophage infiltration, and evidence of increased inflammation, hypoxia, and inhibition of proximal insulin signaling (190). Angiogenesis and adipose tissue vascularization is unlikely to play a role in improved glycemic control after Ad36 infection, since Ad2, which does not improve glycemic control, also increases adipose tissue vascularization. In addition, Ad36 and Ad2 were not angiogenic in human adipose tissue.

In making these conclusions, however, several limitations must be considered. All histochemical and morphological analysis of chow fed adipose tissue was of retroperitoneal adipose tissue, because these animals were lean and other depots were used for signaling studies. All adipose tissue histochemical analyses for the HFD model, on the other hand, were conducted in epididymal fat pads. Therefore, findings from this analysis cannot be generalized to all adipose tissue depots. Also, it is unknown if other depots would have demonstrated alternative results in the parameters measured. In addition, histochemistry involves certain caveats, such as ensuring the stained sample is representative of the entire tissue. For this reason, an effort was made to collect tissue from the same general area of the particular depot, and as many animals per group were analyzed as possible. Slide to slide variation can also cause variability in results, so all slides in a given analysis were stained at the same time, and great care was taken to ensure each slide was treated as equally as possible. Lastly, it is possible to bias results by taking

unrepresentative images of certain groups. Therefore, pictures were taken in a blinded fashion, and several pictures were taken of each slide so that the overall morphology was represented in those pictures. Therefore, these data are likely to accurately represent morphology associated with Ad36 infection, within the limitations of histochemical techniques.

### 4.3.3 Ad36 and Hepatic Lipid and Glycogen Accumulation

Other viruses such as HCV have been implicated in altering hepatic lipid metabolism during the process of viral replication(256-258). It is therefore conceivable that an adenoviral infection of the liver may alter hepatic lipid metabolism. A potential role of liver in Ad36 induced improvement in glycemic control was determined by staining liver of Mock, Ad36, and Ad2 infected mice on HFD for glycogen content. During processing, lipid leaves the sample, and therefore could be quantified as white space in the image. Ad36 significantly increased hepatic glycogen stores and reduced lipid accumulation compared to Mock and Ad2 infected animals, despite a high fat diet. This evidence is supported by increased expression of genes involved in lipid export and fatty acid oxidation, both of which would reduce hepatic triglyceride accumulation(190). This effect may be due to presence of the virus in the liver, since viral DNA and RNA were detected in liver following Ad36 infection(190). Moreover, Ad36 DNA in the liver correlated with glycemic control in mice(190).

Reduced hepatic lipid accumulation may be mediated indirectly through the effect of Ad36 on adipose tissue or a direct effect of the virus on liver. Ad36 increases adiponectin abundance in adipose tissue, and adiponectin is a strong activator of AMPK and fatty acid oxidation in the liver and is associated with lower hepatic lipid accumulation (141; 283). In addition, Ad36 infection increases adiponectin receptor levels(190), which would also increase adiponectin action. Upregulation of adiponectin receptors is mediated by PI3K mediated

FOXO1 nuclear exclusion (138). Ad36 significantly up-regulates AKT phosphorylation in the liver (190), which is indicative of PI3K activation and may be due to local infection in the liver. It could therefore be hypothesized that PI3K activation by Ad36 infection of the liver could work synergistically with the effect of Ad36 on adiponectin in adipose tissue for concomitant increase in both the hormone and the receptor. These dynamics will need to be tested in the future to determine which tissues are key players in improvement of hepatic metabolism and glycemic control induced by Ad36. In addition, these data are subject to the same limitations mentioned for the adipose tissue histochemistry data; however, the same precautions were taken to ensure the staining was as representative as possible. Also, it is encouraging that the gene expression data supported these conclusions(190).

### 4.4 E4orf1 Modulates Glucose and Lipid Metabolism of Adipocytes and Hepatocytes

E4orf1 was investigated as the candidate anti-diabetic protein of Ad36 in order to harness its therapeutic potential. It has been demonstrated that E4orf1 is sufficient and necessary for induction of adipogenesis(203), and it is well known that some adipogenic factors improve insulin sensitivity. In addition, E4orf1 is sufficient and necessary for PI3K activation by the virus, one of the main components up-regulated by Ad36 infection for induction of glucose uptake (188).

In 3T3-L1 cells, E4orf1 was sufficient and necessary to increase glucose uptake. Knockdown of E4orf1 suppressed increased glucose uptake increased by Ad36, and E4orf1 transfection increased glucose uptake in preadipocytes and adipocytes. In adipocytes, glucose uptake was significantly greater in E4orf1 transfected cells compared to Null in both the basal and insulin stimulated condition. E4orf1 did not suppress insulin stimulated glucose uptake. In fact, E4orf1 increased it further compared to the insulin treated Null group. Therefore, it is

likely that E4orf1 does not suppress proximal insulin signaling. This is in contrast to infection with Ad36, which inhibits IRS1 signaling (188).

Because Ad36 relies on Ras mediated activation of PI3K signaling for Glut4 upregulation and glucose uptake, it was next determined if E4orf1 is sufficient to activate the same pathway in 3T3-L1. Importantly, induction of E4orf1 robustly up-regulated Ras abundance and activation. Specifically, H-Ras isoform was activated by E4orf1, which is the same isoform that improves insulin sensitivity upon overexpression in adipose tissue of transgenic mice (225). Distal insulin signaling was also increased by E4orf1, and up-regulation of AKT phosphorylation and Glut4 abundance supports glucose uptake and upregulation of the same pathway used by Ad36 for glucose disposal. Ras activation is known to mimic the effect of insulin on glucose transporters(226), and therefore may be particularly important for glucose clearance when insulin signaling is impaired, as is often the case in T2DM or obesity. Glut1 abundance is also increased by the virus and E4orf1, which may contribute to glucose disposal. Glut1 is commonly expressed in response to Ras activation, and is involved in glucose clearance in transformed cells (278). Therefore, E4orf1 is sufficient to increase the same Ras-PI3K pathway used by the whole virus for glucose uptake, and may also promote glucose uptake through Glut1.

E4orf1 also increases DNL in 3T3-L1 preadipocytes. This effect needs to be verified in humans since the contribution of DNL to lipid accumulation is unclear in human adipose tissue, as discussed for this effect of Ad36. E4orf1 appears to increase both glucose uptake in to an adipocyte, and its conversion to lipid. Therefore, synergy between glucose disposal and adipogenesis induced by E4orf1 may be beneficial for insulin sensitivity.

Because Ras activation is increased by E4orf1, the ability of E4orf1 to transform cells was tested. E4orf1 constitutive expression was not sufficient to induce cell transformation, and

Ad36 infection did not induce cell transformation either. This supports the idea that E4orf1 is unlikely to be tumorgenic *in vivo*. For progression of Ras-PI3K induced tumors, dysfunctional focal-adhesion kinase signaling is required, which suggests that Ras-PI3K activation alone is not sufficient to induce cell transformation (235). In addition, neither the H-Ras overexpression in mice induced tumor formation (225), nor the Ad36 infection of several mammal models induced tumors(192-194; 197; 198). Importantly, the E4orf1 gene of Ad9, which is highly homologous to that of Ad36, induces Ras-PI3K activation. It is sufficient to transform cells and induce estrogen-dependent mammary tumors in rats , but these tumors do not undergo metastasis and appear to be benign (284). In addition, adenoviruses are not associated with cancer in humans. Therefore, if E4orf1 is targeted to adipose tissue for anti-diabetic therapeutic purpose, it may be unlikely to cause tumor formation, although this needs to be tested thoroughly *in vivo*. E4orf1 also increases adiponectin mRNA and protein in 3T3-L1, and suppresses inflammatory cytokine mRNA expression. The beneficial effect of E4orf1 may consequently not be limited to glucose disposal in adipose tissue, but may be beneficial at the level of systemic insulin sensitivity. Adiponectin up-regulates hepatic and skeletal muscle fatty acid oxidation, and is associated with insulin sensitivity (141; 157). In addition, adiponectin is anti-inflammatory and may prevent insulin resistance in adipose tissue if expressed at high levels (68; 285). In line with the potential anti-inflammatory actions of E4orf1 induced adiponectin secretion, E4orf1 also suppressed gene expression of several inflammation genes in 3T3-L1.

MCP-1, MCSF, and TLR-4 expression were down-regulated by E4orf1 in 3T3-L1. Although chronic infection of Ad36 in combination with high fat diet may increase adipose tissue inflammation (unpublished observations), acute Ad36 infection suppresses inflammation in adipose tissue (198). Several early adenoviral genes suppress immune function to aid initial

viral entry and replication, which may be responsible for acute suppression of inflammation by Ad36 infection. The ability of E4orf1 to suppress inflammatory cytokines may add to its therapeutic potential. MCP-1 expression is associated with insulin resistance, adipose tissue macrophage infiltration, and hepatic lipid accumulation (90; 157). In addition, MCP-1 mediates the switch of macrophages to a pro-inflammatory state(286). Reduction of TLR-4 by E4orf1 may also be of benefit, since TLR-4 activation in adipocytes can lead to TNF-α secretion(287). Although suppression of inflammatory cytokines by E4orf1 may improve inflammation associated with insulin resistance that does not necessarily mean this reduction will automatically lead to increased glucose uptake (288). The glucose uptake and anti-inflammatory effects of E4orf1 seem to be independent of each other, and one may not influence the other. Future studies are needed to determine these dynamics.

Interestingly, E4orf1 is sufficient to increase glucose uptake in mouse embryonic fibroblasts that lack PPARγ. Considering the key role of PPARγ in adipogenesis, this suggests that E4orf1 can potentially induce glucose uptake without its adipogenic effect, and that these two phenomena may be uncoupled from each other. Because PPARγ activation as a treatment for T2DM has many unwanted side effects(289-291), agents which up-regulate glucose uptake independent of PPARγ may be the next generation of ant diabetic drugs(292; 293). E4orf1 may be such an agent, and its signaling pathways can be studied in the future for identification of the divergence of these two effects. E4orf1 activates PI3K, which activates both AKT1 and AKT2. AKT1 activation induces adipogenesis and PPARγ(285; 294; 295), while AKT2 activation induces Glut4 translocation (296). Therefore, AKT1/AKT2 signaling may be where E4orf1 induced signaling diverges for these two independent effects and future studies will further elucidate this hypothesis. If E4orf1 does indeed depend on AKT1 for its adipogenic effect, a

drug cocktail of E4orf1 or an E4orf1 analog and an AKT1 inhibitor may be a promising new anti-diabetic drug.

The effect of E4orf1 in hepatocytes is also promising for improvement of glycemic control. E4orf1 suppressed glucose output in HepG2 in glucose starved and gluconeogenic conditions, and had a similar effect in primary mouse hepatocytes in serum and glucose starved and glucagon stimulated conditions. In HepG2, E4orf1 suppressed glucose output in the basal and insulin stimulated condition, which again suggests E4orf1 does not interfere with insulin mediated suppression of glucose output or insulin signaling, in contrast to Ad36 infection(190). In addition, Ad2 E4orf1 did not suppress glucose output in HepG2 cells; however, it was able to suppress glucose output in primary mouse hepatocytes in the glucose starved, but not glucagon stimulated condition. This suggests that Ad2 E4orf1 may have some effect on glucose output in murine, but not human hepatocytes. In murine hepatocytes, Ad36 E4orf1 was more effective suppressor of glucose output compared to Ad2 E4orf1, since it was able to suppress output in the presence of glucagon.

E4orf1 also demonstrated several effects on hepatic lipid metabolism, and E4orf1 may be sufficient for prevention of steatosis by Ad36. Several metabolic processes can contribute to hepatic lipid accumulation and insulin resistance such as impaired fatty acid oxidation, decreased lipid export, and increased DNL, although impaired export and increased DNL are the two major contributors to NAFLD (164-166). E4orf1 did not increase total fatty acid oxidation, however, it up-regulated complete oxidation and decreased the ratio of partial to complete oxidation. As a result, E4orf1 may prevent buildup of fatty acid intermediates and subsequent inhibition of insulin signaling (182). Ad2 E4orf1 also decreased the ratio of partial to complete oxidation, and since Ad2 infection did not prevent hepatic lipid accumulation or insulin resistance in HFD

mouse model, alterations in fatty acid oxidation by E4orf1 may not play a large role in Ad36 induced improvements in hepatic insulin sensitivity. Ad36 E4orf1 did, however, suppress DNL and increase ApoB secretion, which is indicative of lipid export, in HepG2 cells, whereas Ad2 E4orf1 did not. Since these are two main hepatic lipid metabolism parameters that contribute to development of NAFLD, Ad36 E4orf1 may be sufficient for suppression of hepatic triglyceride accumulation demonstrated in HFD C57BL/6J mice. This hypothesis will be tested in future studies. Such a finding could have profound implications for prevention of NAFLD and insulin resistance.

The mechanism for how Ad36 E4orf1 may modulate hepatic lipid metabolism is unknown at this time. It is interesting that E4orf1 has a marked direct effect on hepatic lipid metabolism; this suggests the presence of E4orf1 in the liver alone may be sufficient to improve steatosis. Adiponectin secretion from adipose tissue induced by Ad36 E4orf1 may, however, add to these benefits *in vivo*, and produce a more pronounced effect on fatty acid oxidation. Future studies will determine if these tissues act independently or synergistically for improvement of glycemic control and hepatic steatosis, in response to E4orf1.

Several limitations of the aforementioned studies with E4orf1 must be considered. First, all conclusions are based on *in vitro* studies and need to be verified *in vivo*. Although E4orf1 alters glucose and lipid metabolism in preadipocytes, adipocytes, and hepatocytes, improvement in glycemic control *in vivo* due to E4orf1 remains undetermined. Second, HepG2 cells have a low capacity for DNL from [14C] glucose; however, radioactive counts per minute (CPM) readings of [14C]-Glucose incorporation into lipid were low, but detectable and above the blank readings. Also, E4orf1 has several limitations as a potential therapeutic protein. It is not a secretory protein, and therefore does not have a cell surface receptor for cell entry. As a result, a

delivery mechanism such as nanoparticle delivery or adenoviral vector must be developed. Alternatively, a chemical analog of E4orf1 could be developed and packaged for delivery to the bloodstream. Nonetheless, the metabolic effects of E4orf1 are highly promising, and these caveats present challenges, which need to be overcome.

### 4.5 Conclusions and Future Directions

The studies presented herein lay the foundation for further elucidation of Ad36 induced improvements in glycemic control. A three-tiered approach was adapted to identify the role of Ad36 in improving in glycemic control. First, Ad36 seropositivity was associated with improved glycemic control in children. Next, *in vitro* characterization of adipocyte differentiation and metabolism, and post hoc tissue histological analysis of C57BL/6J mice was conducted. These studies suggest Ad36 may increase insulin sensitivity through up-regulation of adipogenesis and hyperplastic adipose tissue expansion, improved lipid accumulation and glucose clearance through DNL, and hypertrophy in response to a high fat diet. Macrophage infiltration and adipose tissue vascularization were ruled out as potential contributors to Ad36 induced improvements in insulin sensitivity. In addition, prevention of hepatic steatosis by Ad36 infection was observed for the first time. Finally, *in vitro* studies verified that Ad36 E4orf1 protein is sufficient and necessary for Ad36 induced glucose disposal.

Future studies will thus focus on E4orf1 as a potential therapeutic agent. First the molecular mechanism must be determined more in detail. Although E4orf1 up-regulates the Ras-PI3K pathway used by the virus for glucose uptake, a H-Ras knockdown experiment is necessary to demonstrate definitively that E4orf1 depends on this pathway for glucose uptake. Also, uncoupling of the signaling involved in adipogenic and glucose uptake effects of E4orf1 would add greatly to its therapeutic value. Identification of tissues targeted by E4orf1 to improve

glycemic control is needed so the development of any drug therapeutic may be targeted to that particular tissue. Chemical analogs are useful because they can be modified for different solubility and delivery requirements, and are not as fragile as a protein. And finally, such an analog will then be tested for safety and efficacy in a T2DM nonhuman primate model. The studies herein provide the foundation for this future work, and highlight Ad36 viral protein E4orf1 as a promising anti-diabetic and anti-steatotic agent.

**Table 4. Summary of the Effect of Ad36/E4orf1 on Glycemic Control.** Factors related to glycemic control modulated by Ad36, and/or E4orf1. Factors grouped according to conventionally "positive" or "negative" modulators of glycemic control.

| | **Insulin sensitizing factors which** | | |
|---|---|---|---|
| | **Ad36/E4orf1 does not modulate** | **Ad36/E4orf1 modulates positively** | **Ad36/E4orf1 modulates negatively** |
| **Adipose tissue** | - Macrophage Infiltration<br>- Angiogenesis | - ↑ Glucose uptake<br>- ↑ Adipogenesis<br>- ↑ Lipid uptake<br>- ↑ DNL<br>- ↑ Fat Oxidation<br>- ↑ Adiponectin<br>- ↓ Leptin<br>- ↓ Inflammatory cytokines (acute infection) | - ↓ Proximal insulin signaling<br>- ↑ Hypoxia<br>- ↑ TNF-α (chronic infection)<br>- ↑ Large adipocytes (HFD) |
| **Liver** | - Total fat oxidation | - ↓ Steatosis<br>- ↑ Glycogen stores<br>- ↓ Glucose output<br>- ↑ Lipid Export<br>- ↓ DNL<br>- ↑ Complete oxidation<br>- ↑AMPK activation<br>- ↓ Inflammation<br>- ↑ AdipoR1 and AdipoR2 | |

## References


1. Caballero B: The global epidemic of obesity: an overview. *Epidemiol Rev* 29:1-5, 2007

2. Keith SW, Redden DT, Katzmarzyk PT, Boggiano MM, Hanlon EC, Benca RM, Ruden D, Pietrobelli A, Barger JL, Fontaine KR, Wang C, Aronne LJ, Wright SM, Baskin M, Dhurandhar NV, Lijoi MC, Grilo CM, DeLuca M, Westfall AO, Allison DB: Putative contributors to the secular increase in obesity: exploring the roads less traveled. *Int J Obes (Lond)* 30:1585-1594, 2006

3. Breslow L: Public health aspects of weight control. *Am J Public Health Nations Health* 42:1116-1120, 1952

4. Flegal KM, Carroll MD, Kuczmarski RJ, Johnson CL: Overweight and obesity in the United States: prevalence and trends, 1960-1994. *Int J Obes Relat Metab Disord* 22:39-47, 1998

5. Kuczmarski RJ, Flegal KM, Campbell SM, Johnson CL: Increasing prevalence of overweight among US adults. The National Health and Nutrition Examination Surveys, 1960 to 1991. *JAMA* 272:205-211, 1994

6. Flegal KM, Carroll MD, Ogden CL, Johnson CL: Prevalence and trends in obesity among US adults, 1999-2000. *JAMA* 288:1723-1727, 2002

7. Flegal KM, Carroll MD, Ogden CL, Curtin LR: Prevalence and trends in obesity among US adults, 1999-2008. *JAMA* 303:235-241

8. Ogden CL, Flegal KM, Carroll MD, Johnson CL: Prevalence and trends in overweight among US children and adolescents, 1999-2000. *JAMA* 288:1728-1732, 2002

9. Ogden CL, Carroll MD, Flegal KM: High body mass index for age among US children and adolescents, 2003-2006. *JAMA* 299:2401-2405, 2008

10. Division of Nutrition and Physical Activity NCfCDPaHP: Department of Health and Human Services Centers for Disease Control and Prevention. In *Overweight and Obesity* Atlanta, Centers for Disease Control and Prevention, 2007, p. Co-morbities associated with obesity.

11. Tsai AG, Wadden TA: Systematic review: an evaluation of major commercial weight loss programs in the United States. *Ann Intern Med* 142:56-66, 2005

12. Foster GD, Wadden TA, Vogt RA, Brewer G: What is a reasonable weight loss? Patients' expectations and evaluations of obesity treatment outcomes. *J Consult Clin Psychol* 65:79-85, 1997

13. Lindberg NM, Stevens VJ: Review: weight-loss interventions with Hispanic populations. *Ethn Dis* 17:397-402, 2007

14. Thomas H: Obesity prevention programs for children and youth: why are their results so modest? *Health Educ Res* 21:783-795, 2006

15. Dolan MS, Weiss LA, Lewis RA, Pietrobelli A, Heo M, Faith MS: 'Take the stairs instead of the escalator': effect of environmental prompts on community stair use and implications for a national 'Small Steps' campaign. *Obes Rev* 7:25-32, 2006

16. Elbel B, Gyamfi J, Kersh R: Child and adolescent fast-food choice and the influence of calorie labeling: a natural experiment. *Int J Obes (Lond)* 35:493-500

17. Curioni CC, Lourenco PM: Long-term weight loss after diet and exercise: a systematic review. *Int J Obes (Lond)* 29:1168-1174, 2005

18. Dansinger ML, Tatsioni A, Wong JB, Chung M, Balk EM: Meta-analysis: the effect of dietary counseling for weight loss. *Ann Intern Med* 147:41-50, 2007

19. Lowe MR, Tappe KA, Annunziato RA, Riddell LJ, Coletta MC, Crerand CE, Didie ER, Ochner CN, McKinney S: The Effect of Training in Reduced Energy Density Eating and Food Self-monitoring Accuracy on Weight Loss Maintenance. *Obesity (Silver Spring)*, 2008

20. Butryn ML, Phelan S, Hill JO, Wing RR: Consistent self-monitoring of weight: a key component of successful weight loss maintenance. *Obesity (Silver Spring)* 15:3091-3096, 2007

21. Tate DF, Jeffery RW, Sherwood NE, Wing RR: Long-term weight losses associated with prescription of higher physical activity goals. Are higher levels of physical activity protective against weight regain? *Am J Clin Nutr* 85:954-959, 2007

22. Rucker D, Padwal R, Li SK, Curioni C, Lau DC: Long term pharmacotherapy for obesity and overweight: updated meta-analysis. *BMJ* 335:1194-1199, 2007

23. Dvorak RV, Sharma AM, Astrup A: Anti-obesity drugs: to be or not to be? *Obes Rev* 11:833-834

24. Sjostrom L, Narbro K, Sjostrom CD, Karason K, Larsson B, Wedel H, Lystig T, Sullivan M, Bouchard C, Carlsson B, Bengtsson C, Dahlgren S, Gummesson A, Jacobson P, Karlsson J, Lindroos AK, Lonroth H, Naslund I, Olbers T, Stenlof K, Torgerson J, Agren G, Carlsson LM: Effects of bariatric surgery on mortality in Swedish obese subjects. *N Engl J Med* 357:741-752, 2007

25. Karlsson J, Taft C, Ryden A, Sjostrom L, Sullivan M: Ten-year trends in health-related quality of life after surgical and conventional treatment for severe obesity: the SOS intervention study. *Int J Obes (Lond)* 31:1248-1261, 2007

26. Jeffery RW, Harnack LJ: Evidence implicating eating as a primary driver for the obesity epidemic. *Diabetes* 56:2673-2676, 2007

27. Harnack LJ, Jeffery RW, Boutelle KN: Temporal trends in energy intake in the United States: an ecologic perspective. *Am J Clin Nutr* 71:1478-1484, 2000

28. Stubbs CO, Lee AJ: The obesity epidemic: both energy intake and physical activity contribute. *Med J Aust* 181:489-491, 2004

29. Nielsen SJ, Siega-Riz AM, Popkin BM: Trends in energy intake in U.S. between 1977 and 1996: similar shifts seen across age groups. *Obes Res* 10:370-378, 2002

30. Papas MA, Alberg AJ, Ewing R, Helzlsouer KJ, Gary TL, Klassen AC: The built environment and obesity. *Epidemiol Rev* 29:129-143, 2007

31. Bouchard C: The biological predisposition to obesity: beyond the thrifty genotype scenario. *Int J Obes (Lond)* 31:1337-1339, 2007

32. Badman MK, Flier JS: The gut and energy balance: visceral allies in the obesity wars. *Science* 307:1909-1914, 2005

33. Spiegelman BM, Flier JS: Obesity and the regulation of energy balance. *Cell* 104:531-543, 2001
34. Tremblay A, Despres JP, Theriault G, Fournier G, Bouchard C: Overfeeding and energy expenditure in humans. *Am J Clin Nutr* 56:857-862, 1992

35. Leibel RL, Rosenbaum M, Hirsch J: Changes in energy expenditure resulting from altered body weight. *N Engl J Med* 332:621-628, 1995

36. Ravussin E, Lillioja S, Anderson TE, Christin L, Bogardus C: Determinants of 24-hour energy expenditure in man. Methods and results using a respiratory chamber. *J Clin Invest* 78:1568-1578, 1986

37. Goran MI, Beer WH, Wolfe RR, Poehlman ET, Young VR: Variation in total energy expenditure in young healthy free-living men. *Metabolism* 42:487-496, 1993

38. Ravussin E, Lillioja S, Knowler WC, Christin L, Freymond D, Abbott WG, Boyce V, Howard BV, Bogardus C: Reduced rate of energy expenditure as a risk factor for body-weight gain. *N Engl J Med* 318:467-472, 1988

39. Bouchard C, Tremblay A, Despres JP, Nadeau A, Lupien PJ, Theriault G, Dussault J, Moorjani S, Pinault S, Fournier G: The response to long-term overfeeding in identical twins. *N Engl J Med* 322:1477-1482, 1990

40. Bouchard C, Tremblay A, Despres JP, Theriault G, Nadeau A, Lupien PJ, Moorjani S, Prudhomme D, Fournier G: The response to exercise with constant energy intake in identical twins. *Obes Res* 2:400-410, 1994

41. Rankinen T, Zuberi A, Chagnon YC, Weisnagel SJ, Argyropoulos G, Walts B, Perusse L, Bouchard C: The human obesity gene map: the 2005 update. *Obesity (Silver Spring)* 14:529-644, 2006

42. Clement K, Vaisse C, Lahlou N, Cabrol S, Pelloux V, Cassuto D, Gourmelen M, Dina C, Chambaz J, Lacorte JM, Basdevant A, Bougneres P, Lebouc Y, Froguel P, Guy-Grand B: A mutation in the human leptin receptor gene causes obesity and pituitary dysfunction. *Nature* 392:398-401, 1998

43. Haupt A, Thamer C, Staiger H, Tschritter O, Kirchhoff K, Machicao F, Haring HU, Stefan N, Fritsche A: Variation in the FTO gene influences food intake but not energy expenditure. *Exp Clin Endocrinol Diabetes* 117:194-197, 2009

44. McAllister EJ, Dhurandhar NV, Keith SW, Aronne LJ, Barger J, Baskin M, Benca RM, Biggio J, Boggiano MM, Eisenmann JC, Elobeid M, Fontaine KR, Gluckman P, Hanlon EC, Katzmarzyk P, Pietrobelli A, Redden DT, Ruden DM, Wang C, Waterland RA, Wright SM, Allison DB: Ten putative contributors to the obesity epidemic. *Crit Rev Food Sci Nutr* 49:868-913, 2009

45. Reaven GM: Banting lecture 1988. Role of insulin resistance in human disease. *Diabetes* 37:1595-1607, 1988

46. Reaven GM: Insulin resistance, hyperinsulinemia, hypertriglyceridemia, and hypertension. Parallels between human disease and rodent models. *Diabetes Care* 14:195-202, 1991

47. DeFronzo RA, Ferrannini E: Insulin resistance. A multifaceted syndrome responsible for NIDDM, obesity, hypertension, dyslipidemia, and atherosclerotic cardiovascular disease. *Diabetes Care* 14:173-194, 1991

48. Park YW, Zhu S, Palaniappan L, Heshka S, Carnethon MR, Heymsfield SB: The metabolic syndrome: prevalence and associated risk factor findings in the US population from the Third National Health and Nutrition Examination Survey, 1988-1994. *Arch Intern Med* 163:427-436, 2003

49. Weiss R, Dziura J, Burgert TS, Tamborlane WV, Taksali SE, Yeckel CW, Allen K, Lopes M, Savoye M, Morrison J, Sherwin RS, Caprio S: Obesity and the metabolic syndrome in children and adolescents. *N Engl J Med* 350:2362-2374, 2004

50. Pessin JE, Saltiel AR: Signaling pathways in insulin action: molecular targets of insulin resistance. *J Clin Invest* 106:165-169, 2000

51. Sesti G, Federici M, Hribal ML, Lauro D, Sbraccia P, Lauro R: Defects of the insulin receptor substrate (IRS) system in human metabolic disorders. *FASEB J* 15:2099-2111, 2001

52. Pagliassotti MJ, Kang J, Thresher JS, Sung CK, Bizeau ME: Elevated basal PI 3-kinase activity and reduced insulin signaling in sucrose-induced hepatic insulin resistance. *Am J Physiol Endocrinol Metab* 282:E170-176, 2002

53. Goodyear LJ, Giorgino F, Sherman LA, Carey J, Smith RJ, Dohm GL: Insulin receptor phosphorylation, insulin receptor substrate-1 phosphorylation, and phosphatidylinositol 3-kinase activity are decreased in intact skeletal muscle strips from obese subjects. *J Clin Invest* 95:2195-2204, 1995

54. Butler AE, Janson J, Bonner-Weir S, Ritzel R, Rizza RA, Butler PC: Beta-cell deficit and increased beta-cell apoptosis in humans with type 2 diabetes. *Diabetes* 52:102-110, 2003

55. Unger RH, Grundy S: Hyperglycaemia as an inducer as well as a consequence of impaired islet cell function and insulin resistance: implications for the management of diabetes. *Diabetologia* 28:119-121, 1985

56. Pi J, Zhang Q, Fu J, Woods CG, Hou Y, Corkey BE, Collins S, Andersen ME: ROS signaling, oxidative stress and Nrf2 in pancreatic beta-cell function. *Toxicol Appl Pharmacol* 244:77-83

57. Hayes L, Pearce MS, Unwin NC: Lifecourse predictors of normal metabolic parameters in overweight and obese adults. *Int J Obes (Lond)* 30:970-976, 2006

58. Wildman RP, Muntner P, Reynolds K, McGinn AP, Rajpathak S, Wylie-Rosett J, Sowers MR: The obese without cardiometabolic risk factor clustering and the normal weight with cardiometabolic risk factor clustering: prevalence and correlates of 2 phenotypes among the US population (NHANES 1999-2004). *Arch Intern Med* 168:1617-1624, 2008

59. Brochu M, Tchernof A, Dionne IJ, Sites CK, Eltabbakh GH, Sims EA, Poehlman ET: What are the physical characteristics associated with a normal metabolic profile despite a high level of obesity in postmenopausal women? *J Clin Endocrinol Metab* 86:1020-1025, 2001

60. Karelis AD, Faraj M, Bastard JP, St-Pierre DH, Brochu M, Prud'homme D, Rabasa-Lhoret R: The metabolically healthy but obese individual presents a favorable inflammation profile. *J Clin Endocrinol Metab* 90:4145-4150, 2005

61. Andres R: Effect of obesity on total mortality. *Int J Obes* 4:381-386, 1980

62. Conus F, Allison DB, Rabasa-Lhoret R, St-Onge M, St-Pierre DH, Tremblay-Lebeau A, Poehlman ET: Metabolic and behavioral characteristics of metabolically obese but normal-weight women. *J Clin Endocrinol Metab* 89:5013-5020, 2004

63. Conus F, Rabasa-Lhoret R, Peronnet F: Characteristics of metabolically obese normal-weight (MONW) subjects. *Appl Physiol Nutr Metab* 32:4-12, 2007

64. Vikram NK, Misra A, Dwivedi M, Sharma R, Pandey RM, Luthra K, Chatterjee A, Dhingra V, Jailkhani BL, Talwar KK, Guleria R: Correlations of C-reactive protein levels with anthropometric profile, percentage of body fat and lipids in healthy adolescents and young adults in urban North India. *Atherosclerosis* 168:305-313, 2003

65. Misra A, Athiko D, Sharma R, Pandey RM, Khanna N: Non-obese hyperlipidemic Asian northern Indian males have adverse anthropometric profile. *Nutr Metab Cardiovasc Dis* 12:178-183, 2002

66. Misra A, Sinha S, Kumar M, Jagannathan NR, Pandey RM: Proton magnetic resonance spectroscopy study of soleus muscle in non-obese healthy and Type 2 diabetic Asian Northern Indian males: high intramyocellular lipid content correlates with excess body fat and abdominal obesity. *Diabet Med* 20:361-367, 2003

67. Kershaw EE, Flier JS: Adipose tissue as an endocrine organ. *J Clin Endocrinol Metab* 89:2548-2556, 2004

68. Kim JY, van de Wall E, Laplante M, Azzara A, Trujillo ME, Hofmann SM, Schraw T, Durand JL, Li H, Li G, Jelicks LA, Mehler MF, Hui DY, Deshaies Y, Shulman GI, Schwartz GJ, Scherer PE: Obesity-associated improvements in metabolic profile through expansion of adipose tissue. *J Clin Invest* 117:2621-2637, 2007

69. Steppan CM, Bailey ST, Bhat S, Brown EJ, Banerjee RR, Wright CM, Patel HR, Ahima RS, Lazar MA: The hormone resistin links obesity to diabetes. *Nature* 409:307-312, 2001

70. Pajvani UB, Trujillo ME, Combs TP, Iyengar P, Jelicks L, Roth KA, Kitsis RN, Scherer PE: Fat apoptosis through targeted activation of caspase 8: a new mouse model of inducible and reversible lipoatrophy. *Nat Med* 11:797-803, 2005

71. Shimomura I, Hammer RE, Ikemoto S, Brown MS, Goldstein JL: Leptin reverses insulin resistance and diabetes mellitus in mice with congenital lipodystrophy. *Nature* 401:73-76, 1999

72. Chan JM, Rimm EB, Colditz GA, Stampfer MJ, Willett WC: Obesity, fat distribution, and weight gain as risk factors for clinical diabetes in men. *Diabetes Care* 17:961-969, 1994

73. Ohlson LO, Larsson B, Svardsudd K, Welin L, Eriksson H, Wilhelmsen L, Bjorntorp P, Tibblin G: The influence of body fat distribution on the incidence of diabetes mellitus. 13.5 years of follow-up of the participants in the study of men born in 1913. *Diabetes* 34:1055-1058, 1985

74. Zamboni M, Armellini F, Cominacini L, Turcato E, Todesco T, Bissoli L, Micciolo R, Bergamo-Andreis IA, Bosello O: Obesity and regional body-fat distribution in men: separate and joint relationships to glucose tolerance and plasma lipoproteins. *Am J Clin Nutr* 60:682-687, 1994

75. Krotkiewski M, Bjorntorp P, Sjostrom L, Smith U: Impact of obesity on metabolism in men and women. Importance of regional adipose tissue distribution. *J Clin Invest* 72:1150-1162, 1983

76. Bergman RN, Kim SP, Catalano KJ, Hsu IR, Chiu JD, Kabir M, Hucking K, Ader M: Why visceral fat is bad: mechanisms of the metabolic syndrome. *Obesity (Silver Spring)* 14 Suppl 1:16S-19S, 2006

77. Despres JP, Lemieux I: Abdominal obesity and metabolic syndrome. *Nature* 444:881-887, 2006

78. Fontana L, Eagon JC, Trujillo ME, Scherer PE, Klein S: Visceral fat adipokine secretion is associated with systemic inflammation in obese humans. *Diabetes* 56:1010-1013, 2007

79. Gabriely I, Ma XH, Yang XM, Atzmon G, Rajala MW, Berg AH, Scherer P, Rossetti L, Barzilai N: Removal of visceral fat prevents insulin resistance and glucose intolerance of aging: an adipokine-mediated process? *Diabetes* 51:2951-2958, 2002

80. Curat CA, Wegner V, Sengenes C, Miranville A, Tonus C, Busse R, Bouloumie A: Macrophages in human visceral adipose tissue: increased accumulation in obesity and a source of resistin and visfatin. *Diabetologia* 49:744-747, 2006

81. Cancello R, Tordjman J, Poitou C, Guilhem G, Bouillot JL, Hugol D, Coussieu C, Basdevant A, Bar Hen A, Bedossa P, Guerre-Millo M, Clement K: Increased infiltration of macrophages in omental adipose tissue is associated with marked hepatic lesions in morbid human obesity. *Diabetes* 55:1554-1561, 2006

82. Yatagai T, Nagasaka S, Taniguchi A, Fukushima M, Nakamura T, Kuroe A, Nakai Y, Ishibashi S: Hypoadiponectinemia is associated with visceral fat accumulation and insulin resistance in Japanese men with type 2 diabetes mellitus. *Metabolism* 52:1274-1278, 2003

83. Tilg H, Moschen AR: Inflammatory mechanisms in the regulation of insulin resistance. *Mol Med* 14:222-231, 2008

84. Ridker PM: Clinical application of C-reactive protein for cardiovascular disease detection and prevention. *Circulation* 107:363-369, 2003

85. Hotamisligil GS, Shargill NS, Spiegelman BM: Adipose expression of tumor necrosis factor-alpha: direct role in obesity-linked insulin resistance. *Science* 259:87-91, 1993

86. Uysal KT, Wiesbrock SM, Marino MW, Hotamisligil GS: Protection from obesity-induced insulin resistance in mice lacking TNF-alpha function. *Nature* 389:610-614, 1997

87. Bastard JP, Maachi M, Van Nhieu JT, Jardel C, Bruckert E, Grimaldi A, Robert JJ, Capeau J, Hainque B: Adipose tissue IL-6 content correlates with resistance to insulin activation of glucose uptake both in vivo and in vitro. *J Clin Endocrinol Metab* 87:2084-2089, 2002

88. Jager J, Gremeaux T, Cormont M, Le Marchand-Brustel Y, Tanti JF: Interleukin-1beta-induced insulin resistance in adipocytes through down-regulation of insulin receptor substrate-1 expression. *Endocrinology* 148:241-251, 2007

89. Zirlik A, Abdullah SM, Gerdes N, MacFarlane L, Schonbeck U, Khera A, McGuire DK, Vega GL, Grundy S, Libby P, de Lemos JA: Interleukin-18, the metabolic syndrome, and subclinical atherosclerosis: results from the Dallas Heart Study. *Arterioscler Thromb Vasc Biol* 27:2043-2049, 2007

90. Kanda H, Tateya S, Tamori Y, Kotani K, Hiasa K, Kitazawa R, Kitazawa S, Miyachi H, Maeda S, Egashira K, Kasuga M: MCP-1 contributes to macrophage infiltration into adipose tissue, insulin resistance, and hepatic steatosis in obesity. *J Clin Invest* 116:1494-1505, 2006

91. Barbarroja N, Lopez-Pedrera R, Mayas MD, Garcia-Fuentes E, Garrido-Sanchez L, Macias-Gonzalez M, El Bekay R, Vidal-Puig A, Tinahones FJ: The obese healthy paradox: is inflammation the answer? *Biochem J* 430:141-149

92. Yuan M, Konstantopoulos N, Lee J, Hansen L, Li ZW, Karin M, Shoelson SE: Reversal of obesity- and diet-induced insulin resistance with salicylates or targeted disruption of Ikkbeta. *Science* 293:1673-1677, 2001

93. Hirosumi J, Tuncman G, Chang L, Gorgun CZ, Uysal KT, Maeda K, Karin M, Hotamisligil GS: A central role for JNK in obesity and insulin resistance. *Nature* 420:333-336, 2002

94. Clement K, Viguerie N, Poitou C, Carette C, Pelloux V, Curat CA, Sicard A, Rome S, Benis A, Zucker JD, Vidal H, Laville M, Barsh GS, Basdevant A, Stich V, Cancello R, Langin D: Weight loss regulates inflammation-related genes in white adipose tissue of obese subjects. *FASEB J* 18:1657-1669, 2004

95. Weisberg SP, McCann D, Desai M, Rosenbaum M, Leibel RL, Ferrante AW, Jr.: Obesity is associated with macrophage accumulation in adipose tissue. *J Clin Invest* 112:1796-1808, 2003

96. Curat CA, Miranville A, Sengenes C, Diehl M, Tonus C, Busse R, Bouloumie A: From blood monocytes to adipose tissue-resident macrophages: induction of diapedesis by human mature adipocytes. *Diabetes* 53:1285-1292, 2004

97. Cancello R, Henegar C, Viguerie N, Taleb S, Poitou C, Rouault C, Coupaye M, Pelloux V, Hugol D, Bouillot JL, Bouloumie A, Barbatelli G, Cinti S, Svensson PA, Barsh GS, Zucker JD, Basdevant A, Langin D, Clement K: Reduction of macrophage infiltration and chemoattractant gene expression changes in white adipose tissue of morbidly obese subjects after surgery-induced weight loss. *Diabetes* 54:2277-2286, 2005

98. Weisberg SP, Hunter D, Huber R, Lemieux J, Slaymaker S, Vaddi K, Charo I, Leibel RL, Ferrante AW, Jr.: CCR2 modulates inflammatory and metabolic effects of high-fat feeding. *J Clin Invest* 116:115-124, 2006

99. Cinti S, Mitchell G, Barbatelli G, Murano I, Ceresi E, Faloia E, Wang S, Fortier M, Greenberg AS, Obin MS: Adipocyte death defines macrophage localization and function in adipose tissue of obese mice and humans. *J Lipid Res* 46:2347-2355, 2005

100. Cursiefen C, Chen L, Borges LP, Jackson D, Cao J, Radziejewski C, D'Amore PA, Dana MR, Wiegand SJ, Streilein JW: VEGF-A stimulates lymphangiogenesis and hemangiogenesis in inflammatory neovascularization via macrophage recruitment. *J Clin Invest* 113:1040-1050, 2004

101. Khmelewski E, Becker A, Meinertz T, Ito WD: Tissue resident cells play a dominant role in arteriogenesis and concomitant macrophage accumulation. *Circ Res* 95:E56-64, 2004

102. Pang C, Gao Z, Yin J, Zhang J, Jia W, Ye J: Macrophage infiltration into adipose tissue may promote angiogenesis for adipose tissue remodeling in obesity. *Am J Physiol Endocrinol Metab* 295:E313-322, 2008

103. Cancello R, Clement K: Is obesity an inflammatory illness? Role of low-grade inflammation and macrophage infiltration in human white adipose tissue. *BJOG* 113:1141-1147, 2006

104. Patton JS, Shepard HM, Wilking H, Lewis G, Aggarwal BB, Eessalu TE, Gavin LA, Grunfeld C: Interferons and tumor necrosis factors have similar catabolic effects on 3T3 L1 cells. *Proc Natl Acad Sci U S A* 83:8313-8317, 1986

105. Zhou YP, Grill VE: Long-term exposure of rat pancreatic islets to fatty acids inhibits glucose-induced insulin secretion and biosynthesis through a glucose fatty acid cycle. *J Clin Invest* 93:870-876, 1994

106. Milburn JL, Jr., Hirose H, Lee YH, Nagasawa Y, Ogawa A, Ohneda M, BeltrandelRio H, Newgard CB, Johnson JH, Unger RH: Pancreatic beta-cells in obesity. Evidence for induction of functional, morphologic, and metabolic abnormalities by increased long chain fatty acids. *J Biol Chem* 270:1295-1299, 1995

107. Ye J: Role of insulin in the pathogenesis of free fatty acid-induced insulin resistance in skeletal muscle. *Endocr Metab Immune Disord Drug Targets* 7:65-74, 2007

108. Itani SI, Ruderman NB, Schmieder F, Boden G: Lipid-induced insulin resistance in human muscle is associated with changes in diacylglycerol, protein kinase C, and IkappaB-alpha. *Diabetes* 51:2005-2011, 2002

109. Ye J: Emerging role of adipose tissue hypoxia in obesity and insulin resistance. *Int J Obes (Lond)* 33:54-66, 2009

110. Yin J, Gao Z, He Q, Zhou D, Guo Z, Ye J: Role of hypoxia in obesity-induced disorders of glucose and lipid metabolism in adipose tissue. *Am J Physiol Endocrinol Metab* 296:E333-342, 2009

111. Rupnick MA, Panigrahy D, Zhang CY, Dallabrida SM, Lowell BB, Langer R, Folkman MJ: Adipose tissue mass can be regulated through the vasculature. *Proc Natl Acad Sci U S A* 99:10730-10735, 2002

112. Trayhurn P, Wang B, Wood IS: Hypoxia in adipose tissue: a basis for the dysregulation of tissue function in obesity? *Br J Nutr* 100:227-235, 2008

113. Ye J, Gao Z, Yin J, He Q: Hypoxia is a potential risk factor for chronic inflammation and adiponectin reduction in adipose tissue of ob/ob and dietary obese mice. *Am J Physiol Endocrinol Metab* 293:E1118-1128, 2007

114. Higami Y, Barger JL, Page GP, Allison DB, Smith SR, Prolla TA, Weindruch R: Energy restriction lowers the expression of genes linked to inflammation, the cytoskeleton, the extracellular matrix, and angiogenesis in mouse adipose tissue. *J Nutr* 136:343-352, 2006

115. Strissel KJ, Stancheva Z, Miyoshi H, Perfield JW, 2nd, DeFuria J, Jick Z, Greenberg AS, Obin MS: Adipocyte death, adipose tissue remodeling, and obesity complications. *Diabetes* 56:2910-2918, 2007

116. Ambrosini G, Nath AK, Sierra-Honigmann MR, Flores-Riveros J: Transcriptional activation of the human leptin gene in response to hypoxia. Involvement of hypoxia-inducible factor 1. *J Biol Chem* 277:34601-34609, 2002

117. Wang B, Wood IS, Trayhurn P: Dysregulation of the expression and secretion of inflammation-related adipokines by hypoxia in human adipocytes. *Pflugers Arch* 455:479-492, 2007

118. Chen B, Lam KS, Wang Y, Wu D, Lam MC, Shen J, Wong L, Hoo RL, Zhang J, Xu A: Hypoxia dysregulates the production of adiponectin and plasminogen activator inhibitor-1 independent of reactive oxygen species in adipocytes. *Biochem Biophys Res Commun* 341:549-556, 2006

119. Ravussin E, Smith SR: Increased fat intake, impaired fat oxidation, and failure of fat cell proliferation result in ectopic fat storage, insulin resistance, and type 2 diabetes mellitus. *Ann N Y Acad Sci* 967:363-378, 2002

120. Smith SA: Peroxisome proliferator-activated receptors and the regulation of mammalian lipid metabolism. *Biochem Soc Trans* 30:1086-1090, 2002

121. Lehmann JM, Moore LB, Smith-Oliver TA, Wilkison WO, Willson TM, Kliewer SA: An antidiabetic thiazolidinedione is a high affinity ligand for peroxisome proliferator-activated receptor gamma (PPAR gamma). *J Biol Chem* 270:12953-12956, 1995

122. Okuno A, Tamemoto H, Tobe K, Ueki K, Mori Y, Iwamoto K, Umesono K, Akanuma Y, Fujiwara T, Horikoshi H, Yazaki Y, Kadowaki T: Troglitazone increases the number of small adipocytes without the change of white adipose tissue mass in obese Zucker rats. *J Clin Invest* 101:1354-1361, 1998

123. Adams M, Montague CT, Prins JB, Holder JC, Smith SA, Sanders L, Digby JE, Sewter CP, Lazar MA, Chatterjee VK, O'Rahilly S: Activators of peroxisome proliferator-activated receptor gamma have depot-specific effects on human preadipocyte differentiation. *J Clin Invest* 100:3149-3153, 1997

124. Sewter CP, Blows F, Vidal-Puig A, O'Rahilly S: Regional differences in the response of human pre-adipocytes to PPARgamma and RXRalpha agonists. *Diabetes* 51:718-723, 2002

125. de Souza CJ, Eckhardt M, Gagen K, Dong M, Chen W, Laurent D, Burkey BF: Effects of pioglitazone on adipose tissue remodeling within the setting of obesity and insulin resistance. *Diabetes* 50:1863-1871, 2001

126. Boden G, Cheung P, Mozzoli M, Fried SK: Effect of thiazolidinediones on glucose and fatty acid metabolism in patients with type 2 diabetes. *Metabolism* 52:753-759, 2003

127. Okamoto Y, Higashiyama H, Inoue H, Kanematsu M, Kinoshita M, Asano S: Quantitative image analysis in adipose tissue using an automated image analysis system: differential effects of peroxisome proliferator-activated receptor-alpha and -gamma agonist on white and brown adipose tissue morphology in AKR obese and db/db diabetic mice. *Pathol Int* 57:369-377, 2007

128. Barnard RJ, Roberts CK, Varon SM, Berger JJ: Diet-induced insulin resistance precedes other aspects of the metabolic syndrome. *J Appl Physiol* 84:1311-1315, 1998

129. Yang X, Jansson PA, Nagaev I, Jack MM, Carvalho E, Sunnerhagen KS, Cam MC, Cushman SW, Smith U: Evidence of impaired adipogenesis in insulin resistance. *Biochem Biophys Res Commun* 317:1045-1051, 2004

130. Khan T, Muise ES, Iyengar P, Wang ZV, Chandalia M, Abate N, Zhang BB, Bonaldo P, Chua S, Scherer PE: Metabolic dysregulation and adipose tissue fibrosis: role of collagen VI. *Mol Cell Biol* 29:1575-1591, 2009

131. Henegar C, Tordjman J, Achard V, Lacasa D, Cremer I, Guerre-Millo M, Poitou C, Basdevant A, Stich V, Viguerie N, Langin D, Bedossa P, Zucker JD, Clement K: Adipose tissue transcriptomic

signature highlights the pathological relevance of extracellular matrix in human obesity. *Genome Biol* 9:R14, 2008

132. Divoux A, Tordjman J, Lacasa D, Veyrie N, Hugol D, Aissat A, Basdevant A, Guerre-Millo M, Poitou C, Zucker JD, Bedossa P, Clement K: Fibrosis in human adipose tissue: composition, distribution, and link with lipid metabolism and fat mass loss. *Diabetes* 59:2817-2825

133. Arita Y, Kihara S, Ouchi N, Takahashi M, Maeda K, Miyagawa J, Hotta K, Shimomura I, Nakamura T, Miyaoka K, Kuriyama H, Nishida M, Yamashita S, Okubo K, Matsubara K, Muraguchi M, Ohmoto Y, Funahashi T, Matsuzawa Y: Paradoxical decrease of an adipose-specific protein, adiponectin, in obesity. *Biochem Biophys Res Commun* 257:79-83, 1999

134. Hu E, Liang P, Spiegelman BM: AdipoQ is a novel adipose-specific gene dysregulated in obesity. *J Biol Chem* 271:10697-10703, 1996

135. Gilardini L, McTernan PG, Girola A, da Silva NF, Alberti L, Kumar S, Invitti C: Adiponectin is a candidate marker of metabolic syndrome in obese children and adolescents. *Atherosclerosis* 189:401-407, 2006

136. Hotta K, Funahashi T, Bodkin NL, Ortmeyer HK, Arita Y, Hansen BC, Matsuzawa Y: Circulating concentrations of the adipocyte protein adiponectin are decreased in parallel with reduced insulin sensitivity during the progression to type 2 diabetes in rhesus monkeys. *Diabetes* 50:1126-1133, 2001

137. Ryo M, Nakamura T, Kihara S, Kumada M, Shibazaki S, Takahashi M, Nagai M, Matsuzawa Y, Funahashi T: Adiponectin as a biomarker of the metabolic syndrome. *Circ J* 68:975-981, 2004

138. Tsuchida A, Yamauchi T, Ito Y, Hada Y, Maki T, Takekawa S, Kamon J, Kobayashi M, Suzuki R, Hara K, Kubota N, Terauchi Y, Froguel P, Nakae J, Kasuga M, Accili D, Tobe K, Ueki K, Nagai R, Kadowaki T: Insulin/Foxo1 pathway regulates expression levels of adiponectin receptors and adiponectin sensitivity. *J Biol Chem* 279:30817-30822, 2004

139. Civitarese AE, Jenkinson CP, Richardson D, Bajaj M, Cusi K, Kashyap S, Berria R, Belfort R, DeFronzo RA, Mandarino LJ, Ravussin E: Adiponectin receptors gene expression and insulin sensitivity in non-diabetic Mexican Americans with or without a family history of Type 2 diabetes. *Diabetologia* 47:816-820, 2004

140. Combs TP, Pajvani UB, Berg AH, Lin Y, Jelicks LA, Laplante M, Nawrocki AR, Rajala MW, Parlow AF, Cheeseboro L, Ding YY, Russell RG, Lindemann D, Hartley A, Baker GR, Obici S, Deshaies Y, Ludgate M, Rossetti L, Scherer PE: A transgenic mouse with a deletion in the collagenous domain of adiponectin displays elevated circulating adiponectin and improved insulin sensitivity. *Endocrinology* 145:367-383, 2004

141. Yamauchi T, Kamon J, Minokoshi Y, Ito Y, Waki H, Uchida S, Yamashita S, Noda M, Kita S, Ueki K, Eto K, Akanuma Y, Froguel P, Foufelle F, Ferre P, Carling D, Kimura S, Nagai R, Kahn BB, Kadowaki T: Adiponectin stimulates glucose utilization and fatty-acid oxidation by activating AMP-activated protein kinase. *Nat Med* 8:1288-1295, 2002

142. Combs TP, Berg AH, Obici S, Scherer PE, Rossetti L: Endogenous glucose production is inhibited by the adipose-derived protein Acrp30. *J Clin Invest* 108:1875-1881, 2001

143. Tomas E, Tsao TS, Saha AK, Murrey HE, Zhang Cc C, Itani SI, Lodish HF, Ruderman NB: Enhanced muscle fat oxidation and glucose transport by ACRP30 globular domain: acetyl-CoA

carboxylase inhibition and AMP-activated protein kinase activation. *Proc Natl Acad Sci U S A* 99:16309-16313, 2002

144. Yamauchi T, Kamon J, Ito Y, Tsuchida A, Yokomizo T, Kita S, Sugiyama T, Miyagishi M, Hara K, Tsunoda M, Murakami K, Ohteki T, Uchida S, Takekawa S, Waki H, Tsuno NH, Shibata Y, Terauchi Y, Froguel P, Tobe K, Koyasu S, Taira K, Kitamura T, Shimizu T, Nagai R, Kadowaki T: Cloning of adiponectin receptors that mediate antidiabetic metabolic effects. *Nature* 423:762-769, 2003

145. Maeda N, Shimomura I, Kishida K, Nishizawa H, Matsuda M, Nagaretani H, Furuyama N, Kondo H, Takahashi M, Arita Y, Komuro R, Ouchi N, Kihara S, Tochino Y, Okutomi K, Horie M, Takeda S, Aoyama T, Funahashi T, Matsuzawa Y: Diet-induced insulin resistance in mice lacking adiponectin/ACRP30. *Nat Med* 8:731-737, 2002

146. Tsatsanis C, Zacharioudaki V, Androulidaki A, Dermitzaki E, Charalampopoulos I, Minas V, Gravanis A, Margioris AN: Adiponectin induces TNF-alpha and IL-6 in macrophages and promotes tolerance to itself and other pro-inflammatory stimuli. *Biochem Biophys Res Commun* 335:1254-1263, 2005

147. Lovren F, Pan Y, Quan A, Szmitko PE, Singh KK, Shukla PC, Gupta M, Chan L, Al-Omran M, Teoh H, Verma S: Adiponectin primes human monocytes into alternative anti-inflammatory M2 macrophages. *Am J Physiol Heart Circ Physiol* 299:H656-663

148. Wu X, Motoshima H, Mahadev K, Stalker TJ, Scalia R, Goldstein BJ: Involvement of AMP-activated protein kinase in glucose uptake stimulated by the globular domain of adiponectin in primary rat adipocytes. *Diabetes* 52:1355-1363, 2003

149. Ouchi N, Kobayashi H, Kihara S, Kumada M, Sato K, Inoue T, Funahashi T, Walsh K: Adiponectin stimulates angiogenesis by promoting cross-talk between AMP-activated protein kinase and Akt signaling in endothelial cells. *J Biol Chem* 279:1304-1309, 2004

150. Goldstein BJ, Scalia R: Adiponectin: A novel adipokine linking adipocytes and vascular function. *J Clin Endocrinol Metab* 89:2563-2568, 2004

151. Lundgren M, Svensson M, Lindmark S, Renstrom F, Ruge T, Eriksson JW: Fat cell enlargement is an independent marker of insulin resistance and 'hyperleptinaemia'. *Diabetologia* 50:625-633, 2007

152. Lillioja S, Mott DM, Spraul M, Ferraro R, Foley JE, Ravussin E, Knowler WC, Bennett PH, Bogardus C: Insulin resistance and insulin secretory dysfunction as precursors of non-insulin-dependent diabetes mellitus. Prospective studies of Pima Indians. *N Engl J Med* 329:1988-1992, 1993

153. Weyer C, Foley JE, Bogardus C, Tataranni PA, Pratley RE: Enlarged subcutaneous abdominal adipocyte size, but not obesity itself, predicts type II diabetes independent of insulin resistance. *Diabetologia* 43:1498-1506, 2000

154. Skurk T, Alberti-Huber C, Herder C, Hauner H: Relationship between adipocyte size and adipokine expression and secretion. *J Clin Endocrinol Metab* 92:1023-1033, 2007

155. Wueest S, Rapold RA, Rytka JM, Schoenle EJ, Konrad D: Basal lipolysis, not the degree of insulin resistance, differentiates large from small isolated adipocytes in high-fat fed mice. *Diabetologia* 52:541-546, 2009

156. O'Connell J, Lynch L, Cawood TJ, Kwasnik A, Nolan N, Geoghegan J, McCormick A, O'Farrelly C, O'Shea D: The relationship of omental and subcutaneous adipocyte size to metabolic disease in severe obesity. *PLoS One* 5:e9997

157. Kloting N, Fasshauer M, Dietrich A, Kovacs P, Schon MR, Kern M, Stumvoll M, Bluher M: Insulin-sensitive obesity. *Am J Physiol Endocrinol Metab* 299:E506-515

158. Kubota N, Terauchi Y, Miki H, Tamemoto H, Yamauchi T, Komeda K, Satoh S, Nakano R, Ishii C, Sugiyama T, Eto K, Tsubamoto Y, Okuno A, Murakami K, Sekihara H, Hasegawa G, Naito M, Toyoshima Y, Tanaka S, Shiota K, Kitamura T, Fujita T, Ezaki O, Aizawa S, Kadowaki T, et al.: PPAR gamma mediates high-fat diet-induced adipocyte hypertrophy and insulin resistance. *Mol Cell* 4:597-609, 1999

159. Fabbrini E, Sullivan S, Klein S: Obesity and nonalcoholic fatty liver disease: biochemical, metabolic, and clinical implications. *Hepatology* 51:679-689

160. Hilden M, Christoffersen P, Juhl E, Dalgaard JB: Liver histology in a 'normal' population--examinations of 503 consecutive fatal traffic casualties. *Scand J Gastroenterol* 12:593-597, 1977

161. Gholam PM, Kotler DP, Flancbaum LJ: Liver pathology in morbidly obese patients undergoing Roux-en-Y gastric bypass surgery. *Obes Surg* 12:49-51, 2002

162. Ruhl CE, Everhart JE: Determinants of the association of overweight with elevated serum alanine aminotransferase activity in the United States. *Gastroenterology* 124:71-79, 2003

163. Marcos A, Fisher RA, Ham JM, Olzinski AT, Shiffman ML, Sanyal AJ, Luketic VA, Sterling RK, Olbrisch ME, Posner MP: Selection and outcome of living donors for adult to adult right lobe transplantation. *Transplantation* 69:2410-2415, 2000

164. Diraison F, Moulin P, Beylot M: Contribution of hepatic de novo lipogenesis and reesterification of plasma non esterified fatty acids to plasma triglyceride synthesis during non-alcoholic fatty liver disease. *Diabetes Metab* 29:478-485, 2003

165. Petersen KF, Dufour S, Savage DB, Bilz S, Solomon G, Yonemitsu S, Cline GW, Befroy D, Zemany L, Kahn BB, Papademetris X, Rothman DL, Shulman GI: The role of skeletal muscle insulin resistance in the pathogenesis of the metabolic syndrome. *Proc Natl Acad Sci U S A* 104:12587-12594, 2007

166. Adiels M, Taskinen MR, Packard C, Caslake MJ, Soro-Paavonen A, Westerbacka J, Vehkavaara S, Hakkinen A, Olofsson SO, Yki-Jarvinen H, Boren J: Overproduction of large VLDL particles is driven by increased liver fat content in man. *Diabetologia* 49:755-765, 2006

167. Fabbrini E, Mohammed BS, Magkos F, Korenblat KM, Patterson BW, Klein S: Alterations in adipose tissue and hepatic lipid kinetics in obese men and women with nonalcoholic fatty liver disease. *Gastroenterology* 134:424-431, 2008

168. Targher G, Bertolini L, Padovani R, Rodella S, Tessari R, Zenari L, Day C, Arcaro G: Prevalence of nonalcoholic fatty liver disease and its association with cardiovascular disease among type 2 diabetic patients. *Diabetes Care* 30:1212-1218, 2007

169. Younossi ZM, Gramlich T, Matteoni CA, Boparai N, McCullough AJ: Nonalcoholic fatty liver disease in patients with type 2 diabetes. *Clin Gastroenterol Hepatol* 2:262-265, 2004

170. Chitturi S, Abeygunasekera S, Farrell GC, Holmes-Walker J, Hui JM, Fung C, Karim R, Lin R, Samarasinghe D, Liddle C, Weltman M, George J: NASH and insulin resistance: Insulin hypersecretion and specific association with the insulin resistance syndrome. *Hepatology* 35:373-379, 2002

171. Fabbrini E, Magkos F, Mohammed BS, Pietka T, Abumrad NA, Patterson BW, Okunade A, Klein S: Intrahepatic fat, not visceral fat, is linked with metabolic complications of obesity. *Proc Natl Acad Sci U S A* 106:15430-15435, 2009

172. Korenblat KM, Fabbrini E, Mohammed BS, Klein S: Liver, muscle, and adipose tissue insulin action is directly related to intrahepatic triglyceride content in obese subjects. *Gastroenterology* 134:1369-1375, 2008

173. Vega GL, Chandalia M, Szczepaniak LS, Grundy SM: Metabolic correlates of nonalcoholic fatty liver in women and men. *Hepatology* 46:716-722, 2007

174. Bugianesi E, Gastaldelli A, Vanni E, Gambino R, Cassader M, Baldi S, Ponti V, Pagano G, Ferrannini E, Rizzetto M: Insulin resistance in non-diabetic patients with non-alcoholic fatty liver disease: sites and mechanisms. *Diabetologia* 48:634-642, 2005

175. Seppala-Lindroos A, Vehkavaara S, Hakkinen AM, Goto T, Westerbacka J, Sovijarvi A, Halavaara J, Yki-Jarvinen H: Fat accumulation in the liver is associated with defects in insulin suppression of glucose production and serum free fatty acids independent of obesity in normal men. *J Clin Endocrinol Metab* 87:3023-3028, 2002

176. Klein S, Mittendorfer B, Eagon JC, Patterson B, Grant L, Feirt N, Seki E, Brenner D, Korenblat K, McCrea J: Gastric bypass surgery improves metabolic and hepatic abnormalities associated with nonalcoholic fatty liver disease. *Gastroenterology* 130:1564-1572, 2006

177. Kolak M, Westerbacka J, Velagapudi VR, Wagsater D, Yetukuri L, Makkonen J, Rissanen A, Hakkinen AM, Lindell M, Bergholm R, Hamsten A, Eriksson P, Fisher RM, Oresic M, Yki-Jarvinen H: Adipose tissue inflammation and increased ceramide content characterize subjects with high liver fat content independent of obesity. *Diabetes* 56:1960-1968, 2007

178. Nov O, Kohl A, Lewis EC, Bashan N, Dvir I, Ben-Shlomo S, Fishman S, Wueest S, Konrad D, Rudich A: Interleukin-1beta may mediate insulin resistance in liver-derived cells in response to adipocyte inflammation. *Endocrinology* 151:4247-4256

179. Musso G, Gambino R, Durazzo M, Biroli G, Carello M, Faga E, Pacini G, De Michieli F, Rabbione L, Premoli A, Cassader M, Pagano G: Adipokines in NASH: postprandial lipid metabolism as a link between adiponectin and liver disease. *Hepatology* 42:1175-1183, 2005

180. Xu A, Wang Y, Keshaw H, Xu LY, Lam KS, Cooper GJ: The fat-derived hormone adiponectin alleviates alcoholic and nonalcoholic fatty liver diseases in mice. *J Clin Invest* 112:91-100, 2003

181. Cai D, Yuan M, Frantz DF, Melendez PA, Hansen L, Lee J, Shoelson SE: Local and systemic insulin resistance resulting from hepatic activation of IKK-beta and NF-kappaB. *Nat Med* 11:183-190, 2005

182. Samuel VT, Liu ZX, Wang A, Beddow SA, Geisler JG, Kahn M, Zhang XM, Monia BP, Bhanot S, Shulman GI: Inhibition of protein kinase Cepsilon prevents hepatic insulin resistance in nonalcoholic fatty liver disease. *J Clin Invest* 117:739-745, 2007

183. Wing RR, Jeffery RW: Effect of modest weight loss on changes in cardiovascular risk factors: are there differences between men and women or between weight loss and maintenance? *Int J Obes Relat Metab Disord* 19:67-73, 1995

184. Wing RR, Koeske R, Epstein LH, Nowalk MP, Gooding W, Becker D: Long-term effects of modest weight loss in type II diabetic patients. *Arch Intern Med* 147:1749-1753, 1987

185. Hickman IJ, Jonsson JR, Prins JB, Ash S, Purdie DM, Clouston AD, Powell EE: Modest weight loss and physical activity in overweight patients with chronic liver disease results in sustained improvements in alanine aminotransferase, fasting insulin, and quality of life. *Gut* 53:413-419, 2004

186. Sesti G, Federici M, Lauro D, Sbraccia P, Lauro R: Molecular mechanism of insulin resistance in type 2 diabetes mellitus: role of the insulin receptor variant forms. *Diabetes Metab Res Rev* 17:363-373, 2001

187. Semple RK, Cochran EK, Soos MA, Burling KA, Savage DB, Gorden P, O'Rahilly S: Plasma adiponectin as a marker of insulin receptor dysfunction: clinical utility in severe insulin resistance. *Diabetes Care* 31:977-979, 2008

188. Rogers PM, Mashtalir N, Rathod MA, Dubuisson O, Wang Z, Dasuri K, Babin S, Gupta A, Markward N, Cefalu WT, Dhurandhar NV: Metabolically favorable remodeling of human adipose tissue by human adenovirus type 36. *Diabetes* 57:2321-2331, 2008

189. Wang ZQ, Cefalu WT, Zhang XH, Yu Y, Qin J, Son L, Rogers PM, Mashtalir N, Bordelon JR, Ye J, Dhurandhar NV: Human adenovirus type 36 enhances glucose uptake in diabetic and nondiabetic human skeletal muscle cells independent of insulin signaling. *Diabetes* 57:1805-1813, 2008

190. Krishnapuram R, Dhurandhar EJ, Dubuisson O, Kirk-Ballard H, Bajpeyi S, Butte NF, Sothern MS, Larsen-Meyer E, Chalew S, Bennett B, Gupta AK, Greenway FL, Johnson WD, Brashear M, Reinhart G, Rankinen T, Bouchard C, Cefalu WT, Ye J, Javier R, Zuberi A, Dhurandhar NV: A Template to Improve Glycemic Control without Reducing Adiposity or Dietary Fat. *Am J Physiol Endocrinol Metab*

191. Wigand R, Gelderblom H, Wadell G: New human adenovirus (candidate adenovirus 36), a novel member of subgroup D. *Arch Virol* 64:225-233, 1980

192. Dhurandhar NV, Israel BA, Kolesar JM, Mayhew G, Cook ME, Atkinson RL: Transmissibility of adenovirus-induced adiposity in a chicken model. *Int J Obes Relat Metab Disord* 25:990-996, 2001
193. Dhurandhar NV, Israel BA, Kolesar JM, Mayhew GF, Cook ME, Atkinson RL: Increased adiposity in animals due to a human virus. *Int J Obes Relat Metab Disord* 24:989-996, 2000

194. Dhurandhar NV, Whigham LD, Abbott DH, Schultz-Darken NJ, Israel BA, Bradley SM, Kemnitz JW, Allison DB, Atkinson RL: Human adenovirus Ad-36 promotes weight gain in male rhesus and marmoset monkeys. *J Nutr* 132:3155-3160, 2002

195. Atkinson RL, Dhurandhar NV, Allison DB, Bowen RL, Israel BA, Albu JB, Augustus AS: Human adenovirus-36 is associated with increased body weight and paradoxical reduction of serum lipids. *Int J Obes (Lond)* 29:281-286, 2005

196. Trovato GM, Castro A, Tonzuso A, Garozzo A, Martines GF, Pirri C, Trovato F, Catalano D: Human obesity relationship with Ad36 adenovirus and insulin resistance. *Int J Obes (Lond)*, 2009

197. Pasarica M, Shin AC, Yu M, Ou Yang HM, Rathod M, Jen KL, MohanKumar S, MohanKumar PS, Markward N, Dhurandhar NV: Human adenovirus 36 induces adiposity, increases insulin sensitivity, and alters hypothalamic monoamines in rats. *Obesity (Silver Spring)* 14:1905-1913, 2006

198. Pasarica M, Loiler S, Dhurandhar NV: Acute effect of infection by adipogenic human adenovirus Ad36. *Arch Virol* 153:2097-2102, 2008

199. Heiman ML, Ahima RS, Craft LS, Schoner B, Stephens TW, Flier JS: Leptin inhibition of the hypothalamic-pituitary-adrenal axis in response to stress. *Endocrinology* 138:3859-3863, 1997

200. Rathod M, Vangipuram SD, Krishnan B, Heydari AR, Holland TC, Dhurandhar NV: Viral mRNA expression but not DNA replication is required for lipogenic effect of human adenovirus Ad-36 in preadipocytes. *Int J Obes (Lond)* 31:78-86, 2007

201. Vangipuram SD, Sheele J, Atkinson RL, Holland TC, Dhurandhar NV: A human adenovirus enhances preadipocyte differentiation. *Obes Res* 12:770-777, 2004

202. Pasarica M, Mashtalir N, McAllister EJ, Kilroy GE, Koska J, Permana P, de Courten B, Yu M, Ravussin E, Gimble JM, Dhurandhar NV: Adipogenic human adenovirus Ad-36 induces commitment, differentiation, and lipid accumulation in human adipose-derived stem cells. *Stem Cells* 26:969-978, 2008

203. Rogers PM, Fusinski KA, Rathod MA, Loiler SA, Pasarica M, Shaw MK, Kilroy G, Sutton GM, McAllister EJ, Mashtalir N, Gimble JM, Holland TC, Dhurandhar NV: Human adenovirus Ad-36 induces adipogenesis via its E4 orf-1 gene. *Int J Obes (Lond)* 32:397-406, 2008

204. Shen Y, Shenk TE: Viruses and apoptosis. *Curr Opin Genet Dev* 5:105-111, 1995

205. Trovato GM, Castro A, Tonzuso A, Garozzo A, Martines GF, Pirri C, Trovato F, Catalano D: Human obesity relationship with Ad36 adenovirus and insulin resistance. *Int J Obes (Lond)* 33:1402-1409, 2009

206. Goossens VJ, deJager SA, Grauls GE, Gielen M, Vlietinck RF, Derom CA, Loos RJ, Rensen SS, Buurman WA, Greve JW, van Baak MA, Wolffs PF, Bruggeman CA, Hoebe CJ: Lack of evidence for the role of human adenovirus-36 in obesity in a European cohort. *Obesity (Silver Spring)* 19:220-221

207. Broderick MP, Hansen CJ, Irvine M, Metzgar D, Campbell K, Baker C, Russell KL: Adenovirus 36 seropositivity is strongly associated with race and gender, but not obesity, among US military personnel. *Int J Obes (Lond)* 34:302-308

208. Gabbert C, Donohue M, Arnold J, Schwimmer JB: Adenovirus 36 and obesity in children and adolescents. *Pediatrics* 126:721-726

209. Atkinson RL, Lee I, Shin HJ, He J: Human adenovirus-36 antibody status is associated with obesity in children. *Int J Pediatr Obes* 5:157-160

210. Na HN, Hong YM, Kim J, Kim HK, Jo I, Nam JH: Association between human adenovirus-36 and lipid disorders in Korean schoolchildren. *Int J Obes (Lond)* 34:89-93

211. Vangipuram SD, Yu M, Tian J, Stanhope KL, Pasarica M, Havel PJ, Heydari AR, Dhurandhar NV: Adipogenic human adenovirus-36 reduces leptin expression and secretion and increases glucose uptake by fat cells. *Int J Obes (Lond)* 31:87-96, 2007

212. Trovato GM, Martines GF, Garozzo A, Tonzuso A, Timpanaro R, Pirri C, Trovato FM, Catalano D: Ad36 adipogenic adenovirus in human non-alcoholic fatty liver disease. *Liver Int* 30:184-190

213. Reuter CW, Morgan MA, Bergmann L: Targeting the Ras signaling pathway: a rational, mechanism-based treatment for hematologic malignancies? *Blood* 96:1655-1669, 2000

214. Benito M, Porras A, Nebreda AR, Santos E: Differentiation of 3T3-L1 fibroblasts to adipocytes induced by transfection of ras oncogenes. *Science* 253:565-568, 1991

215. Porras A, Nebreda AR, Benito M, Santos E: Activation of Ras by insulin in 3T3 L1 cells does not involve GTPase-activating protein phosphorylation. *J Biol Chem* 267:21124-21131, 1992

216. Uehara T, Tokumitsu Y, Nomura Y: Wortmannin inhibits insulin-induced Ras and mitogen-activated protein kinase activation related to adipocyte differentiation in 3T3-L1 fibroblasts. *Biochem Biophys Res Commun* 210:574-580, 1995

217. Magun R, Burgering BM, Coffer PJ, Pardasani D, Lin Y, Chabot J, Sorisky A: Expression of a constitutively activated form of protein kinase B (c-Akt) in 3T3-L1 preadipose cells causes spontaneous differentiation. *Endocrinology* 137:3590-3593, 1996

218. Engelman JA, Lisanti MP, Scherer PE: Specific inhibitors of p38 mitogen-activated protein kinase block 3T3-L1 adipogenesis. *J Biol Chem* 273:32111-32120, 1998

219. Engelman JA, Berg AH, Lewis RY, Lin A, Lisanti MP, Scherer PE: Constitutively active mitogen-activated protein kinase kinase 6 (MKK6) or salicylate induces spontaneous 3T3-L1 adipogenesis. *J Biol Chem* 274:35630-35638, 1999

220. Font de Mora J, Porras A, Ahn N, Santos E: Mitogen-activated protein kinase activation is not necessary for, but antagonizes, 3T3-L1 adipocytic differentiation. *Mol Cell Biol* 17:6068-6075, 1997

221. Reginato MJ, Krakow SL, Bailey ST, Lazar MA: Prostaglandins promote and block adipogenesis through opposing effects on peroxisome proliferator-activated receptor gamma. *J Biol Chem* 273:1855-1858, 1998

222. Mo X, Kowenz-Leutz E, Xu H, Leutz A: Ras induces mediator complex exchange on C/EBP beta. *Mol Cell* 13:241-250, 2004

223. Dorrestijn J, Ouwens DM, Van den Berghe N, Bos JL, Maassen JA: Expression of a dominant-negative Ras mutant does not affect stimulation of glucose uptake and glycogen synthesis by insulin. *Diabetologia* 39:558-563, 1996

224. Flier JS, Mueckler MM, Usher P, Lodish HF: Elevated levels of glucose transport and transporter messenger RNA are induced by ras or src oncogenes. *Science* 235:1492-1495, 1987

225. Houseknecht KL, Zhu AX, Gnudi L, Hamann A, Zierath JR, Tozzo E, Flier JS, Kahn BB: Overexpression of Ha-ras selectively in adipose tissue of transgenic mice. Evidence for enhanced sensitivity to insulin. *J Biol Chem* 271:11347-11355, 1996

226. Kozma L, Baltensperger K, Klarlund J, Porras A, Santos E, Czech MP: The ras signaling pathway mimics insulin action on glucose transporter translocation. *Proc Natl Acad Sci U S A* 90:4460-4464, 1993

227. Tal M, Wu YJ, Leiser M, Surana M, Lodish H, Fleischer N, Weir G, Efrat S: [Val12] HRAS downregulates GLUT2 in beta cells of transgenic mice without affecting glucose homeostasis. *Proc Natl Acad Sci U S A* 89:5744-5748, 1992

228. Kranenburg O, Gebbink MF, Voest EE: Stimulation of angiogenesis by Ras proteins. *Biochim Biophys Acta* 1654:23-37, 2004

229. Goossens GH: The role of adipose tissue dysfunction in the pathogenesis of obesity-related insulin resistance. *Physiol Behav* 94:206-218, 2008

230. Hamada K, Sasaki T, Koni PA, Natsui M, Kishimoto H, Sasaki J, Yajima N, Horie Y, Hasegawa G, Naito M, Miyazaki J, Suda T, Itoh H, Nakao K, Mak TW, Nakano T, Suzuki A: The PTEN/PI3K pathway governs normal vascular development and tumor angiogenesis. *Genes Dev* 19:2054-2065, 2005

231. Dong G, Chen Z, Li ZY, Yeh NT, Bancroft CC, Van Waes C: Hepatocyte growth factor/scatter factor-induced activation of MEK and PI3K signal pathways contributes to expression of proangiogenic cytokines interleukin-8 and vascular endothelial growth factor in head and neck squamous cell carcinoma. *Cancer Res* 61:5911-5918, 2001

232. Shiojima I, Walsh K: Role of Akt signaling in vascular homeostasis and angiogenesis. *Circ Res* 90:1243-1250, 2002

233. Wang M, Crisostomo PR, Herring C, Meldrum KK, Meldrum DR: Human progenitor cells from bone marrow or adipose tissue produce VEGF, HGF, and IGF-I in response to TNF by a p38 MAPK-dependent mechanism. *Am J Physiol Regul Integr Comp Physiol* 291:R880-884, 2006

234. Yen ML, Su JL, Chien CL, Tseng KW, Yang CY, Chen WF, Chang CC, Kuo ML: Diosgenin induces hypoxia-inducible factor-1 activation and angiogenesis through estrogen receptor-related phosphatidylinositol 3-kinase/Akt and p38 mitogen-activated protein kinase pathways in osteoblasts. *Mol Pharmacol* 68:1061-1073, 2005

235. Pylayeva Y, Gillen KM, Gerald W, Beggs HE, Reichardt LF, Giancotti FG: Ras- and PI3K-dependent breast tumorigenesis in mice and humans requires focal adhesion kinase signaling. *J Clin Invest* 119:252-266, 2009

236. Hanlon GW: Bacteriophages: an appraisal of their role in the treatment of bacterial infections. *Int J Antimicrob Agents* 30:118-128, 2007

237. Crompton AM, Kirn DH: From ONYX-015 to armed vaccinia viruses: the education and evolution of oncolytic virus development. *Curr Cancer Drug Targets* 7:133-139, 2007

238. Lee SS, Weiss RS, Javier RT: Binding of human virus oncoproteins to hDlg/SAP97, a mammalian homolog of the Drosophila discs large tumor suppressor protein. *Proc Natl Acad Sci U S A* 94:6670-6675, 1997

239. Frese KK, Latorre IJ, Chung SH, Caruana G, Bernstein A, Jones SN, Donehower LA, Justice MJ, Garner CC, Javier RT: Oncogenic function for the Dlg1 mammalian homolog of the Drosophila discs-large tumor suppressor. *EMBO J* 25:1406-1417, 2006

240. Frese KK, Lee SS, Thomas DL, Latorre IJ, Weiss RS, Glaunsinger BA, Javier RT: Selective PDZ protein-dependent stimulation of phosphatidylinositol 3-kinase by the adenovirus E4-ORF1 oncoprotein. *Oncogene* 22:710-721, 2003

241. Deckelbaum RJ, Williams CL: Childhood obesity: the health issue. *Obes Res* 9 Suppl 4:239S-243S, 2001

242. Larson-Meyer DE, Newcomer BR, VanVrancken-Tompkins CL, Sothern M: Feasibility of assessing liver lipid by proton magnetic resonance spectroscopy in healthy normal and overweight prepubertal children. *Diabetes Technol Ther* 12:207-212

243. Butte NF, Cai G, Cole SA, Wilson TA, Fisher JO, Zakeri IF, Ellis KJ, Comuzzie AG: Metabolic and behavioral predictors of weight gain in Hispanic children: the Viva la Familia Study. *Am J Clin Nutr* 85:1478-1485, 2007

244. Tompkins CL, Cefalu W, Ravussin E, Goran M, Soros A, Volaufova J, Vargas A, Sothern MS: Feasibility of intravenous glucose tolerance testing prior to puberty. *Int J Pediatr Obes* 5:51-55

245. Greenway FL, Liu Z, Yu Y, Caruso MK, Roberts AT, Lyons J, Schwimer JE, Gupta AK, Bellanger DE, Guillot TS, Woltering EA: An assay to measure angiogenesis in human fat tissue. *Obes Surg* 17:510-515, 2007

246. Aoki F, Honda S, Kishida H, Kitano M, Arai N, Tanaka H, Yokota S, Nakagawa K, Asakura T, Nakai Y, Mae T: Suppression by licorice flavonoids of abdominal fat accumulation and body weight gain in high-fat diet-induced obese C57BL/6J mice. *Biosci Biotechnol Biochem* 71:206-214, 2007

247. Rathod MA, Rogers PM, Vangipuram SD, McAllister EJ, Dhurandhar NV: Adipogenic cascade can be induced without adipogenic media by a human adenovirus. *Obesity (Silver Spring)* 17:657-664, 2009

248. Zhang J, Fu M, Cui T, Xiong C, Xu K, Zhong W, Xiao Y, Floyd D, Liang J, Li E, Song Q, Chen YE: Selective disruption of PPARgamma 2 impairs the development of adipose tissue and insulin sensitivity. *Proc Natl Acad Sci U S A* 101:10703-10708, 2004

249. Dong XC, Copps KD, Guo S, Li Y, Kollipara R, DePinho RA, White MF: Inactivation of hepatic Foxo1 by insulin signaling is required for adaptive nutrient homeostasis and endocrine growth regulation. *Cell Metab* 8:65-76, 2008

250. Kim JY, Hickner RC, Cortright RL, Dohm GL, Houmard JA: Lipid oxidation is reduced in obese human skeletal muscle. *Am J Physiol Endocrinol Metab* 279:E1039-1044, 2000

251. Lee JM, Okumura MJ, Davis MM, Herman WH, Gurney JG: Prevalence and determinants of insulin resistance among U.S. adolescents: a population-based study. *Diabetes Care* 29:2427-2432, 2006

252. Cruz ML, Weigensberg MJ, Huang TT, Ball G, Shaibi GQ, Goran MI: The metabolic syndrome in overweight Hispanic youth and the role of insulin sensitivity. *J Clin Endocrinol Metab* 89:108-113, 2004

253. Trovato GM, Martines GF, Garozzo A, Tonzuso A, Timpanaro R, Pirri C, Trovato FM, Catalano D: Ad36 adipogenic adenovirus in human non-alcoholic fatty liver disease. *Liver Int*, 2009

254. Ambinder RF: Gammaherpesviruses and "Hit-and-Run" oncogenesis. *Am J Pathol* 156:1-3, 2000

255. Fernandez-Real JM, Lopez-Bermejo A, Vendrell J, Ferri MJ, Recasens M, Ricart W: Burden of infection and insulin resistance in healthy middle-aged men. *Diabetes Care* 29:1058-1064, 2006

256. Shintani Y, Fujie H, Miyoshi H, Tsutsumi T, Tsukamoto K, Kimura S, Moriya K, Koike K: Hepatitis C virus infection and diabetes: direct involvement of the virus in the development of insulin resistance. *Gastroenterology* 126:840-848, 2004

257. Perlemuter G, Sabile A, Letteron P, Vona G, Topilco A, Chretien Y, Koike K, Pessayre D, Chapman J, Barba G, Brechot C: Hepatitis C virus core protein inhibits microsomal triglyceride transfer protein activity and very low density lipoprotein secretion: a model of viral-related steatosis. *FASEB J* 16:185-194, 2002

258. Lonardo A, Adinolfi LE, Loria P, Carulli N, Ruggiero G, Day CP: Steatosis and hepatitis C virus: mechanisms and significance for hepatic and extrahepatic disease. *Gastroenterology* 126:586-597, 2004

259. Combs TP, Nagajyothi, Mukherjee S, de Almeida CJ, Jelicks LA, Schubert W, Lin Y, Jayabalan DS, Zhao D, Braunstein VL, Landskroner-Eiger S, Cordero A, Factor SM, Weiss LM, Lisanti MP, Tanowitz HB, Scherer PE: The adipocyte as an important target cell for Trypanosoma cruzi infection. *J Biol Chem* 280:24085-24094, 2005

260. Dyrberg T, Schwimmbeck PL, Oldstone MB: Inhibition of diabetes in BB rats by virus infection. *J Clin Invest* 81:928-931, 1988

261. Schwimmbeck PL, Dyrberg T, Oldstone MB: Abrogation of diabetes in BB rats by acute virus infection. Association of viral-lymphocyte interactions. *J Immunol* 140:3394-3400, 1988

262. Tilg H, Moschen AR: Adipocytokines: mediators linking adipose tissue, inflammation and immunity. *Nat Rev Immunol* 6:772-783, 2006

263. Charriere G, Cousin B, Arnaud E, Andre M, Bacou F, Penicaud L, Casteilla L: Preadipocyte conversion to macrophage. Evidence of plasticity. *J Biol Chem* 278:9850-9855, 2003

264. Cousin B, Munoz O, Andre M, Fontanilles AM, Dani C, Cousin JL, Laharrague P, Casteilla L, Penicaud L: A role for preadipocytes as macrophage-like cells. *FASEB J* 13:305-312, 1999

265. Villena JA, Cousin B, Penicaud L, Casteilla L: Adipose tissues display differential phagocytic and microbicidal activities depending on their localization. *Int J Obes Relat Metab Disord* 25:1275-1280, 2001

266. Scott RE, Florine DL, Wille JJ, Jr., Yun K: Coupling of growth arrest and differentiation at a distinct state in the G1 phase of the cell cycle: GD. *Proc Natl Acad Sci U S A* 79:845-849, 1982

267. Ntambi JM, Young-Cheul K: Adipocyte differentiation and gene expression. *J Nutr* 130:3122S-3126S, 2000

268. Morrison RF, Farmer SR: Role of PPARgamma in regulating a cascade expression of cyclin-dependent kinase inhibitors, p18(INK4c) and p21(Waf1/Cip1), during adipogenesis. *J Biol Chem* 274:17088-17097, 1999

269. Diraison F, Yankah V, Letexier D, Dusserre E, Jones P, Beylot M: Differences in the regulation of adipose tissue and liver lipogenesis by carbohydrates in humans. *J Lipid Res* 44:846-853, 2003

270. Strawford A, Antelo F, Christiansen M, Hellerstein MK: Adipose tissue triglyceride turnover, de novo lipogenesis, and cell proliferation in humans measured with 2H2O. *Am J Physiol Endocrinol Metab* 286:E577-588, 2004

271. Boden G, Homko C, Mozzoli M, Showe LC, Nichols C, Cheung P: Thiazolidinediones upregulate fatty acid uptake and oxidation in adipose tissue of diabetic patients. *Diabetes* 54:880-885, 2005

272. Chaput E, Saladin R, Silvestre M, Edgar AD: Fenofibrate and rosiglitazone lower serum triglycerides with opposing effects on body weight. *Biochem Biophys Res Commun* 271:445-450, 2000

273. Bogacka I, Xie H, Bray GA, Smith SR: Pioglitazone induces mitochondrial biogenesis in human subcutaneous adipose tissue in vivo. *Diabetes* 54:1392-1399, 2005

274. Jo J, Gavrilova O, Pack S, Jou W, Mullen S, Sumner AE, Cushman SW, Periwal V: Hypertrophy and/or Hyperplasia: Dynamics of Adipose Tissue Growth. *PLoS Comput Biol* 5:e1000324, 2009

275. Lang P, van Harmelen V, Ryden M, Kaaman M, Parini P, Carneheim C, Cassady AI, Hume DA, Andersson G, Arner P: Monomeric tartrate resistant acid phosphatase induces insulin sensitive obesity. *PLoS One* 3:e1713, 2008

276. MacKellar J, Cushman SW, Periwal V: Differential effects of thiazolidinediones on adipocyte growth and recruitment in Zucker fatty rats. *PLoS One* 4:e8196, 2009

277. Gao Z, Hwang D, Bataille F, Lefevre M, York D, Quon MJ, Ye J: Serine phosphorylation of insulin receptor substrate 1 by inhibitor kappa B kinase complex. *J Biol Chem* 277:48115-48121, 2002

278. Chen C, Pore N, Behrooz A, Ismail-Beigi F, Maity A: Regulation of glut1 mRNA by hypoxia-inducible factor-1. Interaction between H-ras and hypoxia. *J Biol Chem* 276:9519-9525, 2001

279. Seandel M, Butler JM, Kobayashi H, Hooper AT, White IA, Zhang F, Vertes EL, Kobayashi M, Zhang Y, Shmelkov SV, Hackett NR, Rabbany S, Boyer JL, Rafii S: Generation of a functional and durable vascular niche by the adenoviral E4ORF1 gene. *Proc Natl Acad Sci U S A* 105:19288-19293, 2008

280. Su C, Na M, Chen J, Wang X, Liu Y, Wang W, Zhang Q, Li L, Long J, Liu X, Wu M, Fan X, Qian Q: Gene-viral cancer therapy using dual-regulated oncolytic adenovirus with antiangiogenesis gene for increased efficacy. *Mol Cancer Res* 6:568-575, 2008

281. Tysome JR, Lemoine NR, Wang Y: Combination of anti-angiogenic therapy and virotherapy: arming oncolytic viruses with anti-angiogenic genes. *Curr Opin Mol Ther* 11:664-669, 2009

282. Thomas MA, Broughton RS, Goodrum FD, Ornelles DA: E4orf1 limits the oncolytic potential of the E1B-55K deletion mutant adenovirus. *J Virol* 83:2406-2416, 2009

283. Furler SM, Gan SK, Poynten AM, Chisholm DJ, Campbell LV, Kriketos AD: Relationship of adiponectin with insulin sensitivity in humans, independent of lipid availability. *Obesity (Silver Spring)* 14:228-234, 2006

284. Javier RT: Adenovirus type 9 E4 open reading frame 1 encodes a transforming protein required for the production of mammary tumors in rats. *J Virol* 68:3917-3924, 1994

285. Baudry A, Yang ZZ, Hemmings BA: PKBalpha is required for adipose differentiation of mouse embryonic fibroblasts. *J Cell Sci* 119:889-897, 2006

286. Lumeng CN, Bodzin JL, Saltiel AR: Obesity induces a phenotypic switch in adipose tissue macrophage polarization. *J Clin Invest* 117:175-184, 2007

287. Bes-Houtmann S, Roche R, Hoareau L, Gonthier MP, Festy F, Caillens H, Gasque P, Lefebvre d'Hellencourt C, Cesari M: Presence of functional TLR2 and TLR4 on human adipocytes. *Histochem Cell Biol* 127:131-137, 2007

288. Tang T, Zhang J, Yin J, Staszkiewicz J, Gawronska-Kozak B, Jung DY, Ko HJ, Ong H, Kim JK, Mynatt R, Martin RJ, Keenan M, Gao Z, Ye J: Uncoupling of inflammation and insulin resistance by NF-kappaB in transgenic mice through elevated energy expenditure. *J Biol Chem* 285:4637-4644

289. Lipscombe LL, Gomes T, Levesque LE, Hux JE, Juurlink DN, Alter DA: Thiazolidinediones and cardiovascular outcomes in older patients with diabetes. *JAMA* 298:2634-2643, 2007

290. Schwartz AV, Sellmeyer DE: Thiazolidinedione therapy gets complicated: is bone loss the price of improved insulin resistance? *Diabetes Care* 30:1670-1671, 2007

291. Semenkovich CF: TZDs and diabetes: testing the waters. *Nat Med* 11:822-824, 2005

292. Knouff C, Auwerx J: Peroxisome proliferator-activated receptor-gamma calls for activation in moderation: lessons from genetics and pharmacology. *Endocr Rev* 25:899-918, 2004

293. Mukherjee R, Hoener PA, Jow L, Bilakovics J, Klausing K, Mais DE, Faulkner A, Croston GE, Paterniti JR, Jr.: A selective peroxisome proliferator-activated receptor-gamma (PPARgamma) modulator blocks adipocyte differentiation but stimulates glucose uptake in 3T3-L1 adipocytes. *Mol Endocrinol* 14:1425-1433, 2000

294. Xu J, Liao K: Protein kinase B/AKT 1 plays a pivotal role in insulin-like growth factor-1 receptor signaling induced 3T3-L1 adipocyte differentiation. *J Biol Chem* 279:35914-35922, 2004

295. Yun SJ, Kim EK, Tucker DF, Kim CD, Birnbaum MJ, Bae SS: Isoform-specific regulation of adipocyte differentiation by Akt/protein kinase Balpha. *Biochem Biophys Res Commun* 371:138-143, 2008

296. Hill MM, Clark SF, Tucker DF, Birnbaum MJ, James DE, Macaulay SL: A role for protein kinase Bbeta/Akt2 in insulin-stimulated GLUT4 translocation in adipocytes. *Mol Cell Biol* 19:7771-7781, 1999

# APPENDIX

## LETTERS OF PERMISSION

**The American Physiological Society**
**9650 Rockville Pike, Bethesda, MD 20814-3991, USA**
**Publications Department Phone: (301) 634-7070**
**Fax: (301) 634-7243**

**June 6, 2011**

**Emily Mcallister Dhurandhar**
**11152 S. Lakeside Oaks Ave.**
**Baton Rouge, LA 70810**

**Dear Ms. Dhurandhar**

**The American Physiological Society grants you permission to use figure 4 from the following *American Journal of Physiology Endocrinology and Metabolism* article in your PhD dissertation for Louisiana State University:**

R. Krishnapuram, E. J. Dhurandhar, O. Dubuisson, et al.
Template to improve glycemic control without reducing adiposity or dietary fat. *Am J Physiol Endocrinol Metab May 2011 300:E779-E789; published ahead of print January 25, 2011, doi:10.1152/ajpendo.00703.2010*

**This permission includes the electronic version of the dissertation.**

**Please have the APS author and journal name, the year the article was published, and "Am Physiol Soc, used with permission" in the figure legend so one could find the source article.**

**The full citation would be in the reference list.**

**Thank you.**

**Sincerely,**

Rita Scheman

**Ms. Rita Scheman**
**Director of Publications**
**The American Physiological Society**

# The American Physiological Society

**9650 Rockville Pike, Bethesda, MD 20814-3991, USA**
**Publications Department Phone: (301) 634-7070**
**Fax: (301) 634-7243**


**June 6, 2011**

**Emily Mcallister Dhurandhar**
**11152 S. Lakeside Oaks Avenue**
**Baton Rouge, LA 70810**

**Dear Ms. Dhurandhar:**

**The American Physiological Society grants you permission to use Table 2 from the following *American Journal of Physiology Endocrinology and Metabolism* article in your PhD dissertation for Louisiana State University:**

R. Krishnapuram, E. J. Dhurandhar, O. Dubuisson, Bajpeyi, N. Butte, M. S. Sothern, E. Larsen-Meyer, S. Chalew, B. Bennett, A. K. Gupta, F. L. Greenway, W. Johnson, M. Brashear, G. Reinhart, T. Rankinen, C. Bouchard, W. T. Cefalu, J. Ye, R. Javier, A. Zuberi, and N. V. Dhurandhar

**Template to improve glycemic control without reducing adiposity or dietary fat.** *Am J Physiol Endocrinol Metab May 2011 300:E779-E789; published ahead of print January 25, 2011, doi:10.1152/ajpendo.00703.2010*

**The permission includes the electronic version of the dissertation.**

**The American Physiological Society publication must be credited as the source with the words "used with permission" added when referencing the *Journal of Physiology Heart and Circulatory Physiology* article. The full citation would be in the reference list.**

**Thank you.**

**Sincerely,**

Rita Scheman

**Ms. Rita Scheman**
**Director of Publications**
**The American Physiological Society**

**RS/pr**

# Vita

Emily Jane Dhurandhar completed her Bachelor of Science degree in nutritional sciences at Michigan State University in May of 2006. She then began her doctoral studies in Fall of 2006 at Louisiana State University School of Human Ecology, with a focus in human nutrition. She received an assistantship throughout her graduate work, and received several scholarships as a result of her academic achievements including the Neva Olsen Nelson Graduate Scholarship, the Clara Tucker Graduate Scholarship, and the Lillie and Alvin Harper Graduate Scholarship. In addition, she received the LSU Dissertation Year Fellowship to support the final year of her graduate studies. During her graduate work, she attended three professional conferences of The Obesity Society and presented five posters and two oral abstracts at these conferences. She received the Harvey Lewis Travel Award and The Obesity Society Travel Award. Before completion of her graduate studies, she also contributed to seven publications.